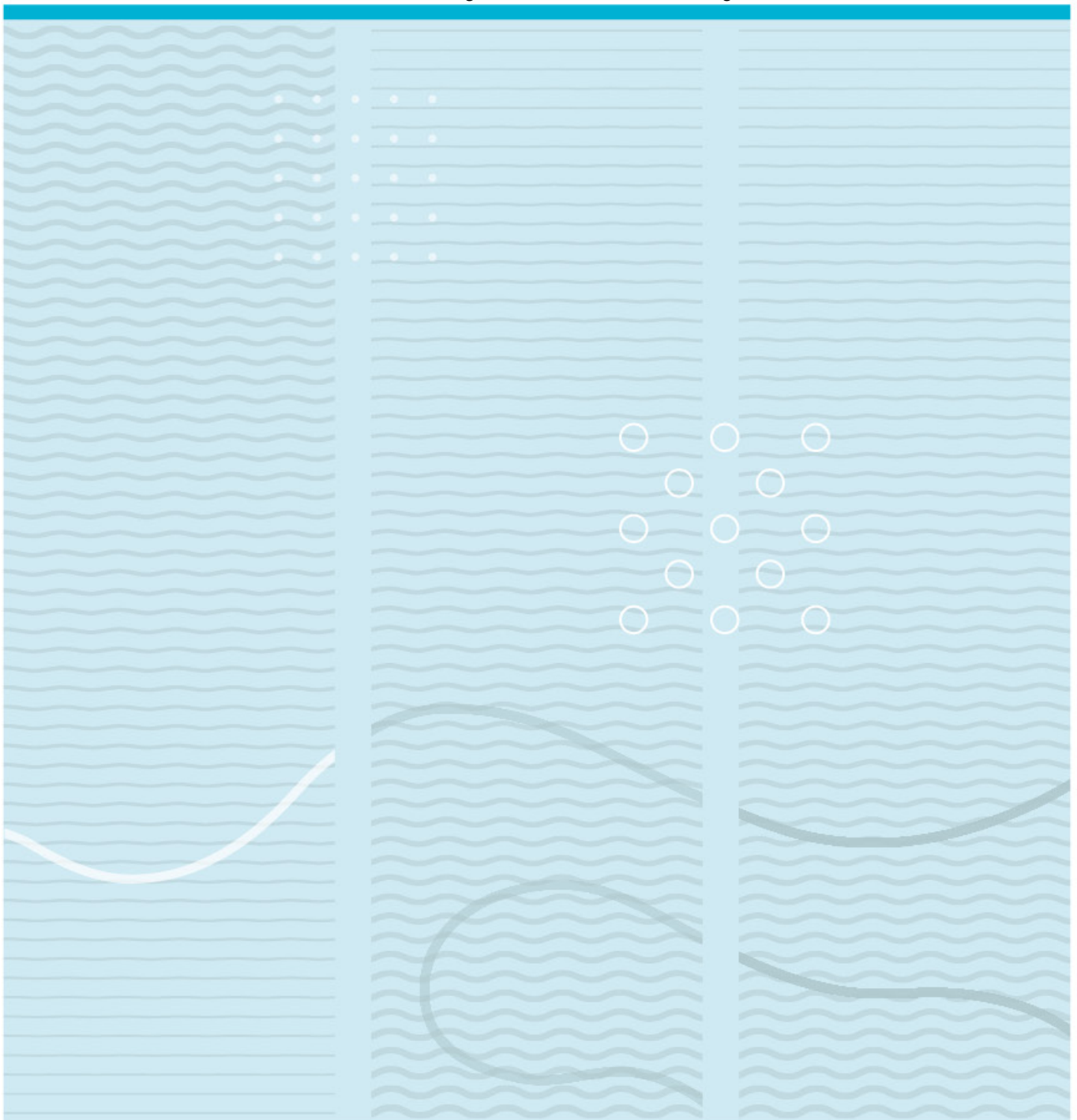


Anders Mæhlum Halvorsen

A Comparison Between Unmanned Aerial Vehicle (UAV) Corridors & Placements To Understand Their Effects on Traffic Safety & Efficiency



University of South-Eastern Norway
Faculty of Technology, Natural Sciences, and Maritime Sciences
Department of Science and Industry Systems
PO Box 235
NO-3603 Kongsberg, Norway

<http://www.usn.no>

© 2022 Anders Mæhlum Halvorsen

This thesis is worth 60 study points

Abstract

With the increasing interest and utilization of unmanned aircraft, also known as drones, current predictions and simulations of the future airspace have found that the existing approach toward drone operation is not sufficient to ensure traffic safety. To cope with the future demand, structuring the airspace has been found beneficial and necessary. Accordingly, various structuring concepts have been proposed, with various concepts suggesting the adaptation of drone corridors. Drone corridors are similar to roads and highways and provide rules of engagement to navigate and improve traffic safety. Understanding how different corridor types, rules, parameters, and placements affect the efficiency and safety of the traffic are all crucial areas of research to improve and influence the future structuring of the airspace. Therefore, in this thesis, we have explored different corridor types, rules, parameters, and placements to observe beneficial characteristics for traffic efficiency and safety. By conducting fast-time simulations with randomized traffic within the metropolitan area of Paris, we observed from our simulational results that structuring the airspace with the utilization of drone corridors significantly improved traffic safety compared to current high-density operations. Moreover, we observed that layering the corridor airspace into different layers is beneficial for the safety and efficiency of the traffic. We further discovered that by assigning similar drone specifications to the same layers, the efficiency of the traffic increased by allowing more optimal speeds and altitudes. We noticed that a lower separation distance of 20 meters amongst drones increased efficiency and safety. Similarly, we found that a higher base speed limit of 18 m/s increased traffic efficiency and safety. On the other hand, no significant efficiency or safety benefit was observed with the increase or decrease in look-ahead time. Finally, a significant contrast in the efficiency and safety of the traffic was observed for different corridor placements. It was observed that a more spread-out corridor placement with a higher number of junctions improved the safety and efficiency of the traffic.

Acknowledgments

I wish to express my gratitude towards my supervisors, Vimala Nunavath and Olaf Hallan Graven, at the University of South-Eastern Norway for both guidance and support throughout the entire duration of the thesis, providing constructive and valuable advice in our weekly meetings and through the development of the thesis.

Furthermore, I would like to express my sincere gratitude to Ole Henrik Dahle, and the people at Indra, for providing me with an exciting area of research and introducing me to the fun and exciting future vision of the integration of drones into both urban and rural airspace.

Finally, I would like to give my deepest gratitude to my family, particularly my parents, Tone Charlotte Mæhlum and Runar Halvorsen, my girlfriend, and my friends, for supporting and cheering for me to complete my thesis at times when things felt a bit hopeless.

P.S. And a special thank you to imposter syndrome for always being there for me.

Contents

| | | |
|----------|--|-----------|
| 1 | Introduction | 1 |
| 1.1 | Motivation and Problem Statement | 2 |
| 1.2 | Approach | 2 |
| 1.3 | Research Questions | 2 |
| 1.4 | Assumptions and Limitations | 3 |
| 1.4.1 | Assumptions | 3 |
| 1.4.2 | Limitations | 3 |
| 1.5 | Contributions | 4 |
| 1.6 | Thesis Outline | 4 |
| 2 | Background | 6 |
| 2.1 | Unmanned Aerial Vehicles (UAVs) | 6 |
| 2.2 | Rules of Conduct for UAV Operation | 9 |
| 2.3 | Unmanned Aircraft Systems Traffic Management (UTM) | 12 |
| 2.4 | UAV Corridors | 16 |
| 2.5 | Topologically Available Airspace | 17 |
| 3 | Literature Review | 20 |
| 3.1 | Proposed Corridor Frameworks | 20 |
| 3.2 | Corridor Simulations | 23 |
| 3.3 | Rules and Parameters simulations | 27 |
| 3.4 | Summary | 30 |
| 4 | Methodology | 32 |
| 4.1 | Experimental Area | 32 |
| 4.2 | Simulator | 34 |
| 4.3 | Conduction of the Simulations | 36 |
| 4.4 | Traffic Generation | 37 |
| 4.5 | Corridor Construction and Routing | 38 |
| 4.6 | Conflict Detection and Resolution (CD&R) | 41 |
| 4.7 | Key Performance Indicators (KPIs) | 42 |

| | | |
|----------|------------------------------------|-----------|
| 4.8 | Data Collection | 44 |
| 4.9 | Data Analysis | 48 |
| 4.10 | Statistical Significance Testing | 48 |
| 5 | Experiments | 50 |
| 5.1 | Corridor Types | 50 |
| 5.2 | Rules and Parameters | 52 |
| 5.2.1 | Separation Distances | 53 |
| 5.2.2 | Speed Limits | 53 |
| 5.2.3 | Look-Ahead Times | 54 |
| 5.3 | Corridor Placements | 54 |
| 5.4 | Unstructured Free-Flight | 56 |
| 6 | Results | 58 |
| 6.1 | Corridor Types | 58 |
| 6.2 | Rules and Parameters | 60 |
| 6.2.1 | Separation Distances | 61 |
| 6.2.2 | Speed Limits | 63 |
| 6.2.3 | Look-Ahead Times | 66 |
| 6.3 | Corridor Placements | 68 |
| 6.4 | Unstructured Free-Flight | 72 |
| 7 | Discussion | 75 |
| 7.1 | Introduction | 75 |
| 7.2 | Discussion of Results | 76 |
| 7.2.1 | Corridor Types | 76 |
| 7.2.2 | Rules and Parameters | 78 |
| 7.2.2.1 | Separation Distances | 78 |
| 7.2.2.2 | Speed Limits | 79 |
| 7.2.2.3 | Look-Ahead Times | 80 |
| 7.2.3 | Corridor Placements | 80 |
| 7.2.4 | Unstructured Free-Flight | 82 |
| 7.3 | Summary | 82 |
| 8 | Conclusions and Future Work | 84 |
| 8.1 | Conclusion | 84 |
| 8.2 | Future Work | 85 |
| | References | 86 |
| | Appendix | 94 |

| | | |
|----------|---|-----------|
| A | Simulational Parameters | 94 |
| A.1 | Corridor types simulation(s) specifications | 94 |
| B | Corridor Coordinates | 95 |
| B.1 | Park coordinates | 95 |
| B.2 | Roundabout coordinates | 96 |
| B.3 | Ring road coordinates | 97 |
| B.4 | River coordinates | 97 |
| C | Numerical Results | 98 |
| C.1 | Numeric corridor types results | 98 |
| C.2 | Numeric separation distances results | 100 |
| C.3 | Numeric speed limits results | 101 |
| C.4 | Numeric look-ahead times results | 102 |
| C.5 | Numeric corridor placements results | 103 |
| C.6 | Numeric unstructured free-flight results | 106 |

List of Figures

| | | |
|------|--|----|
| 2.1 | Multi-rotor UAV (DJI Matrice 100) [24] | 7 |
| 2.2 | Fixed-wing UAV (Delair DT26X LiDAR) [25] | 8 |
| 2.3 | Single-rotor UAV (PRODRONE) [26] | 8 |
| 2.4 | Hybrid UAV (Wings hybrid delivery UAV) [28] | 9 |
| 2.5 | Illustrational comparison between the various operational lines of sights [31] | 10 |
| 2.6 | Notional US-UTM architectural design [44] | 13 |
| 2.7 | US-UTM levels [45] | 14 |
| 2.8 | Generic architectural design of U-space ConOps [46] | 15 |
| 2.9 | The four phases of U-space [49] | 15 |
| 2.10 | Illustrative figure of geofencing (left) and geocaging (right) technology [57] | 17 |
| 2.11 | Possible no-fly zone depending on the combined awareness of buildings (a), wind (b), privacy (c), and noise (d), where the possible accumulated no-fly zone is created in (e) and (f) [55] | 18 |
| 4.1 | 153.94 km^2 simulation area in Paris seen from map- and simulation overview, with latitude/longitude origin coordinate (48.8590239723895, 2.3345907131722807) | 33 |
| 4.2 | An illustrative figure of the structural build of a weighted corridor network. The blue crosses inside the blue circles are the junction nodes. The green squares are the outer crossing nodes. The black arrows are the directional heading of the lane to the left of the directional heading. The purple line is the divider between the directional traffic direction. | 39 |
| 4.3 | The UAV flight protocol for the direct route | 40 |
| 4.4 | The eight step corridor flight protocol | 40 |
| 5.1 | Bi-directional corridor | 51 |
| 5.2 | Layered bi-directional corridor | 51 |
| 5.3 | Unstructured corridor layers | 52 |
| 5.4 | Structured corridor layers | 52 |
| 5.5 | A 3x3 corridor grid network above the metropolitan area of Paris | 55 |
| 5.6 | A 4x4 corridor grid network above the metropolitan area of Paris | 55 |
| 5.7 | A corridor network based of the locations of smaller and larger parks in the metropolitan area of Paris | 55 |

| | | |
|------|---|----|
| 5.8 | A corridor structure around the "Boulevard Périphérique" in the metropolitan area of Paris | 55 |
| 5.9 | A corridor structure above the "Seine" river in the metropolitan area of Paris | 56 |
| 5.10 | A corridor structure above a roundabout network in the metropolitan area of Paris | 56 |
| 5.11 | The UAV flight protocol for the unstructured free-flight simulations | 57 |
| 6.1 | A figure of the average number of conflicts for the different corridor types | 59 |
| 6.2 | A figure of the average number of LoS for the different corridor types | 59 |
| 6.3 | A figure of the average LoS duration for the different corridor types | 59 |
| 6.4 | A figure of the average LoS distance for the different corridor types | 59 |
| 6.5 | A figure of the average travel time for the different corridor types | 60 |
| 6.6 | A figure of the average route deviation for the different corridor types | 60 |
| 6.7 | A figure of the average number of near mid-air collisions for the different corridor types | 60 |
| 6.8 | A figure of the average number of conflicts for the bi-directional- and layered bi-directional (structured) corridor for the different separation distances | 61 |
| 6.9 | A figure of the average number of LoS for the bi-directional- and layered bi-directional (structured) corridor for the different separation distances | 61 |
| 6.10 | A figure of the average LoS duration for the bi-directional- and layered bi-directional (structured) corridor for the different separation distances | 62 |
| 6.11 | A figure of the average LoS distance for the bi-directional- and layered bi-directional (structured) corridor for the different separation distances | 62 |
| 6.12 | A figure of the average travel time for the bi-directional- and layered bi-directional (structured) corridor for the different separation distances | 63 |
| 6.13 | A figure of the average route deviation for the bi-directional- and layered bi-directional (structured) corridor for the different separation distances | 63 |
| 6.14 | A figure of the average number of near mid-air collisions for the different separation distances | 63 |
| 6.15 | A figure of the average number of conflicts for the bi-directional- and layered bi-directional (structured) corridor for the different speed limits | 64 |
| 6.16 | A figure of the average number of LoS for the bi-directional- and layered bi-directional (structured) corridor for the different speed limits | 64 |
| 6.17 | A figure of the average LoS duration for the bi-directional- and layered bi-directional (structured) corridor for the different speed limits | 65 |
| 6.18 | A figure of the average LoS distance for the bi-directional- and layered bi-directional (structured) corridor for the different speed limits | 65 |
| 6.19 | A figure of the average travel time for the bi-directional- and layered bi-directional (structured) corridor for the different speed limits | 65 |
| 6.20 | A figure of the average route deviation for the bi-directional- and layered bi-directional (structured) corridor for the different speed limits | 65 |
| 6.21 | A figure of the average number of near mid-air collisions for the bi-directional- and layered bi-directional (structured) corridor for the different speed limits | 66 |

| | | |
|------|---|----|
| 6.22 | A figure of the average number of conflicts for the bi-directional- and layered bi-directional (structured) corridor for the different look-ahead times | 67 |
| 6.23 | A figure of the average number of LoS for the bi-directional- and layered bi-directional (structured) corridor for the different look-ahead times | 67 |
| 6.24 | A figure of the average LoS duration for the bi-directional- and layered bi-directional (structured) corridor for the different look-ahead times | 67 |
| 6.25 | A figure of the average LoS distance for the bi-directional- and layered bi-directional (structured) corridor for the different look-ahead times | 67 |
| 6.26 | A figure of the average travel time for the bi-directional- and layered bi-directional (structured) corridor for the different look-ahead times | 68 |
| 6.27 | A figure of the average route deviation for the bi-directional- and layered bi-directional (structured) corridor for the different look-ahead times | 68 |
| 6.28 | A figure of the average number of near mid-air collisions for the bi-directional- and layered bi-directional (structured) corridor for the different look-ahead times | 68 |
| 6.29 | A figure of the average number of UAVs not utilising the corridor depending on the corridor placement | 69 |
| 6.30 | A figure of the average direct route deviation for the different corridor placements | 69 |
| 6.31 | A figure of the average number of conflicts for the different corridor placements | 70 |
| 6.32 | A figure of the average number of LoS for the different corridor placements | 70 |
| 6.33 | A figure of the average LoS duration for the different corridor placements | 70 |
| 6.34 | A figure of the average LoS distance for the different corridor placements | 70 |
| 6.35 | A figure of the average travel time for the different corridor placements | 71 |
| 6.36 | A figure of the average route deviation for the different corridor placements | 71 |
| 6.37 | A figure of the average number of near mid-air collisions for the different corridor placements | 72 |
| 6.38 | A figure of the average number of near mid-air collisions for the unstructured free-flight and layered bi-directional corridor (structured) | 73 |
| 6.39 | A figure of the average number of LoS for the unstructured free-flight and layered bi-directional corridor (structured) | 73 |
| 6.40 | A figure of the average LoS duration for the unstructured free-flight and layered bi-directional corridor (structured) | 73 |
| 6.41 | A figure of the average LoS distance for the unstructured free-flight and layered bi-directional corridor (structured) | 73 |
| 6.42 | A figure of the average travel time for the unstructured free-flight and layered bi-directional corridor (structured) | 74 |
| 6.43 | A figure of the average route deviation for the unstructured free-flight and layered bi-directional corridor (structured) | 74 |

List of Tables

| | | |
|------|---|-----|
| 2.1 | Legislation approaches for commercial UAV use by country [4] | 11 |
| 4.1 | Overview of some of the TrafScript commands [14] | 35 |
| 4.2 | UAV specifications | 38 |
| 4.3 | A list of the safety KPIs and a description of their values | 43 |
| 4.4 | A list of the efficiency KPIs and a description of their values | 44 |
| 4.5 | A list of the additional efficiency KPIs for the corridor placement simulations and a description of their values | 44 |
| 4.6 | UAV start log | 45 |
| 4.7 | LoS log | 46 |
| 4.8 | Conflict log | 47 |
| 4.9 | UAV end log | 47 |
| 4.10 | Data analysis output file with a description of the different stored values | 48 |
| 5.1 | A list of the different separation distances simulated for the bi-directional- and structured layered bi-directional corridor | 53 |
| 5.2 | A list of the different speed limits simulated for the bi-directional- and structured layered bi-directional corridor | 54 |
| 5.3 | A list of the different look-ahead times simulated for the bi-directional- and structured layered bi-directional corridor | 54 |
| A.1 | The simulation rules and parameters for the corridor type comparison experiment | 94 |
| B.1 | Park coordinates | 95 |
| B.2 | Roundabout coordinates | 96 |
| B.3 | Ring road coordinates | 97 |
| B.4 | River coordinates | 97 |
| C.1 | Numerical results for the bi-directional corridor | 98 |
| C.2 | Numerical results for the unstructured layered bi-directional corridor | 99 |
| C.3 | Numerical results for the structured layered bi-directional corridor | 99 |
| C.4 | Numerical results for the different separation distance for the bi-directional corridor | 100 |

| | | |
|------|---|-----|
| C.5 | Numerical results for the different separation distances for the structured layered bi-directional corridor | 100 |
| C.6 | Numerical results for the different speed limits for the bi-directional corridor | 101 |
| C.7 | Numerical results for the different speed limits for the structured layered bi-directional corridor | 101 |
| C.8 | Numerical results for the different look-ahead times for the bi-directional corridor | 102 |
| C.9 | Numerical results for the different look-ahead times for the structured layered bi-directional corridor | 102 |
| C.10 | Numerical results for the 3x3 grid network | 103 |
| C.11 | Numerical results for the 4x4 grid network | 103 |
| C.12 | Numerical results for the park network | 104 |
| C.13 | Numerical results for the ring road | 104 |
| C.14 | Numerical results for the river | 105 |
| C.15 | Numerical results for the roundabout network | 105 |
| C.16 | Numerical results for the unstructured free-flight | 106 |

Acronyms

AGL Above Ground Level

ATC Air Traffic Control

ATM Air Traffic Management

ASB Aircraft Safety Bounds

AGI Analytical Graphics, Inc.

BVLOS Beyond Visual Line of Sight

CAA Civil Aviation Authority

CSV Comma-Separated Values

ConOps Concept of Operation

CORUS Concept of operations for European UTM systems

CD&R Conflict Detection and Resolution

CD Conflict Detection

CR Conflict Resolution

DAA Detect and Avoid

DLR Deutsches Zentrum für Luft- und Raumfahrt

EC European Commission

EUROCONTROL European Organisation for the Safety of Air Navigation

EU European Union

EVLOS Extended Visual Line of Sight

GCAA General Civil Aviation Authority

GOS Global Offline Static

GPS Global Positioning System

| | |
|-----------------|---|
| GPD | Global Probabilistic Dynamic |
| GCS | Ground Control Station |
| GCS | Ground Control System |
| ID | Identifier |
| JAXA | Japan Aerospace Exploration Agency |
| KPI | Key Performance Indicator |
| LBSD | Lane Based Strategic Deconfliction |
| LPG | Local Pheromone Guided |
| LoS | Loss of Separation |
| MVP | Modified Voltage Potential |
| NTU | Nanyang Technological University |
| NASA | National Aeronautics and Space Administration |
| NLR | National Aerospace Laboratory of the Netherlands |
| NUARI | Northeast UAS Airspace Integration Research Alliance |
| ORCA | Optimal Reciprocal Collision Avoidance |
| RPS | Remote Pilot Station |
| SSD | Space Solution Diagram |
| STK | System Tool Kit |
| TCL | Technical Capability Level |
| SESAR JU | The Single European Sky ATM Research Joint Undertaking |
| TMX | The Traffic Manager |
| UASSP | UAS Service Provider |
| UNICEF | United Nations International Children's Emergency Fund |
| US-UTM | United State (US) - Unmanned Aircraft System Traffic Management (UTM) |
| US | United States |
| UAS | Unmanned Aerial System |
| UAV | Unmanned Aerial Vehicle |
| UTM | Unmanned Aircraft System Traffic Management |

U-space Urban Space

VO Velocity Obstacle

VTOL Vertical Take-Off and Landing

VLL Very Low-Level Airspace

VLOS Visual Line of Sight

FAA Federal Aviation Administration

Chapter 1

Introduction

Unmanned aircraft, also known as drones, have become an increasing area of interest in recent years. Due to a vast range of versatile designs and operational functionalities, they have been adopted both for recreational and commercial use, ranging from package delivery services [1] to military applications [2]. Depending on the country of operation, different rules and regulations apply, with most of the operations performed in unstructured free-flight [3] in countries where access to the airspace is permitted [4]. In unstructured free-flight, drones can be operated freely in allowed areas directly from origin to destination.

By the year 2050, according to The Single European Sky ATM Research Joint Undertaking (SESAR JU), there will be approximately 7,000,000 recreational drones operating throughout Europe, in addition to a further 400,000 drones expected to be operated by the government and commercial sector [5]. With the current operational body of unstructured free-flight, it has been found that unstructured free-flight is only feasible up until 10,000 flights per day within an area the size of the San Francisco Bay Area and that anywhere above the given range will need a more complex and mature management system [6]. As a consequence of future predictions and simulations, various structuring concepts of the airspace have been proposed, also called Unmanned Aircraft System Traffic Management (UTM).

As implied by the name, UTM aims to efficiently and safely manage future drone traffic in both urban and rural areas. Due to the complexities of the airspace, the vast range of different drone specifications, and the existing Air Traffic Management (ATM) for manned aviation, UTM is still under development, and a complete system is yet to be established and fully operable. To date, airspace structures within UTM remains an open research gap in the literature [7], with most of the drones operating in unstructured free-flight [3]. However, as part of various UTM concepts, drone corridors have been proposed to navigate and contain traffic. Drone corridors are similar to roads and highways and provide rules of engagement to navigate and improve traffic safety.

1.1 Motivation and Problem Statement

To date, a range of different corridor types have been proposed [8][9][10][11][12], ranging in complexity and airspace utilization, with different rules and parameters. However, existing research on corridors' effect on efficiency and traffic safety is limited, restricting the overall knowledge of their viability and impact on the traffic. Exploring and comparing different corridor types, rules, and parameters are crucial in observing and determining beneficial characteristics for traffic efficiency and safety for future development, adaptation, and optimization of corridors in the airspace. Moreover, both the urban and rural environments are complex, and different factors such as the operational safety, social acceptance, integration into the existing ATM, technological capabilities, and more will largely determine the allowed operational airspace in which drone operations will take place in the future [13]. Consequently, topological placements of corridors will likely be restricted and will need to confine to future rules and regulations. Currently, the knowledge of how different corridor placements might impact the efficiency and safety of traffic is limited. Exploring various corridor placements is necessary for observing characteristics of corridor placements that might be beneficial for future corridor placements and the determination to what extent different corridor placements impact the efficiency and safety of the traffic.

1.2 Approach

By adopting the BlueSky simulator [14] and creating an experimental area around the metropolitan area of Paris, randomized drone traffic was generated within the defined simulational area as part of a simple UTM system. Consequently, different corridor types, rules, parameters, and placements were simulated as part of the UTM system. Accordingly, by conducting fast-time simulations, we collected and analyzed the numerical results and compared the related results, ultimately aiding in filling the identified knowledge gap in the literature as discussed in section 1.1.

1.3 Research Questions

In this section, we present the research questions created at the beginning of the thesis, aiding in the exploration of the research area and the conduction of the simulational experiments.

1. *Do different corridor types effect the efficiency and safety of the traffic?*

Three different corridor types were simulated to answer this research question, ranging in airspace utilization and complexity.

2. *Do different corridor placements effect the efficiency and safety of the traffic?*

Six different corridor placements based on proposed and adopted corridor placements in the existing literature and the metropolitan structure of Paris were simulated, utilizing the same corridor type for all placements.

3. *How do changes to the traffic- or corridor rules effect the efficiency and safety of the traffic?*

To answer this question, we explored how different separation distances and corridor speed limits effect the efficiency and safety of the traffic for two of the corridor structures compared in this thesis.

4. *How do changes to the traffic- or corridor parameters effect the efficiency and safety of the traffic?*

To answer this question, we explored how different look-ahead times effect the efficiency and safety of the traffic for two of the corridor structures compared in this thesis.

1.4 Assumptions and Limitations

The assumptions and limitations section aids in clarifying any limitations or assumptions carried out throughout the thesis. In addition, this section helps the reader further understand some of the choices made in this thesis. Lastly, it also limits the overall scope and extent of the research to make it manageable to complete within the provided time frame.

1.4.1 Assumptions

1. In reality, the allowed airspace in which drones can operate is limited. These limitations could be due to buildings, such as the Eiffel tower, no-fly zones instantiated around airports, military zones, or altitude restraints. In this thesis, we assume that all airspace from 0m to 165m Above Ground Level (AGL) was available without limitations within the simulated area.
2. The traffic awareness was not limited by communication delay or data loss. Thus, perfect global knowledge of drone positions, speeds, altitudes, and headings was assumed.
3. While weather conditions, in reality, might effect the drones speed, heading, and altitude, the simulations were based on perfect weather conditions, without wind- or rain vectors.

1.4.2 Limitations

1. In reality, a vast amount of different drone types, with ranging technological capabilities and specifications would be utilizing the airspace. However, in the case of this thesis, four different drone specifications were used, representing four different tiers of drones.
2. The UTM system utilized only provided the drones with access to the airspace and corridor routes based on their origin and destination coordinate. A more complex and mature UTM system might have caused different results.
3. For each simulational scenario, five simulations were conducted. While additional simulations for each scenario would have been preferable, the number of simulations was limited due to time constraints.
4. For the corridor placement experiments, a single corridor type was used. However, different corridor types might have an impact on the results. Furthermore, for the corridor placements based on

geographical structures the corridor junctions were randomly selected, which might have impacted the results.

1.5 Contributions

The main contribution of the thesis are as follows:

- First, we contribute to the existing literature by comparing three different corridor types ranging in airspace utilization and structuring, comparing their efficiency and safety impact on the traffic, and identifying beneficial characteristics for the future implementation and development of corridor structures in UTM.
- Secondly, the thesis contributes to the literature by exploring how different rules and parameters effect the efficiency and safety of two of the corridor types explored in this thesis. Specifically, we explored separation distances, speed limits, and look-ahead times.
- Thirdly, this thesis contributes to the existing literature by exploring how different corridor placements might effect the safety and efficiency of the traffic, identifying beneficial characteristics for corridor placements based on the results.
- Lastly, this thesis contributes to the existing literature by comparing one of the corridor types simulated in this thesis to unstructured free-flight, evaluating the feasibility, efficiency, and safety of the two approaches towards the structuring of the airspace.

1.6 Thesis Outline

Chapter 2 presents an overview of the research area, providing sufficient insight and knowledge to understand the background of the thesis questions and the experiments conducted.

Chapter 3 presents the related research within the area of this thesis. Consequently, positioning the contributions of the thesis into the existing literature and providing a foundation for the structure of the conducted experiments.

Chapter 4 explains the methodological construct of the experiments conducted while discussing and reasoning the choices made.

Chapter 5 provides detailed explanations of the experiments conducted in this thesis, providing the simulational structures and relevant information.

Chapter 6 presents the results gathered from the experiments discussed in chapter 5, alongside their significance.

Chapter 7 discusses explanations of the results, their significance, and their placement in the existing literature. Furthermore, conclusions are drawn.

Chapter 8 concludes the thesis. Additionally, suggestions of both interesting and necessary future work are presented based on the experiences gathered throughout exploration and experimentation within the selected area of research.

Chapter 2

Background

This section starts with outlining the background theory by giving an overview of the concepts that act as the building blocks of the main contributions of this thesis.

2.1 Unmanned Aerial Vehicles (UAVs)

Unmanned Aerial Vehicles (UAVs) are aerial vehicles, controlled by a ground control operator, autonomously governing themselves, or both [15]. UAVs are often referred to as drones, although, unlike the term UAV, which defines itself as an aerial vehicle, drones is a generalized term for any remotely or autonomously controlled vehicle, such as boats, submarines, aircraft, or similar. However, the term UAV only refers to the aircraft itself and excludes the equipment and accessories which make it operational. As such, the term Unmanned Aerial System (UAS) was created, referring to the entire system, including the camera, software, Global Positioning System (GPS), control operator, and similar [16]. However, in this thesis, UAV is used to describe the aircraft itself including its onboard instruments, while UAS, is used to describe both the aircraft along with the control operator.

Combined with its low development cost and vast scope, UAVs rapid development has enabled new opportunities in the civil and non-civil sectors. Surveillance, photography, filming, delivery, and agriculture, are just some of the applications UAVs have been used for, with the scope expanding together with the rapid technological development. However, to date, UAVs still have significant shortcomings, such as battery life, sensor capability, environmental adaptation hurdles, and similar, limiting the UAVs use case [17].

Due to the various use-cases for UAVs, it comes in numerous specifications and features, varying in size, material, attachments, mission goals, and similar. As such, a vast amount of classifications have been proposed. However, due to the vast range of specifications and rapid development of UAV technology, it is challenging to create a suitable classification model appropriately classifying each UAV properly. However, UAVs can mainly be divided into four major UAV types, single-rotor, multi-rotor, fixed-wing, and hybrid [18][19][20][21].

Multi-rotor UAVs use rotors to achieve Vertical Take-Off and Landing (VTOL) and flying. Multi-rotor UAVs can be divided into six sub-groups, bi-copters (2 rotors), tri-copters (3 rotors), quadcopters (4 rotors), penta-copters (5 rotors), hexa-copters (6 rotors), and octo-copters (8 rotors). Due to the varying ranges of rotors, exceptional control over its positioning and framing can be achieved in low wind environments, which is why multi-rotor UAVs are often used for inspections, photography, and filming. However, due to its numerous rotors, stabilizing technology, and other on-board technology, it is significantly energy expensive, which is why most of the multi-rotor UAVs on the market only have around 10-20 minutes of in-air time capability. However, larger multi-rotor UAVs can carry more weight, but consequently, the battery life will be even shorter. Due to the characteristics of the multi-rotor UAVs and the need for quick changes in rotor speed to maintain in-air stability as-well-as achieving safe VTOL, it is currently relying on battery technology to achieve these fast and high-precision throttle changes, which is why it can not run solely on a gas engine due to the latency [18][19][20][22]. However, hybrid gas and electric multi-rotor UAVs have been successfully launched and tested, such as Skyfront's Perimeter 8 octocopter, with a record-breaking multi-rotor UAV flight time of 13 hours and 4 minutes in March 2021 [23]. An illustration of a multi-rotor UAV can be seen in figure 2.1.



Figure 2.1: Multi-rotor UAV (DJI Matrice 100) [24]

The fixed-wing UAV is comparable to a commercial airliner, as can be seen in figure 2.2, as it uses the wings to lift the UAV, unlike the multi-rotor UAV, thrusting down air with enough force to counterweight the gravitational force on the UAV. Because the fixed-wing use the wings to provide a lift, they can keep themselves in the air for a significantly longer duration than a typical multi-rotor UAV. As a consequence, they can be used for long distance travel and map larger areas. Moreover, due to its characteristics, unlike the multi-rotor UAV, the fixed-wing UAV can use gas as the primary source of power since it does not require as fast a reaction time and stabilization as the multi-rotor UAV. As a result, it is common for fixed-wing UAVs to stay in the air for around 16 hours. On the other hand, due to its fixed wings, and use of its wings for lift, it can not hover in the same position as the multi-rotor UAV. Moreover, as the fixed-wing is not capable of VTOL, a takeoff and landing strip is required, especially for the larger fixed-wing UAVs [18][19].



Figure 2.2: Fixed-wing UAV (Delair DT26X LiDAR) [25]

The single-rotor UAV shares some characteristics with multi-rotor UAVs, such as rotors, VTOL, and their ability to hover. On the other hand, it has some distinct characteristics. The single-rotor helicopter is equipped with a single main rotor in addition to a tail rotor to control its heading, unlike the multi-rotor UAV, which can have multiple main rotors and no tail rotor. It is a popular choice within manned aviation, however significantly less utilized as a UAV. The single-rotor UAV has significantly greater power efficiency and does not require rapid thrusting adjustments compared with the multi-rotor UAV. The blade size is also considerably larger and spins slower than the multi-rotor UAV, making it a more power-efficient UAV. Consequently, it can use a gas engine to achieve even longer endurance and carry heavier loads than the multi-rotor UAV. Due to its increased rotor size, the single-rotor UAV is also more dangerous to operate [18][19]. An illustration of a single-rotor UAV can be seen in figure 2.3.



Figure 2.3: Single-rotor UAV (PRODRONE) [26]

The fixed-wing hybrid combines the ability of hovering and VTOL, like the single- and multi-rotor UAV,

and utilizing lift, such as the fixed-wing UAV, as can be seen in figure 2.4. However, due to its complexity and difficulty to operate, it is not until the modern-day they have been found more practical due to the rapid technological development within the aviation industry. Moreover, due to the hybrid solution, hybrid UAVs expand the scope of services like food- and package-delivery, enabling further travel distances using airlift and allowing for VTOL and hovering for package loading and drop-off with the use of multi-rotor UAVs [18][19]. Corporations like Amazon [1] and Alphabet[27] are already well on their way into testing and adopting hybrid UAVs for package delivery.



Figure 2.4: Hybrid UAV (Wings hybrid delivery UAV) [28]

2.2 Rules of Conduct for UAV Operation

There are three different lines of sight operations of a UAV in the aviation industry. The first is called Visual Line of Sight (VLOS). To operate a UAV within VLOS means the UAS operator can see the UAV clearly without the assistance of any additional tools such as telescopes or binoculars. However, this does not include the use of prescription glasses[29][30].

The second operation of a UAV is within Extended Visual Line of Sight (EVLOS). When a UAV is operated within EVLOS, the flight is operated beyond the restrictions of VLOS. This can be achieved by using a trained observer to stay within VLOS of the UAV operated by the UAS operator. The trained observer will then collaborate with the UAS operator to fly the UAV safely and reasonably, avoiding any potential hazards in the airspace or surroundings. The UAS operator and the trained observer can communicate through technologies such as radio, cellular, or similar [29][30].

The final operation of a UAV is Beyond Visual Line of Sight (BVLOS). In BVLOS the UAV is not visible for

the UAS operator. Instead, the UAS operator controls the aircraft through Remote Pilot Station (RPS) / Ground Control System (GCS) instruments, enabling the UAV to travel further distances, this is in contrast to EVLOS, where flights rely on a second party. Since the UAS operator does not have direct sight of the UAV or a second party to navigate the flight, such as a trained observer, this type of operation requires careful planning and execution. Flights operated in BVLOS are controlled by data provided by the on-board instruments on the UAV. Consequently, a telemetry link transmits information to the UAS operator about the UAVs flight, such as speed, altitude, position, and other relevant parameters. As such, not all UAVs are capable of a BVLOS flight due to missing vital instruments [29][30]. A visual illustration of the differences between VLOS, EVLOS, and BVLOS can be seen in figure 2.5.

Several benefits are enabled with BVLOS flights. BVLOS allows UAVs to collect more data in fewer deployments due to the extended travel distance compared to VLOS and EVLOS. As such, they can replace long-range aerial data collection currently performed by satellites and manned aircraft, yielding economic gain and providing higher quality results due to the Above Ground Level (AGL) distance and travel speed. Lastly, BVLOS flights can be deployed instead of humans in places that may be of danger, such as inspections of power lines, providing a level of safety [29][30].

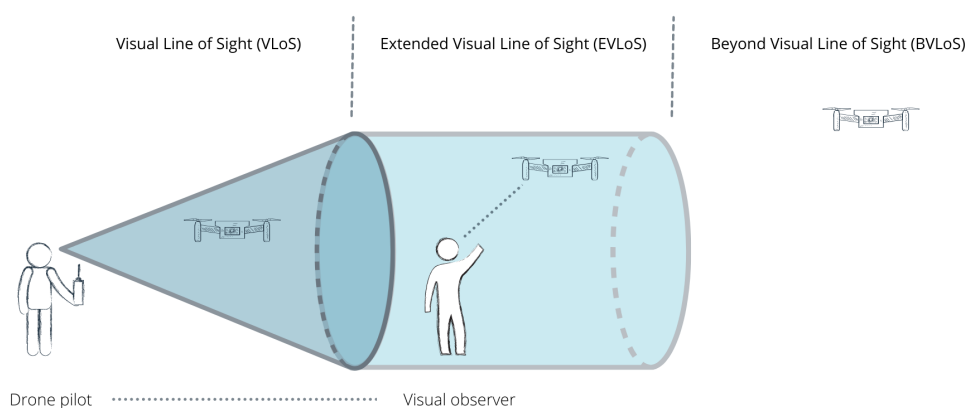


Figure 2.5: Illustrational comparison between the various operational lines of sights [31]

Depending on the country, different rules and regulations may apply when operating commercial or recreational UAVs in the airspace. Jones [4] from the RAND Corporation in Santa Monica, California, explored the existing international commercial UAS rules and regulations within different countries. She found that there are six broad approaches to national commercial UAS regulation.

The first approach is the "Outright ban", these countries do not allow UAVs for commercial use. The second one is "Wait-and-see", these countries have few rules and regulations in place and intend to monitor the other countries to see their regulatory effect. The third is "Effective ban", these countries have instantiated formal rules and processes, although they are almost impossible to meet. The fourth is "VLOS required", in these countries, the UAVs must be operated within VLOS, essentially limiting the commercial potential. The fifth is "Experimental BVLOS", these are countries where exceptions to the VLOS requirements are pos-

sible, although it comes with some restrictions. Finally, the last approach is "Permissive", these countries have instantiated relatively unrestricted legalization of commercial UAV use, providing general guidelines or requiring licensing, insurance, registration, and similar for the operation of the commercial UAV [4]. A list of the approaches, alongside the approaches used by different countries can be seen in table 2.1.

Table 2.1: Legislation approaches for commercial UAV use by country [4]

| Approach | Definition | Countries |
|--------------------|--|--|
| Outright ban | Countries do not allow drones at all for commercial use. | Argentina, Barbados, Cuba, India, Morocco, Saudi Arabia, Slovenia, Uzbekistan, United Arab Emirates |
| Effective ban | Countries have a formal process for commercial UAV licensing, but requirements are either impossible to meet or licenses do not appear to have been approved | Algeria, Belarus, Chile, Colombia, Egypt, Kenya, Nicaragua, Nigeria |
| VLOS required | UAVs must be operated with VLOS of the pilot, this limiting their potential range. | Belgium, Bermuda, Bhutan, Botswana, Croatia, Ecuador, Jamaica, Latvia, Lithuania, Luxembourg, Mexico, Nepal, Netherlands, Slovakia, South Africa, South Korea, Switzerland, Thailand |
| Experimental BVLOS | Exceptions to the constant VLOS requirement are possible with certain restrictions and pilot ratings. | Australia, Austria, Brazil, Canada, China, Czech, Republic, Denmark, Finland, France, Germany, Greece, Guyana, Ireland, Japan, New Zealand, Panama, Poland, Rwanda, Singapore, South Africa, Sri Lanka, Russia, Trinidad and Tobago, Uganda, United Kingdom, United States |
| Permissive | Countries have enacted relatively unrestricted legislation on commercial UAV use. These countries have a body of regulation that may give operational guidelines or require licensing, registration, and insurance, but upon following proper procedures it is straightforward to operate a commercial delivery UAV. | Costa Rica, Iceland, Italy, Norway, Sweden |

Initially, United Arab Emirates was placed as "Permissive" by the author. However, this has been changed as of 2022. At the end of January 2022, a UAS attack on the Abu Dhabi International Airport was conducted, killing three civilians. Consequently, the General Civil Aviation Authority (GCAA) reacted by banning all VLOS, EVLOS, and BVLOS operations, without special permission from the GCAA [32]. However, in Norway, according to the Civil Aviation Authority (CAA), a UAS can be operated within VLOS below 120m AGL within allowed operational areas without permission by the CAA. On the other hand, EVLOS and BVLOS can be conducted above or below 120m AGL with permission from the CAA [33].

2.3 Unmanned Aircraft Systems Traffic Management (UTM)

In an outlook study conducted by The Single European Sky ATM Research Joint Undertaking (SESAR JU), the authors observed that by the year 2050, there will be approximately 7,000,000 recreational UAVs and an additional 400,000 UAVs operated by the governmental and commercial sector throughout Europe. In total, the European UAV market will have a valuation of over EUR 15 billion annually [34]. Moreover, Busulu et al., explored the feasibility of unstructured free-flight, where all UAVs operated BVLOS at the same altitude, in an area the size of the San Francisco Bay Area. The authors simulated 100 to 1,000,000 flights per day with an average travel distance of 40km. The authors used the occurrences of large deconflictions, defined by the number of simultaneous UAVs within a distance of 50m from each other, to estimate the feasibility of the unstructured free-flight. The authors observed that unstructured free-flight is only feasible up to 10,000 flights per day within the restricted area, and that anywhere above the given range will need a more complex and mature management system to avoid drone collisions which might harm the environment, people, animals, or other valuable assets [6].

As can be drawn from the outlook study performed by the SESAR JU, both the interest and availability of UAVs are rapidly increasing. As such, if their estimates for the future airspace are close to their predictions and the current VLOS, EVLOS, and BVLOS operations continue as it currently is, an unsafe airspace can be recognized as observed by Busulu et al. in the paper [6]. Consequently, a more mature and complex management system is needed to regulate the expected future demand for UAVs in low-altitude airspace. Currently, an existing management system is used for manned aviation, called Air Traffic Management (ATM). The ATM aims to create a safe, efficient, and economical movement for various types of aircrafts. As such, services and facilities have been created providing ground-based and airborne functions [35]. However, due to its traditional reliance on voice communication through the Air Traffic Control (ATC), a centralized human-centric ATM can be recognized, limiting the scalability of its operation [36][37].

In 2014 the National Aeronautics and Space Administration (NASA), proposed the idea of a Unmanned Aircraft System Traffic Management (UTM) system for enabling safe and efficient low-altitude airspace operations for UAVs. The idea represented an initial step to start a discussion surrounding UTM and not a concrete solution. As such, NASA discussed that the system would be an extension of the currently implemented ATM system, taking inspiration from its operation and removing the centralized operation limiting its scalability. Since the proposition of the idea, various UTM concepts have been proposed, where two of the most well-known are US-UTM and Urban Space (U-space) [38].

In the United States (US), UTM is currently a collaborative research between the Federal Aviation Administration (FAA), NASA, and industry [39], with the first UTM Concept of Operation (ConOps) published in 2016 [40]. Moreover, in Europe, the European Commission (EC) inaugurated an initiative to assure UAVs secure and safe integration into European airspace. In 2007 the European Organisation for the Safety of Air Navigation (EUROCONTROL) and European Union (EU) founded the SESAR JU with the responsibility of

modernizing the European airspace [41]. As a consequence of the increasing need for the structuring of the future airspace, in 2017 the SESAR JU published a blueprint called U-space. The blueprint was an expansion of the UTM ConOps presented in the US in 2016, presenting their own vision for a possible UTM system [42].

In the US, the FAA created a ConOps for UTM in a collaborative research with NASA in 2016 [40]. Furthermore, two other ConOpses have been released, one in 2018 [43], and the other in 2020 [44]. The first version focused on the collaborative efforts among FAA, NASA, industry partners, government, and non-government organizations. On the other hand, the second version released in 2020 is an updated and expanded document of the previous document.

According to the FAA [44], the UTM system is a cooperative community-based traffic management system, in which the FAA establishes the rules of the roads. The system is based on multiple layers of information sharing from stakeholder to stakeholder to achieve its safe operation. The UAS operators will share their flight intent amongst each other in which it is used to de-conflict and create separate safe trajectories. An illustration of the architectural design for the US-UTM can be seen in the figure 2.6.

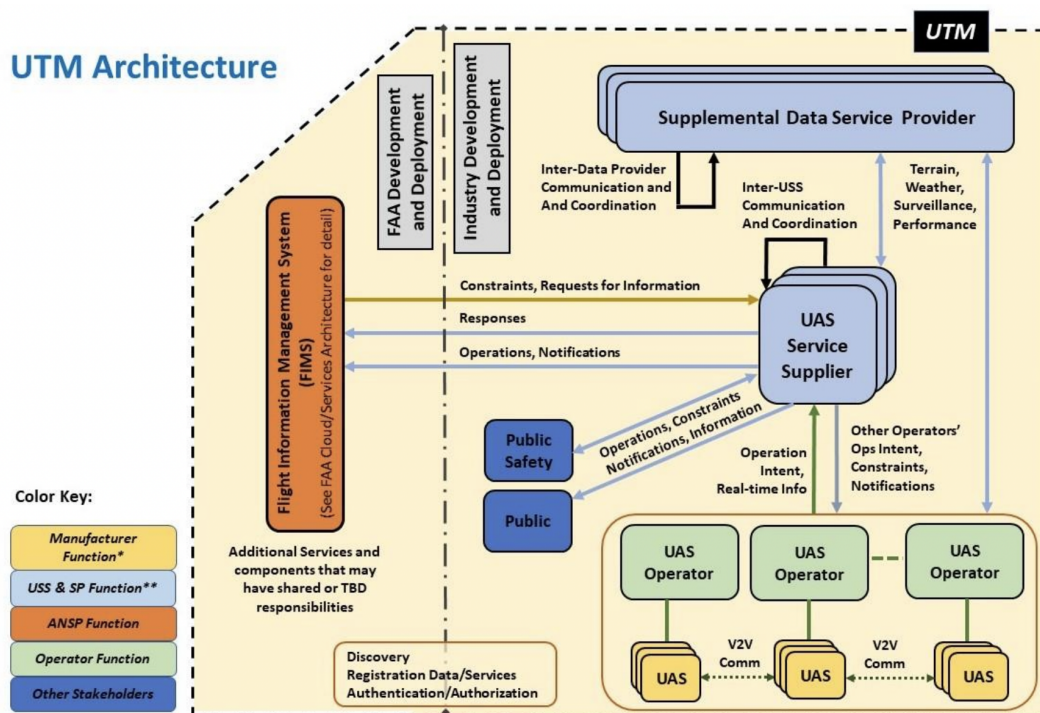


Figure 2.6: Notional US-UTM architectural design [44]

The UTM ConOps has four levels, also referred to as Technical Capability Level (TCL). Each of the levels has an increase in their complexity and different goals to help demonstrate the systems development and maturity. The TCLs are based on a growing complexity, such as population density, air traffic density, flight frequency, and similar. The four levels are TCL1, TCL2, TCL3, and TCL4. Each of them are designed based on an increase in risk. Starting from low air traffic, and low density, to a more complex operational environment, challenging the systems. An illustration of the various TCLs can be seen in figure 2.7

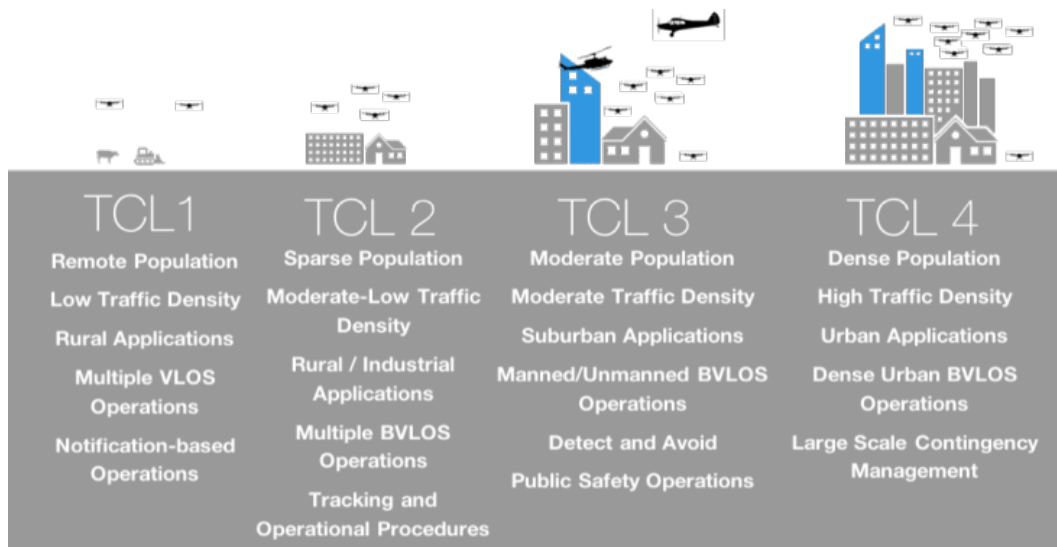


Figure 2.7: US-UTM levels [45]

In Europe, in 2017, the SESAR JU published a blueprint called U-space, expanding on the UTM concept presented in the US. In the blueprint, SESAR JU shares their future vision of the European airspace. According to SESAR JU, U-space aims to enable high complexity UAV operations with a great degree of automation. U-space will be a framework supporting growth and new business opportunities throughout Europe, while ensuring security, safety, and privacy. U-space will be a set of procedures and services designed for secure, efficient, and safe access to the airspace for a large volume of UAVs, with the intent of including allowing access to the airspace for everyone. Moreover, SESAR JU believes this should be achievable by implementing services that rely on high levels of digitization and automation, both on-board the UAVs and ground-based environments. The U-space is envisioned not simply to be its own system but an extension of ATM, providing a straightforward and efficient interface to manned aviation, making the shared airspace possible. Two years after the publication of the blueprint, in 2019, a ConOps for U-space was published. The ConOps was created, written, and published by a project called Concept of operations for European UTM systems (CORUS), a project funded by the SESAR JU, to create a ConOps for U-space [46][47]. An illustration of the architectural design for the U-space system can be seen in figure 2.8.

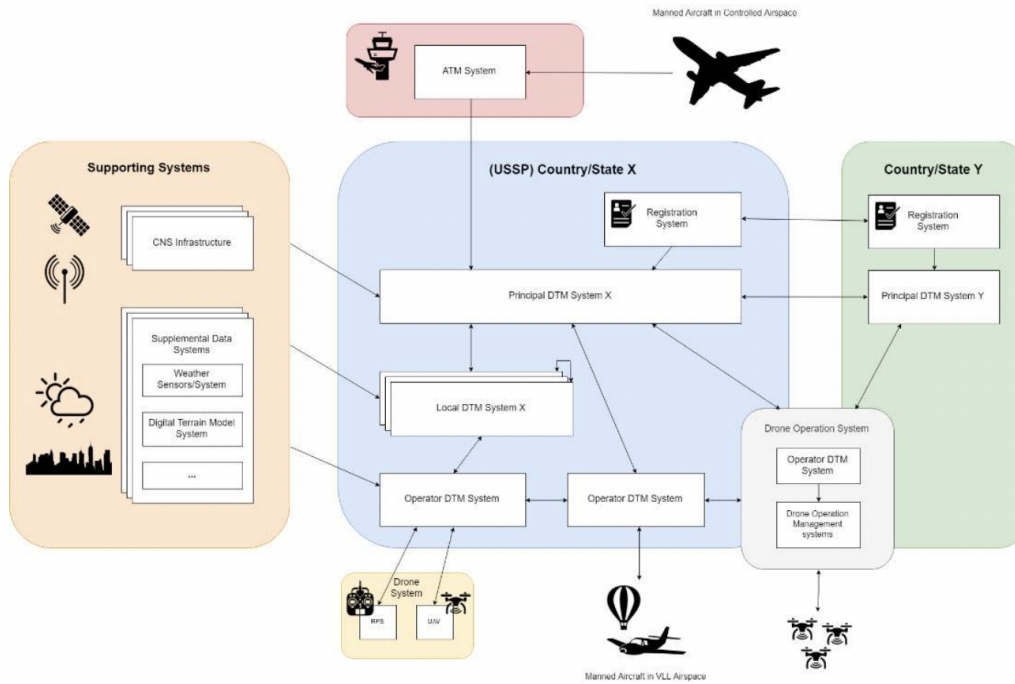


Figure 2.8: Generic architectural design of U-space ConOps [46]

Due to the unavailability of the necessary technologies to achieve the vision for U-space, similarly to US-UTM, a proposed increasingly iterative phase release structure was proposed in the initial blueprint released in 2017, as can be seen in the figure 2.9. The development is divided into four phases, starting on phase U1 and ending on phase U4. Each of the phases is complementary to one another and matures based on the previous phase, slowly implementing new improvements, service groups, safety, and technology. Overall, increasing the automation and connectivity with each phase, similarly to the US-UTMs TCLs [48].

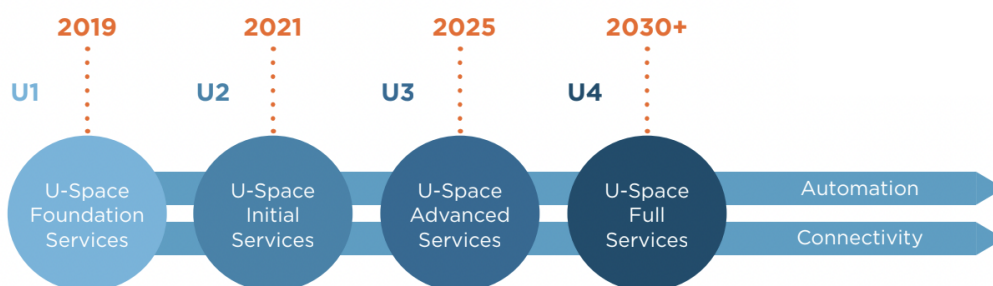


Figure 2.9: The four phases of U-space [49]

The first of the four phases is U1. The U1 level includes the provisioning of e-registration, e-identification, and geofencing. This phase allows UAS operation in low-density traffic locations with manned aircraft and updated on restricted zones where flights are permanently or temporarily forbidden. The second phase of the four is U2. This phase includes planning and approval, tracking, dynamic airspace information, and procedural interface with ATC. In essence, this phase provides safe operations for BVLOS flights. Furthermore, it establishes a general connection and interfaces to ATM, allowing for an even safer integration with

manned aviation. The third phase is U3, and this phase aims to allow for safe operations in dense areas. As such, this phase includes capacity management and assistance for conflict detection. Moreover, it will include the implementation of automatic DAA and better overall communication. The last phase is U4. This phase includes integrated interfaces with manned aviation and additional new services. Finally, the last phase aims to integrate fully with the currently existing ATM system, allowing for U-space vision of the future management system [48].

According to SESAR JU, the currently available U1 and U2 projects demonstrate that the services are ready in low density and low traffic environments. However, SESAR JU also recognized that the services need to be further validated and developed to support the expected density and complexity for future environments. Moreover, U2, U3, and U4 services need further research, with some services being recognized as more important than others, including monitor services, conflict management, and emergency management. These services are especially critical for ensuring scalable and robust operations in U2 to achieve a sufficient transition into U3 and U4 [50].

2.4 UAV Corridors

Dedicated UAV corridors have been proposed as parts of various UTM ConOps such as [10][9]. The word *corridor* is a loosely defined word by definition, and based on the literature, there seem to be different interpretations of the word, and its concept [51][13][52][9]. However, in this thesis, a corridor is a three dimensional road structure in the airspace with different rules of engagement. A corridor can be a simple one way road structure, or a more complex multi-layered highway structure [8][10]. Furthermore, a corridor can be static or dynamic, dependent on the corridor type [8]. A static corridor is a corridor that does not adapt to its environment and is well defined, making flight durations, flight planning, and protocols relatively simple. On the other hand, a dynamic corridor is an adaptable corridor where the route might change or be shut down in the case of temporary no-fly zones. No-fly zones are temporary areas where traffic is forbidden due to local accidents, weather conditions, or similar [8].

To date, various UAV corridors have been created worldwide for testing purposes. In 2016, New York invested 30 million dollars into developing an 80 km flight traffic management system between Syracuse and Griffiss International Airport in Rome. Over the past five years, New York has invested a total of 70 million dollars into the corridor. At the end of 2021, it was announced that the corridor would be provided with 5G network technology with the help of Northeast UAS Airspace Integration Research Alliance (NUARI) [53]. Moreover, in Africa, the first drone corridor was established in a combined effort with United Nations International Children's Emergency Fund (UNICEF), and the Government of Malawi in June 2017. The corridor is placed in Malawi and extends over 5000 km^2 . The corridor aims to provide a platform for universities, the private sector, and other third parties to explore how UAVs can assist various needs, such as medical delivery [54].

In recent years, emerging technologies such as geofencing and geocaging has become an important topic within the area of UTM to enable safety and separation between static and dynamic objects such as buildings, restricted areas, and no-fly zones. While technologies such as geofencing, focuses on the restriction of UAVs to access or bypass restricted areas, geocaging is used to contain UAVs within a certain bound of airspace, and can be used for dedicated UAV corridors [55] or to safely cage a UAV to avoid collisions [56]. An illustrative figure of the two technologies can be seen in figure 2.10.

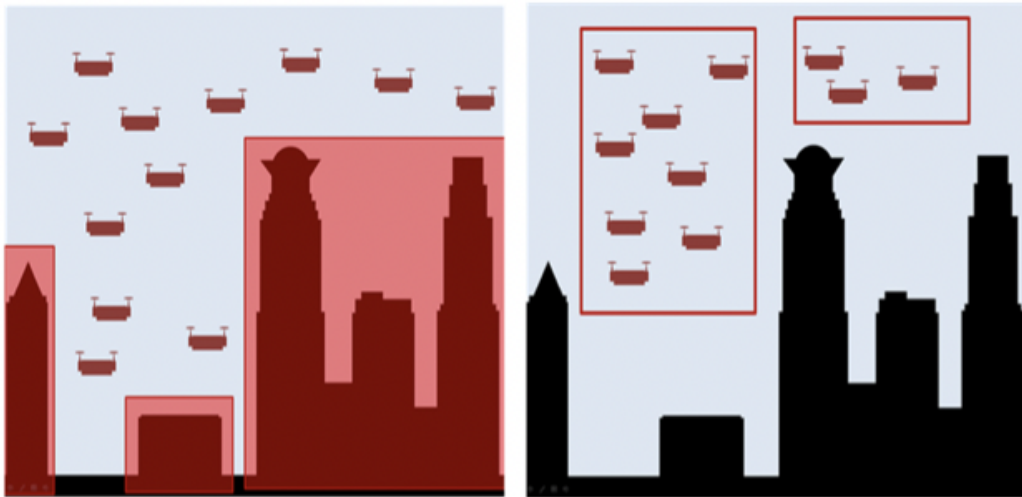


Figure 2.10: Illustrative figure of geofencing (left) and geocaging (right) technology [57]

2.5 Topologically Available Airspace

With the increasing number of UAVs and the emergence of new ways to utilize them, larger-scale operations are expected to operate in urban and rural areas. However, the integration of UAV operations into the existing airspace is challenging due to the complex nature of the existing structural properties of urban and rural design [58]. According to [55], there are three main factors which will determine the available urban and rural airspace in the future, the safety, the social acceptance, and the operational body.

For the safety factor, UAVs will operate in the airspace below 150m AGL, also referred to as Very Low-Level Airspace (VLL), and are expected to keep a safe distance between themselves and static and dynamic objects, such as buildings, poles, power lines, birds, and similar. The safe separation needs to be assured due to the implications that could occur in a collision, where animals, humans, or property might be damaged. As such, UAVs need to be provided with adequate operational areas where separation can be assured. However, weather conditions such as rain and wind can significantly effect UAVs route deviation. As such, the separation distances between static and dynamic objects will also need to take into account the weather impact on the route deviations of the UAVs [55].

The second factor is social acceptance. Like manned aviation and ground traffic, UAV traffic creates noise while operating. In recent research, it has been found that the annoyance levels of UAV traffic are significant

and were found to be annoying. However, in the same research, it was observed that by integrating the traffic noise into the existing highway traffic noise, a reduction in the observed annoyance level was reduced [59]. Moreover, with the future implementation of high-density UAV traffic in VLL airspace, privacy has become a relevant topic. UAVs are often equipped with cameras and other highly technical components, which can collect data on people, businesses, and similar. As such, the social acceptance of the corridor placements and the operational altitude might vary. Based on these observations, UAV operations have been proposed to be conducted over existing structures such as roads, highways, or even above water to mitigate these concerns [55]. In figure 2.11, an illustration of how different factors, such as buildings, weather conditions, privacy, and noise, might collaboratively restrict the available airspace is presented.

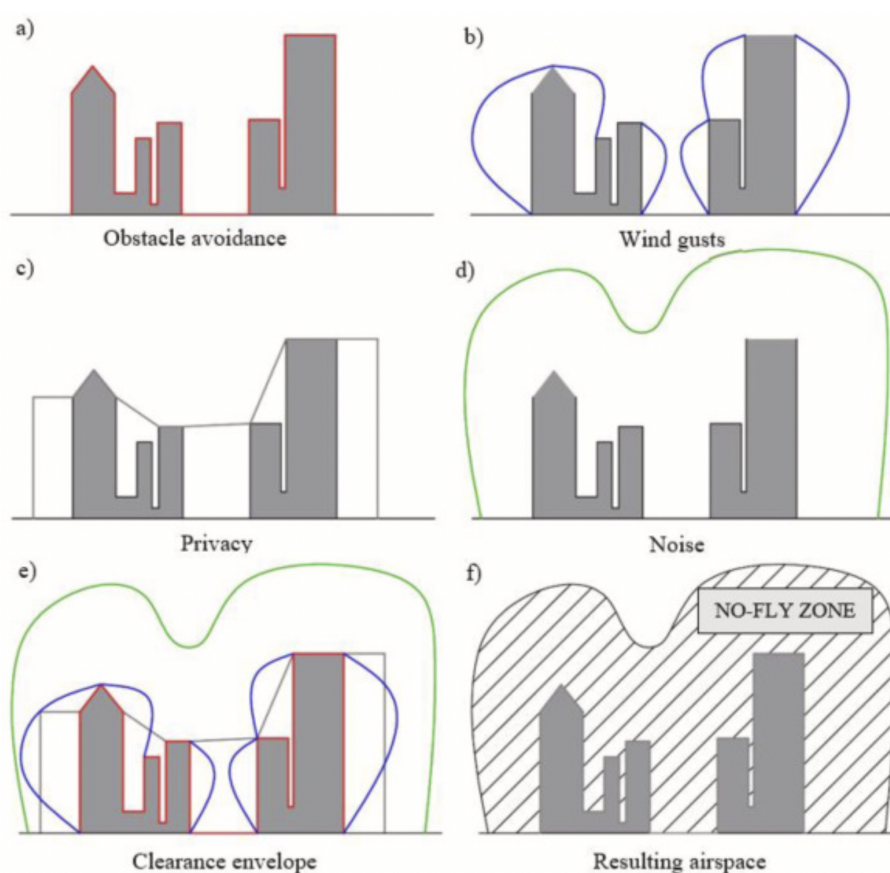


Figure 2.11: Possible no-fly zone depending on the combined awareness of buildings (a), wind (b), privacy (c), and noise (d), where the possible accumulated no-fly zone is created in (e) and (f) [55]

The last factor is the operational body. The integration of the UTM system into the current ATM will further largely effect how much of the airspace will be available for UAV operations. In the paper [60], an analysis of four different integration levels of UTM in ATM was explored. The available airspace was calculated for the different integration levels in San Francisco. The authors observed that if UTM is dynamically integrated into the ATM, UAV operations can operate with a great degree of freedom. However, the available airspace largely decreases with the lower levels of integration. Moreover, U-space 2.8, and other UTM concepts, have proposed a future vision of the airspace where a range of different UAVs will be utilizing the airspace. Consequently, UAVs with different capabilities and specifications will share the same airspace. As such, the airspace will consist of fixed-wing UAVs, multi-rotor UAVs, high-end UAVs, low-end UAVs, and

everything between, with various ranges of operational missions. Consequently, as can be recognized, the airspace will need to be adapted to the complex future environment. Furthermore, due to the reliance on batteries for most UAVs, they will need to get from their origin to their destination as quickly as possible in order to preserve battery life, further limiting the possible construction of the airspace [55].

Chapter 3

Literature Review

Due to the increasing, interest and relevance of Unmanned Aircraft System Traffic Management (UTM), significant research has been conducted within the area to achieve the implementation of UTM in the airspace. This chapter presents the related literature within corridor research related to the aim of this thesis.

3.1 Proposed Corridor Frameworks

In the following section, we present previous research that has been carried out by other researchers on the proposal of different corridor types and frameworks.

Jang et al. [13] proposed three different corridor structures, sky-lanes, sky-tubes, and sky-corridors, all ranging in different degrees of freedom. The sky-lanes concept is similar to the global highway system, where vehicles travel in lanes in either direction and are responsible for maintaining separation distance from the vehicle in front. Depending on the situation, the sky-lane can have multiple layers and lanes in either direction. The authors proposed three different sky-lane concepts depending on their intersection design. In the first sky-lane structure, the intersection of each layer is intertwined, like a typical highway with a traffic light solution. In the second concept, north and south directional traffic are in different layers from east and west traffic. Consequently, there is no traffic light solution at intersections. Furthermore, at intersections on the right side of the highway direction, Unmanned Aerial Vehicle (UAV)s can change to an upper layer and vice versa. However, while a traffic light solution is not established for the intersections, a traffic light solution is created for the UAVs changing layers. In the third sky-lane concept, the UAVs can travel up and down a layer in the right and left lanes, with no traffic light solution for UAVs changing layers, overall creating a more self-managed system. The second corridor concept proposed by the authors was the sky-tubes concept. The sky-tubes concept is similar to the first sky-lane concept. However, there are no lanes. Consequently, traffic is significantly more self-organized and less structured. The authors proposed two concepts for the sky-tubes concept. The first concept uses a traffic light solution for the intersections, while the second concept utilizes time windows. The third and last proposed concept by the authors is the

sky-corridor. In the sky-corridor, UAVs can move freely in any direction, as long as safety is ensured.

Cristian Martín Calvo [9], The Single European Sky ATM Research Joint Undertaking (SESAR JU) proposed a corridor concept where only pre-flight Conflict Detection and Resolution (CD&R)¹ is offered. The author proposed a bi-directional corridor structure with a height and width of 20m. In the corridor structure, the traffic is divided in the middle of the structure. To ensure on-going traffic does not collide, in the case of more significant route deviation, the directional traffic is divided into two different layers, 100m to 110m and 110m to 120m. Inside the corridor structure, the authors proposed a speed limit of 11 m/s with a separation distance of 60m. To access the corridor, Unmanned Aerial System (UAS) operators request access, and the UTM system provides the UAV with a route and access time frame². If the UAV misses the access time frame to the corridor, the UAV will need to hover by the corridor structure until safety can be assured. Although, if the UAV utilizes onboard CD&R³ technology, access can be granted, enabling a level of self-separation.

An Binh Nguyen [8] proposed three different corridor types in his research. Based on the existing literature and requirements for the future airspace, three corridor types, specific-, parallel-, and switching corridors were proposed. The specific corridor is a static mono-directional corridor. The corridor allows only a single UAV to utilize the corridor at a time. Other UAVs attempting to access the corridor are queued until the UAV has reached the end. The corridor is 500m in width so that fixed-wing UAVs have room to turn in the corridor. The parallel corridor is a static bi-directional corridor, allowing for travel in both directions through the appropriate directional lane, and, unlike the specific corridor, as many UAVs as theoretically possible can utilize it simultaneously. Moreover, like the specific corridor, the lane width is 500m, with a 100m separation distance between the UAVs within the corridor. Furthermore, the parallel corridor allows for additional lanes in either direction, depending on the traffic density of its placement. Unlike both of the other corridor types, the switching corridor is a dynamic corridor that allows for both different corridor layers and corridor lanes while also adapting to established no-fly zones or local or global weather impacts. This means that the route distance might be difficult to calculate due to the dynamic approach. The lowest layer(s) in the corridor is for less-equipped or lower-end UAVs, while the higher layers are dedicated to faster UAVs, allowing for more optimal travel altitudes and speeds. Consequently, the slower and lower-end UAVs do not bottleneck higher-end UAVs by having the extra layers.

Balakrishnan et al.[10] proposed a corridor framework based on future traffic demand. The authors proposed that each corridor have a centralized control service controlling the flow and coordination within the corridor. Furthermore, the authors proposed that there might be different UAV requirements based on the corridor placement. For instance, greater technological capabilities should be required for corridors in

¹Pre-flight CD&R is the process where the UTM system analyses the airspace and checks the flight plans of the UAV against other flights to ensure that the separation distance, which can vary depending on multiple factors, are upheld throughout the flight.

²Access time frame is the timestamp the UAV will reach the corridor

³Onboard CD&R, can be utilized for UAVs to share flight information amongst each other in order to keep the provided separation distance between traffic. Conflict is defined as when two or more UAVs are not able to keep their separation distance in the future. Consequently, Conflict Detection (CD) is the process of detecting future conflicts, and Conflict Resolution (CR) is the process of maneuvering in order to avoid a loss in separation.

urban areas due to the more complex nature of an urban environment compared to a rural environment. Consequently, UAVs must be granted approval by the corridor's centralized control service to enter the corridor, depending on its specifications. Furthermore, the authors suggest that specific corridors should be established for lesser capable UAVs to allow their integration into the airspace. Moreover, the authors argued that the general structuring and design of the corridor structure could take on many shapes, as long as safety is ensured for the traffic utilizing the corridor structures. As such, corridor shapes, such as connected tubes, cones, and cylinders, are all viable corridor designs. The authors further addressed that the corridors should be integrated cooperatively with the existing Air Traffic Management (ATM) system to ensure safety. Consequently, the corridor access and traffic were proposed to dynamically adapt to the response of ATM operations.

Deutschen Zentrum für Luft- und Raumfahrt (DLR) [61] proposed a concept for a density-based management system for Urban Space (U-space), with the intent of enabling any UAV into the airspace. DLR proposed segmented airspace, where the airspace is divided into three dimensional grids, dynamically controlled based on current and expected traffic, weather conditions, or other parameters. Each segment is limited to a certain number of UAVs and can be closed if needed. Furthermore, due to the vast range of UAV specifications and capabilities, the authors proposed that Aircraft Safety Bounds (ASB)⁴ are provided to each UAV operating within the airspace. The better the performance and technological equipment on the UAV, the smaller the ASB size, and vice versa. However, the specification of the ASB may change over time due to surrounding conditions such as high winds or internal parameters like changing battery conditions during flight. Moreover, each flight mission is evaluated based on the characteristics of the segments within its calculated path. In the case of a mission request, it is either accepted or rescheduled based on the expected and current traffic density, weather conditions, or if any of the route segments are locked. Moreover, to calculate the number of UAVs within each segment, a centralized system provides four dimensional trajectory information⁵ from each UAV within any given segment. According to the authors, by having a system as described, all types of UAVs in the future could utilize the airspace, allowing for significant freedom at lower densities, although lesser freedom at higher densities. However, segments may be quickly filled if there are multiple low-performance UAVs in the same segment, as these types of UAVs would require a large ASB size to ensure safety.

Tony et al. [12] proposed an on-demand multi-lane corridor called CORRIDRONE, which according to the authors, can fit into any existing UTM concept. The proposed corridor consists of three geocaging levels. The first is the main corridor, composed of all sub-levels of the corridor. The second level is the lanes within the corridor, and the last level is around the UAVs operating in the lanes. Moreover, the authors suggest that the corridor's construction can be created based on a set of vertiports⁶ provided to the Ground Control System (GCS) and geographical locations. The GCS is also responsible for monitoring the UAVs within the system and provides action plans for deviations, critical errors, or dynamic no-fly zones. However, while a

⁴ASB can be recognized as geocaging technology around the body of the UAVs.

⁵Four dimensional trajectory defines where, and when, a UAV will be in the airspace at any time.

⁶A vertiport, similar to helicopter pads, are dedicated Vertical Take-Off and Landing (VTOL) points for the UAVs.

GCS exists for the control of the corridor, UAVs are reliant on ad-hoc communication⁷ amongst each other to ensure a level of safety. Moreover, similar to the DLR concept [61], capability levels were proposed to be used as a means of defining the geocage size around the bodies of the UAVs, while also limiting the allowed mission extents. Consequently, lesser capable UAVs would be required to have larger geocages to ensure a level of safety, while higher capable UAVs, with greater technological capabilities, could have smaller geocages around their bodies. Furthermore, the size of the geocage will further depend on the speed of the UAV. As such, faster-moving UAVs will have larger geocages, while slower-moving UAVs will have smaller geocages. According to the authors, a testbed is currently formed on the Indian Institute of Science campus to research and develop this concept.

EmbraerX [52] proposed a corridor concept as part of their future UTM vision for urban operation. The authors defined corridors as a structure with a pre-defined height and width that could operate multiple UAVs simultaneously, separated horizontally, vertically, or both, comparing the structure to highways. The authors proposed that the corridor structure will have dedicated entrance- and exit points to make the behavior predictable for outward traffic and ATM operation. Moreover, the authors proposed that access to more complex corridors should be restricted to UAVs with appropriate certificates and specifications to ensure safety. The authors further proposed that access to the corridors would be granted by the UTM system before departure, ensuring available airspace for the UAV and access to the corridor. Furthermore, the authors proposed that the placement and availability of the corridor should be dynamically adaptable based on weather conditions, regulations, and similar.

3.2 Corridor Simulations

In the following section, we present the previous research that has been carried out by other researchers on the comparison of different corridor types, and general corridor simulations.

Bulusu et al. [6] simulated the feasibility of unstructured free-flight in the San Francisco Bay Area (100,000 km^2). The authors simulated the simplest form of unstructured free-flight, where all UAVs were operating at the same altitude with uniform speeds evenly distributed across twelve hours, with an average travel distance of 40 km. To compare its viability, as per the aim of the paper, different traffic densities were simulated. The authors simulated traffic densities ranging from 100 to 100,000 UAVs. To observe the viability, the authors used the metric of the number of concurrent UAVs within a provided distance of each other, ranging from 50m to 300m. The authors found that unstructured free-flight is feasible for up to 10,000 flights per day within the restricted area. Moreover, in the same paper [6] the authors simulated a simple corridor grid network with the same simulational parameters and the same viability metric. The corridor grid network was a simple single-layer structure, where UAVs would fly through without any structuring within. As such, the authors did not log any data once the UAVs accessed the corridor structure. The authors observed that the complexity of the traffic was reduced around ten times compared to the un-

⁷Ad-hoc communication is technology based on information sharing amongst the UAVs, which can be used in combination with CD&R to ensure safe separation distances.

structured free-flight, overall drastically improving the safety of the traffic.

Sinul et al. [62][63] simulated four different airspace concepts, full-mix, layers, zones, and tubes (corridors), and compared their efficiency and safety impact on the traffic. In the conduction of the experiments, the authors created a virtual environment in a simulator called The Traffic Manager (TMX), developed by the National Aerospace Laboratory of the Netherlands (NLR). The full-mix concept is similar to the unstructured free-flight simulated in the research [6]. However, in this paper, the UAVs operated at their optimal speed and altitude. Moreover, the airspace was divided into layers in the layers concept, where each layer limited horizontal travel. On the other hand, the zones concept was structured like ring roads around the city, with different directional headings. Inwards and outwards radials were used for the UAVs to change ring roads and directional heading. Lastly, the tube concept was a bi-directional pre-planned conflict-free corridor based on a twelve layered grid network, with fewer nodes for each increasing layer. In the simulator, a $5,476 \text{ km}^2$ area was used for the simulation with four different traffic demand scenarios varying from low to ultra, 4,005 UAVs and 7455 UAVs, respectively, on average per hour. The UAVs were generated from delivery centers with a destination randomly generated within an 11 km range. Additionally, 1,600 runways were created for larger UAVs, spaced evenly throughout the area, where half of these were marked as Vertical Take-Off and Landing (VTOL) capable. Furthermore, randomized vector wind was added in combination with rouge UAVs. The rouge UAVs were introduced at random time intervals and were proportioned to be seven times larger than the other UAVs, flying in random directions and altitudes. The authors observed that extreme density was viable and could be achieved by spreading out traffic in conjunction with a flexible structure. Furthermore, the authors observed that the utilization of corridors with pre-defined conflict-free routes limited the traffic efficiency and overall reduced the performance.

Doole et al. [64] simulated a UAV delivery operation above Manhattan, New York City, comparing a mono-directional- and bi-directional corridor structure. To conduct the experiments, the authors adopted the BlueSky simulator, creating a simulation environment of 59.1 km^2 , where the corridor structures were positioned above the streets of Manhattan, overall forming a grid network. The grid network was divided into layers varying from 23m to 320m, with each layer having different heading ranges the UAVs were allowed to travel. Consequently, to change the heading, a layer change was required. Moreover, speed changes were conducted to resolve conflicts, slowing down their speed in case of a possible Loss of Separation (LoS) instance. The traffic was directly generated into the corridor structure, where a total of 60 randomized simulations involving a total of 200,000 UAVs were conducted. The authors found that the mono-directional corridor performed better than the bi-directional corridor based on throughput, safety, stability, and amount of turns needed to reach their destination. In addition, the simulation results showed that the mono-directional corridor had fewer overall conflicts and LoS and was additionally beneficial for safety in an urban environment.

Jang et al. [13] compared two different corridor types using numerical simulations. The authors created an experimental intersection design to compare the two corridor types, where the corridor lengths from

north to south and east to west were 500m long. For both corridor types, two lanes in both directions were created and duplicated in four layers to simulate a simplified layered corridor. The first corridor type compared in the paper was a highway structure with a traffic light system at the intersection. Four different traffic light frequencies were simulated for this corridor ranging from 10s to 40s with an increase of 10s. The second corridor type compared was a highway-like structure. However, the north-to-south lanes were in a different layer than the east-to-west traffic. Consequently, the corridor height was double that of the first corridor type. Moreover, the corridor type did not utilize a traffic light system but rather a more dynamic approach toward merging traffic, not requiring any stops. Moreover, both corridor types had a ramp on the up-most right lane in either direction 90m before the intersection. In both corridor types, the speed limit was 20 m/s, with a slower speed limit of 18 m/s on the ramp. In each simulation, 20 UAVs were simulated. The authors observed that the more dynamic intersection design of the second corridor type was more beneficial in terms of throughput of UAVs per second and minute compared to the first corridor type, regardless of the different traffic light frequencies of the first corridor type.

Oosedo et al. [65] examined a UTM delivery operation based on estimated parcel delivery numbers in the year 2030. A simulated environment was created in the SKALE simulator, developed by Japan Aerospace Exploration Agency (JAXA), in an area 6 km north-south and 10 km east-west in Sendai, Miyagi Prefecture, Japan. Two delivery point models were created. The first delivery model was based on the area's current ground vehicle delivery points, while the other was created based on school districts in the area. Two on-demand⁸ corridor frameworks for corridor protection were simulated. The first concept protected the entire corridor, including its VTOL zones, while the other concept only protected the horizontal corridor, meaning that two on-demand corridors could be interconnected. In addition, the simulation contained no-fly zones covering areas protected by local laws. Furthermore, wind gusts were implemented to add further realism to the simulated environment. Based on their research and predictions of the future delivery operations in the area, 32,887 daily flights were simulated. The delivery of packages was simulated from the vertiport locations to random locations within its operational delivery radius, based on the delivery radius of the first model's existing ground vehicle delivery point and based on the school district radius for the second model. Once a delivery had been generated, a on-demand corridor was created between the two points, and the UAV delivered the package and traveled back in the same corridor. The authors observed that the configuration with the highest delivery efficiency was the second model with the second corridor protection. However, due to the limited number of vertiports and required waiting times for new on-demand corridors to be generated, only 50.1% of the packages were delivered. Consequently, it was observed that this type of corridor airspace structuring is not viable for future traffic demand. As such, the authors suggested that the VTOL from the delivery points need to be more efficient to transport packages efficiently. Furthermore, the authors observed that UAV-to-UAV communication is needed to sustain a level of safety for high-density UAV operations.

Sacharny et al. [66] compared three different corridor placements, road network, grid network, and Delau-

⁸On-demand corridor, meaning, a corridor structure that is created based on the origin and destination of the UAV going to utilize the corridor structure.

may triangulation network. Furthermore, in the same paper, the authors compared a proposed pre-flight deconfliction method by the Federal Aviation Administration (FAA), called distributed cell-based deconfliction, to a more dynamic corridor deconfliction method called Lane Based Strategic Deconfliction (LBSD). The authors used a Salt Lake City earthquake simulation to compare the placements and deconfliction methods, where 25,000 people would receive 36L of water and 1,4 kg of food each day. The number of vertiports varied from 10 to 50, with 477 distribution sites. In addition, 500 to 1,000 UAVs were simulated. For the comparisons, the authors used the maximum delay, maximum deconfliction time, average deconfliction time, and average delay as performance indicators. The authors observed that the corridor placement did make a difference, as the grid layout showed a higher deconfliction rate compared to the two other layouts, with the Delaunay triangulation yielding the least. Furthermore, the authors observed that the LBSD provided no flight plan delays, unlike the LBSD method, which showed significant delays, indicating that a more dynamic approach towards corridor traffic is beneficial.

Muna et al.[51] proposed an collision-free multi-layered bi-directional corridor framework. The corridor framework is similar to the layered concept proposed in [62]. However, unlike the layered concept, the authors proposed to divide the corridors into three dimensional cubes, where only a single UAV can operate simultaneously. The corridor structure was based on a three-layered structure, where the upper layer has the two headings, North-to-South and South-to-North, while the bottom layer has the directions West-to-East and East-to-West. At intersections, UAVs can change directions by flying down to the middle layer and waiting for an open cube in the new direction. In the same paper, the authors simulated the proposed framework as a one dimensional grid network using discrete-time simulations in python to demonstrate the distribution of UAVs over a prolonged period. A total of 100,000 time-step simulations were performed, varying from 1 to 50 UAVs in the corridor, consisting of 100 air cubes. Moreover, simulations with different UAV speeds were also simulated to explore their effect on the corridor framework. The authors observed that the UAV distribution remained uniform regardless of traffic speed- and volume changes.

Quan et al.[11] proposed a corridor network structure for as part of UTM, combining current swarm- and route technology. The authors proposed a two-way corridor network, allowing for UAV swarms within each lane, relying on ad-hoc communication to uphold separation distances amongst the UAVs within the corridor structure. The proposed corridor concept is similar to highways in its design, with similar rules and designs for roundabouts and turns. In the same paper, the authors simulated a simple corridor network with 80 UAVs with different routes, with the use of a custom simulator in Unreal Engine. The corridor network, consisted of the same junction designed as proposed by the authors. Amongst the UAVs a minimum separation distance of 1m was set. The authors observed that the UAVs kept their separation, with the lowest separation amongst the UAVs being 1.42m throughout the simulation.

Pang et al.[67] proposed a three dimensional grid corridor concept similar to what was proposed in [61]. The authors proposed to divide the airspace into a three dimensional matrix consisting of three different density layers. In the lowest layer, the airspace would be divided into small cubes for further control over

airspace, with a decrease in cube density for the higher layers for further and faster travel. In the same paper, the authors explored the efficiency and safety of the two airspace structures unstructured free-flight and corridor network based on trajectory operations (pre-flight deconfliction). Flights were scheduled to be flown every 10 minutes in different altitude layers in the corridor network. A simulated environment of 2 km^2 above the Nanyang Technological University (NTU) in Singapore was used as their test location, with a traffic density ranging from 20 to 100 UAVs flying below 60 meters. The authors found that unstructured free-flight is more complex in terms of number of crossing routes. However, as the traffic density increases, the trajectory-based corridor network's efficiency significantly decreases.

3.3 Rules and Parameters simulations

In the following section, we present the previous research that has been carried out by other researchers on parameters and rules changes for traffic efficiency and safety in corridors and other airspace concepts.

Ho et al. [68] proposed an improved Optimal Reciprocal Collision Avoidance (ORCA) CD&R method called Adapted ORCA and explored how different look-ahead times, separation distances, and deconfliction distances effect traffic efficiency and safety based on their newly proposed CD&R method. Two different simulation scenarios were conducted, the first was an extreme conflict scenario, where 10 UAVs were forced into direct conflict, and the other was a realistic depiction of a multi UAS Service Provider (UASSP) system in Okutama, Japan. Here, three different UASSPs were considered, health delivery and two food delivery services, with a traffic density varying from 15 to 35 UAVs. In total, 100 simulations were conducted for each scenario, where each scenario was around 4 hours long. The authors simulated separation distances ranging from 5m to 15m, look-ahead times ranging from 4s to 10s, and with and without CD&R, with a max speed of 5m/s. In the extreme conflict scenario, the authors observed that a more considerable separation distance caused more significant route deviations and that a larger look-ahead time minimized the route deviation. Furthermore, the authors observed that for higher look-ahead times, the UAVs tended to deviate more due to pre-mature CR and vice versa. In the real-world UASSP scenario, the authors observed that the larger the separation distance, the larger the route deviation was. Moreover, they observed that the total number of LoS instances increased with the different separation distances. Lastly, the authors observed that with an increase in traffic density, and no CD&R system, the total number of LoS increased, while with CD&R enabled, no LoS were observed.

Aarts et al. [69] developed an analytical model to observe factors influencing the capacity of airspace traffic. To validate the analytical model, the authors conducted fast-time simulations adopting the BlueSky simulator. Moreover, the authors created a two-dimensional single-lane orthogonal corridor grid network, with the identical operational functionality of the corridor network simulated in [64]. As mentioned in their work, the UAVs utilized a one dimensional speed constraint to avoid LoS. The authors conducted three different experiments, a base experiment to validate the created analytical model and two rule experiments exploring speed and separation distance changes, to explore their effect on the traffic in the

corridor. Two different speeds were simulated in the speed experiment, 5m/s and 10m/s. Similarly, two different distances were simulated for the separation distances experiment, 50m and 100m. For each experiment, ten different traffic densities were simulated, ranging from 6 to 60. The authors observed that the whole airspace slows down and becomes unstable when an intersection reaches its maximum capacity using speed resolution as the only resolution factor. Moreover, the authors observed that the maximum density is not effected by increasing cruise speed while the network flow rate increases. However, by utilizing higher separation distances, the authors observed a reduction in the corridor's capacity.

Bulusu et al. [6] explored the feasibility of unstructured free-flight and found that it was feasible up to 10,000 flights a day in an area the size of the San Francisco Bay area. In the same paper, the authors also explored how different separation distances would effect the complexity of the traffic. Consequently, the authors simulated separation distances varying from 50m to 300m with a 50m increase. Based on the results, the authors observed that a separation distance of 50m yielded the slowest conflict complexity growth, meaning concurrent UAVs in LoS, suggesting that the airspace is safer and more efficient with a decrease in separation distance.

Ribeiro et al. [70] compared the efficiency and safety of four commonly used Conflict Resolution (CR) algorithms for manned- and unmanned aviation. A linear state-based algorithm⁹ was adopted for Conflict Detection (CD), while four different CR algorithms were compared and simulated: Modified Voltage Potential (MVP), Space Solution Diagram (SSD), Coordinated Resolution, and Centralized Cost Solution. The BlueSky simulator was used for the simulations, with the DJI Mavic Pro specifications with a 300s look-ahead time and a separation distance of 50m, simulating a simple unstructured free-flight where UAVs travel directly from their origin to their destination at the same altitude and speed. Moreover, three different traffic densities were simulated, ranging from 1,080 to 1,440 UAVs, simulating three times for each scenario. The authors compared the distance traveled, flight duration, number of LoS occurrences, and LoS durations to compare the different resolution algorithms. Based on the results, the authors observed that the two Velocity Obstacle (VO) based resolution methods, MVP and SSD exhibited fewer secondary conflicts than the other algorithms. Furthermore, the authors observed that the MVP algorithm yielded more conflicts than the other algorithms. However, it also had a lower conflict time than the SSD algorithm. Moreover, the authors observed that the selected resolution algorithm and traffic density did not correlate with the LoS duration. Finally, the authors observed that the MVP had the lowest route deviation and travel time, suggesting that the MVP algorithm is more efficient than the other algorithms.

Bulusu et al. [6] explored the feasibility of different airspace volumes for cooperative and non-cooperative UAVs in shared airspace [71]. Furthermore, in the same paper, the authors explored the effect of different separation distances on both the cooperative- and non-cooperative traffic. Each UAV operated at a vertical height of 120 meters Above Ground Level (AGL) in a two dimensional environment, storing information such as origin, destination, start time, and similar. The densities varied from 100 to 200,000 UAVs in the

⁹A linear state-based algorithm looks for conflicts based on the UAV's future linear position, comparing it to the positions of the other UAVs.

simulations, where non-cooperative minimum separation values were simulated from 50-300 meters with an increment of 50 meters, while cooperative separation values were simulated from 5 meters to 300 meters. In the paper, the authors defined UAVs as in LoS when they were within the defined separation distance for the non-cooperative UAVs, while the cooperative UAVs were in LoS when they were within the defined separation distance and converging. The authors observed that having cooperative UAVs significantly improved traffic volumes while reducing the overall computational complexity. Furthermore, the authors observed that the probability of observing large LoS clusters were minimized by having smaller separation distances for both cooperative- and non-cooperative UAVs.

Oosedo et al., [65] simulated a future delivery operation in Japan, as discussed in the previous section. In the same paper, the authors explored how different separation distances would effect traffic. Consequently, the authors simulated three different separation distances for the different experiments, 30m, 60m, and 150m. Based on their experimental results, the authors observed that the number of intrusions, defined when two UAVs were closer than 5m, increased when the separation distance was 30m compared to the separation distance of 60m. However, the authors also observed an increase in the number of intrusions again when the separation distance increased to 150m, suggesting a non-linear increase in safety with an increase in separation distance.

Sacharny et al.,[66] compared three different corridor placements and compared a pre-flight deconfliction method proposed by the FAA, called distributed cell-based deconfliction, to a more dynamic corridor deconfliction method called LBSD. The researchers compared the effect on the corridor traffic depending on two different speed limits, 9 m/s and 18 m/s. The authors observed that an increase in speed limit decreased the average number of deconflictions within the corridor, meaning, the complexity within the corridors decreased with the increase in speed limit.

Tan et al. [72] explored how different separation distances would effect the number of LoS with and without CD&R. The authors created a simulated environment within the software System Tool Kit (STK), developed by Analytical Graphics, Inc. (AGI), and defined an experimental area in Singapore of 0.185 km^2 . The authors simulated traffic densities ranging from 18-42 UAVs with six generative vertiports and three landing vertiports. The traffic was generated based on concurrent waves from the different generative vertiports with a provided time interval. Moreover, in the experiments, LoS instances were defined when two UAVs were within 30m. Finally, simulations were performed with and without CD&R, using a fixed look-ahead time of 10s and a resolution algorithm constraining the speed vector. Based on the results, the authors observed that with an increase in the separation interval/distance, there was a reduction in the number of LoS instances. Moreover, the authors observed that when enabling CD&R, even fewer LoS instances occurred.

Labib et al. [73] simulated a multi-layered corridor network model for distributed UTM, comparing three different traffic knowledge scenarios with corridor traffic awareness, Global Offline Static (GOS), Global Probabilistic Dynamic (GPD), and Local Pheromone Guided (LPG), based on the UAVs travel time, route

changes, layer changes, queuing, and energy consumption. The three knowledge scenarios increased the UAVs knowledge of the traffic, and dynamic route changes were made based on this knowledge. A simulated environment was created adopting the NetworkX library from Python and the multiNetX package, based on the Erdos-Renyi model. A three-layered network was created in the simulated environment, each layer containing 300 vertiports and the same amount of airways. Moreover, the UAVs were assigned random start and end vertiports in the lowest layer in the simulations. Furthermore, the UAVs were permitted to travel at any layer, allowing UAVs to travel at their optimal vertical height and speed. The lower the layer, the lower the speed, and vice versa. In the first and second experiments, a range of 10 to 500 UAVs was simulated, while in the third experiment, 10 to 1,500 UAVs were simulated. The authors observed that for denser traffic, the LPG outperformed both the GOS and GPD based on the performance metrics adopted by the authors, suggesting that more advanced traffic awareness is beneficial for the performance of the traffic within complex corridor networks.

3.4 Summary

To date, significant research has been conducted within the area of UTM research, mainly encouraged by various UTM concepts, such as geofencing, geocaging, pre-flight tactical deconfliction, monitoring, tracking, conflict resolution, and similar. However, literature on the simulational comparison of different corridor types, rules, parameters, and placements was found to be significantly limiting.

Based on the existing literature, a variety of different corridor concepts have been proposed, ranging in complexity and airspace utilization, such as [12][9][8][13]. However, as of yet there is limited simulational experiments on different corridor types, yet alone the comparison of different corridor types, overall limiting the understanding on the different corridor types effect on the safety and efficiency of traffic, making it difficult to determine corridor characteristics which might be beneficial for the safety and efficiency of the traffic. Currently, existing corridor simulations have largely utilized the concept of vertiport-to-vertiport travel with an interconnected corridor network between the vertiports, such as [64][11][68][73].

Several other researchers have simulated vertiport-to-vertiport traffic without simulating the VTOL process for the UAVs, simply generated the traffic directly into the airspace, such as [64][69][13]. On the other hand, other researchers have focused on vertiport-to-destination travel, simulating package delivery services with on-demand corridors, such as [65]. Lastly, others have taken a more dynamic approach, simulating random traffic from origin-to-destination where UAVs access the corridor structure while in the airspace, such as [6]. Based on various proposed UTM concepts, the airspace should be accessible to most, and traffic will likely be more dynamic, as simulated in [6], and will not be limited to flights from vertiport-to-vertiport or vertiport-to-destination, rather a combination of vertiport-to-vertiport, vertiport-to-destination, and origin-to-destination, with a corridor structure which can be accessed by the UAVs requesting access to the airspace and corridor structure. Consequently, the understanding of the efficiency and safety of the traffic is limited in the papers which have simulated from vertiport-to-vertiport

and vertiport-to-destination, as this is likely only one aspect of the future airspace. Moreover, while existing literature exists on the effects of different rules and parameters on UAV traffic, such as [70][6][65], different parameters and rules might impact the efficiency and safety of the traffic differently depending on the structuring of the airspace. As such, limited parameter and rules experiments were observed in the existing literature for the corridor types aimed to be simulated in this thesis.

In the future, the placement of the corridors will likely be limited due to future rules, regulations, and physical restrictions. Corridor placements above water and highways have been proposed to mitigate sound-, visual-, and privacy concerns. However, currently, no literature has addressed how different corridor placements might impact the efficiency and safety of the traffic. On the other hand, while some corridor simulations, have addressed that a different corridor placement effected the results, such as [65] and [66], these simulations provided limited data, due to the main aim of the papers. Furthermore, as these simulations were conducted with the utilization of vertiport-to-destination [65] and vertiport-to-vertiport [66] traffic, limited information on the accessibility to the corridor structure is left unknown, along with performance indicators such as the direct route deviation, travel time, and similar. Moreover, limited experiments on different placements were conducted in both papers, with two different placements for the first paper and three for the second.

This thesis aims to add new scientific knowledge to the literature by conducting fast-time simulations with randomized traffic, comparing three different corridor types raging in their airspace utilization, to observe corridor characteristics that might be beneficial to the safety and efficiency of the traffic. Moreover, this thesis aims to add new scientific knowledge to the literature by conducting different rules and parameter experiments to observe beneficial rules and parameter characteristics for the efficiency and safety of traffic for two of the corridor types in this thesis. Lastly, this thesis aims to add new scientific knowledge to the literature by exploring the impact on the efficiency and safety of the traffic depending on six different corridor placements.

Chapter 4

Methodology

This chapter explains the methodological approach that we have used to perform the experiments conducted in this thesis, which will be further discussed in chapter 5. A rationale for the choice of simulation environment is discussed and presented in section 4.1. In section 4.2 the rationale for choosing the simulator utilized throughout this thesis is presented. Section 4.3 describes different simulational approaches, and the rationale for choosing the approach used. Section 4.4 presents the approaches considered and conducted for the Unmanned Aerial Vehicle (UAV) traffic. Section 4.5 provides explanation of the the creational process of the corridor structures, placements, and corridor routing. Section 4.6 discusses and presents how safety is achieved amongst the UAVs as part of the simple Unmanned Aircraft System Traffic Management (UTM) system created. Section 4.7 discusses and presents the performance indicators used to compare the results in the results chapter 6. Section 4.8 provides a discussion and final approach towards collecting the simulational data. Section 4.9, presents how the collected data was analysed. Lastly, section 4.10 presents how the significance of the results collected were determined.

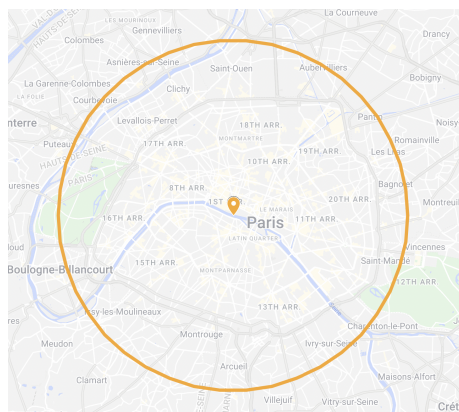
4.1 Experimental Area

In this thesis, different corridor types, rules, parameters, and placements have been explored. In addition, an unstructured free-flight experiment was conducted to compare the feasibility of unstructured free-flight compared to a corridor structure as part of a simple UTM system, further information on the experiments will be provided in chapter 5. Based on the goal of the thesis, the corridor placements' experiment required parts of the placements to be based on the infrastructure of the chosen simulated area. As such, for the purpose of this thesis, a city with compelling infrastructure and size was necessary to collect and observe interesting results while also limiting the necessary traffic density to limit the computational power for each simulation.

According to previous research on corridors and airspace capacity [6][64][62], researchers observed that considering around 1 UAV per km^2 , each hour, presented interesting results. In this thesis, traffic was simulated across a twelve hour period. As such, cities such as Rome, with an area of $1,285 km^2$, would have

required around 15,420 UAVs to be simulated, which would have taken a significant amount of computational power to simulate for each scenario. Moreover, as different corridor placements were going to be explored, having such a large city would make it difficult for most of the UAVs in the area to have access to corridor placements such as ring roads, provided the UAVs were given reasonable travel distances in accordance to current UAV technological capabilities, with randomly generated origin and destination coordinates. Moreover, some cities have significant areas covered in water, such as Amsterdam or Venice, which meant that the UAVs origin and destination locations should have been checked for each instance to achieve more realistic simulation results for each scenario. On the other hand, if lower percentage of the city was covered in water, the need to avoid generative coordinates on water would not be needed while still achieving more realistic and interesting results.

For the experimental area, in this thesis, the metropolitan of Paris was chosen as the simulation area. The metropolitan of Paris was chosen based on a variety of factors. First, the metropolitan of Paris is around 105 km^2 , which allowed fewer concurrent UAVs to be simulated, overall requiring less computational power, making the simulation process manageable and the overall data sizes collected smaller compared to cities such as Rome, while still generating interesting results. For example, in the case of Paris, around 1,260 UAVs should have been simulated over a twelve hour period, compared to the previously mentioned 15,420 for Rome, or 5,448 UAVs in the case of Oslo. Secondly, due to the relatively small size of the Metropolitan area of Paris, the ring-road around its city is, comparably to Rome or Oslo, relatively small. This makes it more accessible to more UAVs, regardless of their origin and destination location. Lastly, only a small portion of Paris is covered in water, with only the "Seine" river going through a small portion of the city.



(a) Aerial overview of simulation area



(b) Simulation area in Paris viewed from the BlueSky simulator

Figure 4.1: 153.94 km^2 simulation area in Paris seen from map- and simulation overview, with latitude/longitude origin coordinate (48.8590239723895, 2.3345907131722807)

Since we used the ring road structure around Paris as one of the corridor placements in the corridor placement experiment, as presented in chapter 5, the circular simulation area was extended from the center of Paris ensuring full coverage. Meaning, the circular radius was extended to 7,000 meters, extending the simulation area to 153.94 km^2 . Moreover, the origin coordinate was chosen based on an estimate of the center of Paris. An image of the simulation area used throughout the experiments in this thesis is pre-

sented in figure 4.1, where figure 4.1(a) is the general map overview, and figure 4.1(b) is the area as defined in the simulator which was used throughout this thesis, which will be further discussed in section 4.2.

4.2 Simulator

As mentioned in section 4.1, in this thesis an exploration of corridor types, parameters, rules, and placements have been conducted, with the experiments presented in chapter 5. In addition, an unstructured free-flight experiment was conducted to compare the feasibility of unstructured free-flight compared to a corridor structure as part of a simple UTM system. To conduct the experiments and collect the necessary data to answer the research questions, as presented in section 1.3, a simulator was utilized. However, before deciding on the adopted simulator, in total, three different simulator alternatives were taken into consideration.

The first alternative was to create a simulator from scratch. By creating a custom simulator, we could have ensured that it contained all the necessary components and features to assist in the exploration of corridors and the answering of the thesis questions (section 1.3). On the other hand, developing a simulator would have been quite extensive and would have become exponentially more advanced for each additional feature implemented. Consequently, the development process was uncertain, and the development time was challenging to predict altogether. As such, most of the thesis duration might have been used to finish the simulator, which was outside of the scope of this thesis. Furthermore, while the simulator was under development, most of the thesis work would have been postponed until the simulator operated satisfactorily, which was not ideal.

The second alternative was to utilize an existing closed-source simulator adapted to UAV, UTM, or Air Traffic Management (ATM) research. By utilizing an existing simulator, a significant amount of labor would have been preserved, compared to the first alternative, and could have been used on the task at hand. However, by utilizing a closed-source simulator, there would have been a lack of transparency due to its private code, altogether making it difficult to compare or verify both results and operational functionality. Moreover, in the case of the simulator not having a particular feature needed for the experiments, it would have been challenging to extend or adapt the simulator to the experiments. Instead, a request would have been needed to be made to the project's developers. However, the requested implementation would have not been guaranteed to be implemented on time, or even implemented at all.

The last alternative was to utilize an existing open-source simulator. Like the closed-source simulator, a significant amount of labor would have been preserved by utilizing an existing simulator. However, unlike the closed-source simulator, an open-source simulator provides a level of transparency by having all of its code publicly available. Consequently, by utilizing publicly available code, the simulation results are more comparable, accessible, and verifiable by other third parties. Furthermore, an open-source simulator allowed for further expansion of its code, which allowed for additional feature implementation and code

changes to fit the experiments. This was especially important, as bug fixes and altering of code could be performed to adapt the simulator to the experimental needs. In the end, after exploring a variety of different simulators, such as [74] [75][76][77][14], the BlueSky simulator, created by Hoekstra and Ellerbroek [14], was adopted.

The BlueSky simulator is open-source, accessible, and free to use by anyone, providing a level of transparency and community-driven development. The transparency of the simulator is in contrast to some of the other similar papers which have utilized in-house simulators [65], where the code is not publicly available, and the results can be difficult to compare and interpret as a consequence. Moreover, the simulator is still maintained and under development by its creators and was reasonably documented, with both test case scenarios to present different functionalities, and a command-line list on a GitHub wiki page. The simulator also supports a sufficient amount of concurrent flights to what was needed in this thesis. The simulator could concurrently simulate around 600-800 flights at the same time without multi-threading, and significantly more with [14]. Furthermore, the simulator also supports plugins, which made it simple to extend the simulator and directly access all of the data and functions without directly altering the code, reducing the amount of written and altered code needed to collect the necessary data.

The simulator is structured around scenario files, simple files with command lines from the language TrafScript. The commands could be provided as input before or during the operation of the simulation. For example, in table 4.1, some of the TrafScript commands within the BlueSky simulator are presented, with a short description of their functionality. Moreover, the BlueSky simulator is built upon modules, which allowed easy adaptation of new functionality. By building the simulator architecture in such a manner, functionality could easily be implemented within a single module without the required understanding of the other modules, which allowed for easy expansion and modification of the simulator.

Table 4.1: Overview of some of the TrafScript commands [14]

| Command (TrafScript) | Command description |
|--------------------------------------|--|
| CRE acid, type,lat, lon,hdg, alt,spd | Create an aircraft |
| HDG acid,hdg | Given an aircraft a heading command (use heading in degrees) |
| LEFT acid,hdg | Given an aircraft a 'turn left' command (use target heading in degrees) |
| ALT acid,alt | Altitude command for autopilot, accepts feet ('30000') or flight levels ('FL300') |
| SPD acid, spd | Speed command, accepts Mach numbers (speeds <1 optionally prefix by an M) and CAS in kts |
| DEST acid, airport/lat, lon | Add a destination as the end waypoint of the route |

4.3 Conduction of the Simulations

Due to the structuring of the BlueSky simulator, there were two main methods of conducting the simulations. The first method was to fully integrate the traffic generation and operation algorithms directly into the BlueSky simulator, creating modules and plugins to handle the generation and deletion of traffic, routing, and similar, creating generalized scenario files to run the experiments. In essence, the results would have been different for each simulational instance by conducting the simulations in such a manner. Furthermore, with this approach, a great degree of control of the traffic would have been achieved during the simulation, allowing for additional micro-managing. However, to adopt this approach, a great degree of knowledge of the simulator and its components was required. While parts of the modules were well documented, the documentation was still lacking, and initial testing observed it to be problematic and time-consuming to discover relevant values and functions in the existing code.

The second method was to create scenario files externally from the BlueSky simulator and load these files onto the simulator once created. Unlike the previous method, by conducting the experiments in such a manner, a re-run of the scenario files would result in identical results for each instance. Furthermore, a less complex structure can be identified by separating them, allowing for quicker adaptation, relying on the available command stack. Furthermore, by keeping them separated, a more flexible structure would be achieved, allowing for a more personal adaption, aiding in the completion of the experiments. Furthermore, in the case where more advanced control of traffic would have been needed, this could have been achieved by creating a plugin, and enabled it in the scenario file.

In the end, adopting an external scenario file generation process was the chosen method for conducting the simulations thought the thesis. The primary motivation behind the approach was quick adaptation. As the simulator was still under development and its documentation was limited, consequently, adopting the first approach could have caused more outstanding issues than the second approach. Consequently, due to the limited time frame of this thesis, a risk-to-reward judgment was taken. Furthermore, by adopting the second approach, the integration of routing algorithms, corridor placements, and similar was easier implemented by creating the scenario files externally.

As mentioned, the second approach towards conducting the simulations was adopted. Consequently, scenario files were created externally from the simulator. With the use of python scripts, scenario files were created. This was achieved by using the python file opener and writing text snippets to the file, ultimately outputting a complete scenario file for the BlueSky simulator to interpret. In total, apart from the standard packages used in python, such as sys, os, random, math, numpy, and re, two external packages were used throughout the creation of the scenario files, geopy [78] and nvector [79]. Both geopy and nvector are geographical calculator packages used to calculate geographical instances like the crossing point between two coordinate lines or calculating a coordinate position based on the heading and distance from another coordinate. Both of which were used in the creation of the corridors and traffic patterns.

4.4 Traffic Generation

Traffic is a critical aspect of UTM, and the accessibility to the airspace is expected to be available to most. As such, in this thesis, traffic was randomly generated within the experimental area with the assumption that people and services will request access to the airspace from anywhere. Moreover, the traffic density pattern is an interesting aspect of future airspace. Currently, knowledge of how the future traffic density pattern will look is yet to be observed. In this thesis, we mainly considered two different traffic density patterns. The first traffic density pattern was similar to a standard deviation curve. Here, traffic was low at the beginning and end of the day, with significant airspace utilization in the middle of the day. The second considered traffic density pattern was an equally distributed pattern, meaning we would expect the airspace to be occupied with an equal concurrent number of UAVs across the day, with no peak hours.

With the assumption that future UAV operations, such as package delivery, surveillance, imagery, and similar, will be highly autonomous, the future operations will primarily, and arguably, be operated without human-in-the-loop. Consequently, we can expect services to automatically start when the airspace is accessible. Based on these assumptions, the second traffic density pattern was chosen for this thesis. Consequently, the traffic was equally distributed across twelve hours, randomly assigning the minutes and seconds within the hour. The UAVs which were left, were assigned to a random hour, minute, and second.

As previously mentioned, the future airspace is expected to be available to most. This entails a vast range of different types of UAVs ranging from highly technological- and physically capable to lower technological- and physically capable UAVs. For instance, larger businesses such as Amazon will likely afford to use more high-end UAVs for their package deliveries than a smaller family-owned restaurant or even a recreational user delivering a forgotten family member's phone back to them. Additionally, the future airspace will most likely contain different types of UAVs, such as the fix-wing-, multi-rotor-, single-rotor-, and hybrid UAVs. In this thesis, to limit the complexity of the experiments, four different UAV configurations were chosen to represent four different tiers of UAVs, mainly focusing on their speed. In increasing order of technological- and physical capable UAVs which were used in this thesis are the DJI Matrice 600, DJI Phantom 4, DJI Matrice 100, and the Amazon Octocopter. A table of the specifications of the different UAVs is presented in table 4.2. Based on the UAVs travel distance capabilities and the size of the experimental area, in this thesis, the UAVs were assigned random origin and destination coordinate with a travel distance randomly picked between 3km and 5km.

Table 4.2: UAV specifications

| Parameter | DJI Matrice 600 | DJI Phantom 4 | DJI Matrice 100 | Amazon Octocopter |
|------------------------------|-----------------|---------------|-----------------|-------------------|
| Number of engines [number] | 6 | 4 | 4 | 8 |
| Power per engine [kW] | 0.482 | 0.0669 | 0.2 | 0.482 |
| Horizontal speed range [m/s] | -18-18 | -20-20 | -22-22 | -44-44 |
| Vertical speed range [m/s] | -5-5 | -4-6 | -4-5 | -8-8 |

As the traffic was randomly generated, it was observed in some instances that the UAVs would be generated into Loss of Separation (LoS), where two UAVs were within their provided separation distances. Moreover, in other cases, it was observed that when two UAV destinations were beside each other, within a 50m range, and the UAVs arrived near their destinations simultaneously, they would end up in an endless spiral of conflict and avoidance. Therefore, a simple access protocol to the airspace was created between the Unmanned Aerial System (UAS) operator and the UTM system to mitigate these two issues. In the first step, the UAS operator request access to the airspace, providing their origin, destination, and UAV specification. In the second step, the UTM system checks against current traffic (200 previous UAVs). In the last step, if the requested origin and destination are within the radius of the separation distance, with a buffer radius of 60m, the flight is declined. While an airspace approval process was adopted, the issue could have also been resolved by forcing UAVs in conflict near their destination to take a slight detour or emergency land. However, a consequence of this could have been that UAVs, on average, landed further away from their original destinations and possibly falsely emergency landed. As such, a "delayed" UAV flight approach was adopted in this thesis, where UAS operators would request access to the airspace to the simple UTM system.

4.5 Corridor Construction and Routing

In this thesis, as will be presented in both section 5.1 and 5.3, we have explored a range of different corridor types and placements. Consequently, various corridor complexities can be recognized, with different angles, junction nodes, and junction routes. To ensure the integrity of the corridor structures, a dynamic corridor creation methodology was adopted. Initially, a trigonometric approach was used to create the corridor structures. In this approach, a set of junction nodes were provided as an input, as represented by the blue crosses in figure 4.2. For each of the junction nodes, the outer nodes, as represented by the green squares in figure 4.2, were calculated based on the crossing nodes of the connected junction nodes, ultimately creating a corridor structure. In addition to the outer nodes, inner nodes were also calculated to define the inner routes of the corridor structure. However, as the corridor networks became more complex, significant issues with the initial corridor creation methodology were observed, where the integrity of the corridor structure was not consistent, most likely due to issues in the initial code or logic. Consequently, another methodological approach was adopted. In the final corridor creation method, an existing geo-

graphical Python package, called *nvector* [79] was used to calculate the crossing nodes, ultimately creating a corridor network with structural integrity, outputting both corridor structure coordinates and corridor lane coordinates.

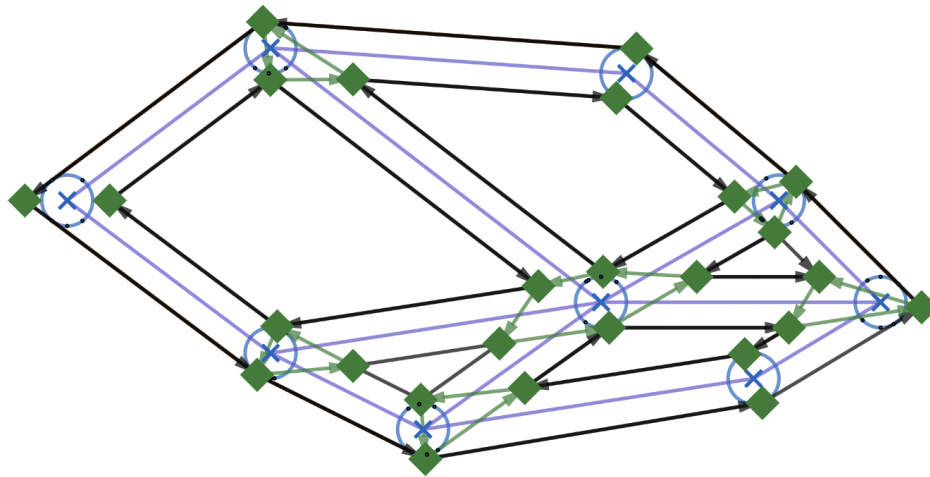


Figure 4.2: An illustrative figure of the structural build of a weighted corridor network. The blue crosses inside the blue circles are the junction nodes. The green squares are the outer crossing nodes. The black arrows are the directional heading of the lane to the left of the directional heading. The purple line is the divider between the directional traffic direction.

As mentioned in section 4.4, in this thesis, the traffic was randomly generated with different travel distances and origin- and destination coordinates. Consequently, instances where UAVs did not benefit from the utilization of the corridor or needed to largely deviate from the direct route, occasionally occurred. Like a real-world scenario, all UAVs utilizing the airspace will not necessarily utilize a corridor structure. As such, an intermediate global travel altitude and travel speed were created. Since the corridor structure was placed at 120m Above Ground Level (AGL), and above, a global intermediate travel altitude of 100m was created in this thesis. Furthermore, to ensure a great level of safety, a slower travel speed of 10.28 m/s was instantiated compared to the corridor speed limit. In this thesis, UAVs did not access the corridor if the origin- and destination coordinate had the same closest corridor junction node or if the corridor route distance exceeded three times the direct route distance. In figure 4.3, the protocol for the direct route travel is illustrated. The protocol consisted of four steps. In the first step, the UAV ascended to the intermediate travel altitude. In the second step, the UAV started traveling towards its destination once the global intermediate altitude was reached. In the third step, once the UAV was close to its destination, the UAV slowed down and stopped when it was reached, then descended to the ground. Finally, the UAV was removed from the simulation once the ground was reached.

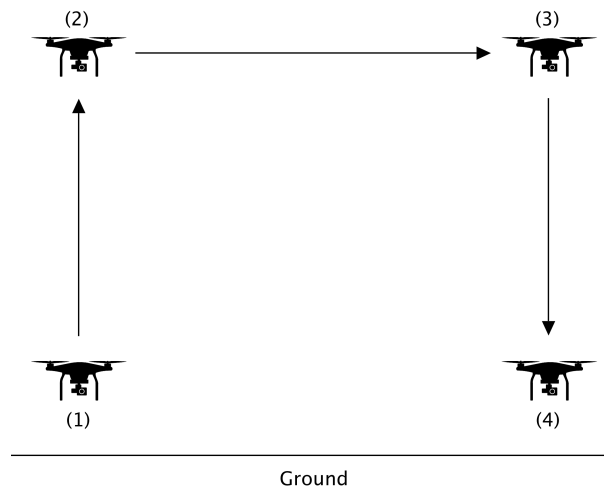


Figure 4.3: The UAV flight protocol for the direct route

For the UAVs which utilized the corridor, an eight-step protocol was created, as is presented in figure 4.3. In the first step, the UAV ascended to the intermediate travel altitude. In the second step, the UAV traveled towards the corridor entrance junction once the intermediate travel altitude was reached. In the third step, the UAV ascended to the corridor altitude once the entrance junction was reached. In the fourth step, the UAV followed its assigned corridor route. Once the UAV reached its exit junction node in the fifth step, it descended to the intermediate travel altitude. In the sixth step, the UAV traveled to its destination. In the seventh step, once the UAV was close to its destination, it would slow down. Once the destination was reached, it would stop and descend to the ground. Lastly, the UAV would be removed from the simulation once the ground was reached.

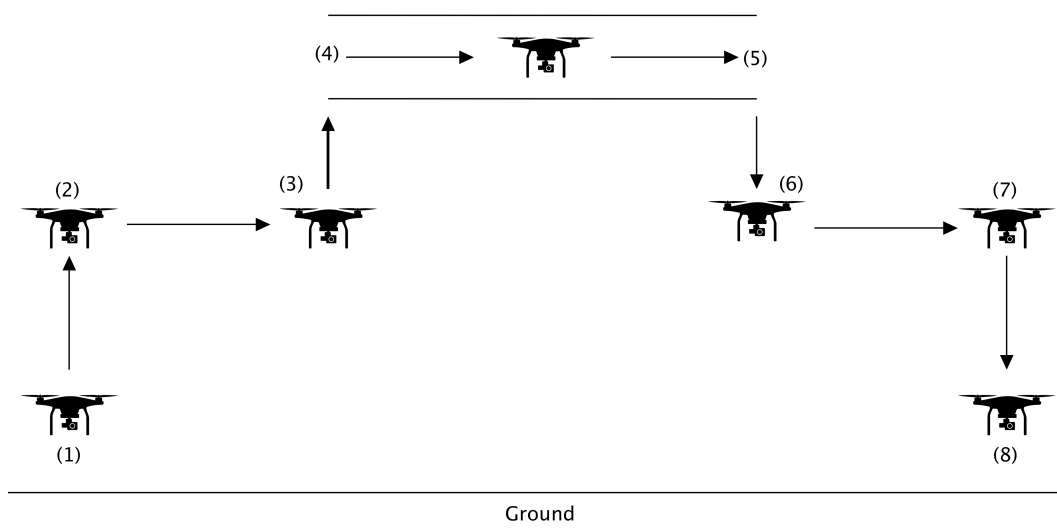


Figure 4.4: The eight step corridor flight protocol

A range of different corridor placements were explored in this thesis, and are presented in chapter 5. The corridor placements included weighted corridor networks (roundabout- and park networks), non-

weighted corridor networks (grid networks), and curved corridors (ring-road and river). Consequently, a range of different corridor routing algorithms was utilized.

For the weighted corridor networks, as implied by the name, the networks consisted of junction-to-junction nodes of varying distances. Consequently, for any UAV, a single shortest route existed within the network. In this thesis, Dijkstra's shortest route algorithm [80] was adopted to calculate the general shortest route between the junction nodes. However, first, the closest junctions to the origin and destination coordinate were calculated. Based on this data, Dijkstra's shortest route algorithm was used to find the general shortest route. Based on this information, the inner corridor route was further calculated based on a counter clock-wise sorted inner junction node lists provided during the creation of the corridor, headings, and distance calculations from junction-to-junction, ultimately generating an inner route. Another possible routing approach for the weighted corridor networks would have been to further structure the corridor data to provide information on allowed routes, thus providing this data to Dijkstra's shortest route algorithm. However, due to the creational process of the corridor structures, the first approach made it simpler while also providing further routing control.

For the non-weighted corridor networks, unlike the weighted corridor networks, all of the junction-to-junction distances were equal, meaning there were multiple shortest routes for any UAV. While Dijkstra's algorithm could have been used for the shortest route, a custom non-weighted algorithm was created as Dijkstra's algorithm would have been biased towards some routes due to slight variations in the geographical distances between junction coordinates. As such, a non-biased custom algorithm was created. The algorithm was based on a two dimensional matrix structure. The algorithm favored the x-axis before the y-axis. Thus, travel would always occur on the x-axis before the y-axis. For the inner routing, the same approach as with the weighted corridor was adopted.

For the curved corridors, similarly to the weighted networks, for any UAV, a shortest route existed. However, unlike the weighted networks, only a single or two possible routes were available depending on if the corridor endings were connected. If the endings were connected, there would be two possible routes for any UAV. However, if the endings were not connected, there was only one possible route. Therefore, for the non-connected curved corridor, the shortest route and inner route were calculated based on a sorted corridor junction list. However, for the connected curved corridor, the shortest route and inner route were calculated based on a sorted corridor junction list and the shortest directional route within.

4.6 Conflict Detection and Resolution (CD&R)

In the aviation industry, Conflict Detection and Resolution (CD&R) is a broad term, ranging from centralized onboard instruments to pre-flight strategies. Currently, UAVs are heavily reliant on onboard systems for a level of safety. However, as the traffic density and complexity increase, simple onboard CD&R instruments are not sufficient to ensure a level of safety. Consequently, additional collaboration/information-sharing

technology, pre-flight planning, or both are necessary and are both parts of UTM concepts such as U-space and US-UTM. In this thesis, we have explored different corridor types, parameters, rules, and placements, while also exploring the feasibility of corridors as part of UTM compared to unstructured free-flight. While UTM systems can range in complexity, depending on the concept, a simple UTM system was created to limit the scope of this thesis. As presented in section 4.4 and 4.5, a UTM system avoiding initial LoS and end-less conflict was created while also providing the UAS operators with the shortest route and access to the airspace. Moreover, while pre-flight conflict detection and corridor access protocols have been proposed as part of UTM concepts [8], in this thesis, a more dynamic and self-structuring approach was adopted to limit the scope. Consequently, the safety of the traffic relies on intercommunication amongst the UAVs. In the case of this thesis, with the use of ad-hoc networks [81]. With the ad-hoc network, UAVs shared their intent and collaboratively organized themselves in an effort to avoid LoS.

The conflict detection method used in this thesis was a state-based algorithm [82]. In the state-based algorithm, the UAVs geographical location, altitude, heading, speed, and separation distance, were used to calculate possible future LoS occurrences in the linear future provided a look-ahead time in seconds. For instance, if a UAV was traveling at 10 m/s with a look-ahead time of 10s, the state-based algorithm would look 100m into the future to observe possible LoS instances. However, as the algorithm calculated possible linear separation violations within a given look-ahead time, it did not consider any potential directional change in the route. Therefore, in the case of ongoing traffic in a corridor, false conflicts occurred when the speed and look-ahead time was high. Consequently, a look-ahead time of 15s was chosen for this thesis.

The Modified Voltage Potential (MVP) algorithm [82] was used for conflict resolution throughout the thesis. In the MVP algorithm, conflicts were resolved pair-wise by speed- and heading changes. However, it is important to note that by solving conflicts in a pair-wise manner, possible chain reactions could have occurred, where one resolution created a new conflict. However, although domino effects could have occurred, in the paper [83], the authors compared different Conflict Resolution (CR) algorithms and observed that the MVP algorithm had the least route deviation, lowest time in conflict and the fewest LoS instances in higher density traffic. Moreover, in the paper [64], the authors only used a speed change as a resolution maneuver for the MVP algorithm. However, in this thesis, the lanes were wider, and a more dynamic approach was adopted for the experiments, allowing UAVs to move more freely, consequently, both speed and heading changes were allowed.

4.7 Key Performance Indicators (KPIs)

Safety and efficiency have been used as general terms to explain what we are comparing and exploring in this thesis. However, safety and efficiency are broad terms, and as such, this section presents the interpretation of these two words in the context of the conducted experiments and presents the values which we have used as indicators for efficiency and safety. These values are collectively called Key Performance Indicators (KPIs).

In this thesis, the UAVs were separated based on provided separation distance values, both horizontally and vertically. Thus, creating a safety area around the bodies of the UAVs. The higher the separation distances were, the longer distances away from each other the UAVs needed to be to uphold the provided separation rules. Provided a horizontal separation distance of 50m, a LoS would have occurred if two UAVs were within a shorter horizontal distance than the provided horizontal separation distance. For instance, if two UAVs were 40m apart, a separation violation of 10m would have occurred. To avoid LoS occurrences, as presented in section 4.6, the UAVs future linear positions were calculated to determine whether or not a future LoS would occur. In the case of a potential future LoS, a conflict would be raised for the two UAVs involved. To avoid the possible LoS, a resolution maneuver would be conducted, changing the speed, heading, or both. Based on this information, we observed five safety KPIs of interest in determining the safety of the traffic.

The first safety KPI utilized in this thesis was the average number of conflicts, as an increase in the number of conflicts conveys the complexity of the traffic in the airspace. As such, the lesser the number of conflicts, the less complex the airspace, and the fewer possible occurrences of collisions. Moreover, for the second safety KPI, the average number of LoS conveys how many failed conflict resolution maneuvers have occurred. Furthermore, for the second and third safety KPI, the LoS duration and distance were chosen, as these values present the severity of the LoS. Generally, the longer the LoS duration and the higher the separation violation, the more severe the LoS occurrence. For the last safety KPI, the number of near mid-air collisions was chosen, defined when two UAVs were closer than 10m from one another. A table of the different safety KPIs used in this thesis, along with a short description, is presented in table 4.3

Table 4.3: A list of the safety KPIs and a description of their values

| KPI | Description |
|--|--|
| Average number of conflicts [number] | The average number maneuvers taken to avoid LoS |
| Average number of LoS [number] | The average number of unique separation violations |
| Average LoS duration [s] | The average number of seconds two UAVs are violating the separation distance |
| Average LoS distance [m] | The average LoS distance between LoS pairs |
| Average near mid-air collisions [number] | The average number of instances where two UAVs were closer than 10m from each other in a LoS |

For the efficiency KPIs, we were mainly interested in how fast the UAVs could reach their destinations. The faster the destinations were reached, the less crowded the corridors were, and the more energy was preserved. Consequently, the collective average travel time for the UAVs was used as the primary indicator

of efficiency in this thesis. However, as previously mentioned for the safety KPIs, with an increase in the average number of conflicts, more complex airspace and traffic pattern can be recognized, leading to both speed and route deviations. Consequently, two additional efficiency KPIs were utilized for this thesis, the average number of conflicts and the average route deviation. A table of the different efficiency KPIs are presented in table 4.4.

Table 4.4: A list of the efficiency KPIs and a description of their values

| KPI | Description |
|--------------------------------------|--|
| Average travel time [s] | The average travel duration for the UAVs to reach their destination |
| Average number of conflicts [number] | The average number maneuvers taken to avoid LoS |
| Average route deviation [m] | The average deviation from the calculated- and provided route by the UTM |

For the corridor placement experiment, as presented in section 5.3, two additional efficiency KPIs were used. As six different corridor placements were simulated, their level of accessibility was expected to vary depending on their coverage of the simulated area. Consequently, the average number of UAVs not utilizing the corridor was used as an additional efficiency KPI for this experiment. Moreover, it was further expected that the provided routes would vary in distances depending on the corridor placements due to the variety of junctions and aerial coverage, either limiting or improving the efficiency of the routes. As such, for the last additional efficiency KPI for the corridor placement experiment, the average direct route deviation was also utilized. A table of the additional efficiency KPIs for the corridor placement experiment is presented in table 4.5

Table 4.5: A list of the additional efficiency KPIs for the corridor placement simulations and a description of their values

| KPI | Description |
|--|---|
| Average number of UAVs not utilizing the corridor [number] | The average number of UAVs which were not provided corridor access by the UTM |
| Average direct deviation [m] | The average direct deviation from the calculated- and provided route by the UTM |

4.8 Data Collection

In the previous section 4.7, we discussed how we defined efficiency and safety for the conducted experiments. However, in this section we will present the methodological approach adopted to collect the necessary data. Overall, three different data collection methods were considered.

The first method was to utilize the existing built-in plugins for the BlueSky simulator, in this case, loggers such as "SNAPLOG" and "CONFLOG". The "SNAPLOG" allowed for periodic logging within an adaptable logging interval. Furthermore, several variables could have been activated or deactivated based on a pre-defined variable list. Moreover, the "CONFLOG" worked similarly, although specified explicitly for conflicts. Using the built-in plugins would have saved both time and development effort. On the other hand, the built-in plugins were limited and would have possibly been challenging to adapt to the need of the thesis. The second method was to utilize a third-party logging plugin. Different values could have been collected depending on how the logger was structured and aimed, similarly to the first method. However, locating a third-party logger compatible with all of the thesis needs would have been difficult, and similarly to the built-in plugins might have been challenging to adapt for this thesis. The third, and last method considered, was to create a plugin from scratch and customize it to the needs of the thesis. The plugin would be created from scratch, so the development effort would be more significant. However, it would allow for a level of customization, ensuring all the needed data was logged. While utilizing an existing plugin would have saved some development effort, it lacked customization and logging information such as the distance between two UAVs in an LoS, the option to log end data of a UAV once it landed, and similar. Consequently, for this thesis, a customized plugin was created from scratch.

Table 4.6: UAV start log

| Data | Description |
|----------------------------|--|
| Creation time [s] | The second the UAV was granted access to the airspace by the UTM |
| UAV ID [string] | The identifier of the UAV |
| UAV type [string] | The specification type of the UAV |
| Direct route [m] | The shortest direct route distance from origin to destination |
| Route distance [m] | The provided route distance provided by the UTM |
| Max altitude [m] | The maximum planned travel altitude for the UAV |
| Max horizontal speed [m/s] | The maximum planned horizontal speed for the UAV |
| Max vertical speed [m/s] | The maximum planned vertical speed the UAV will use |

In theory, all of the data collection in this thesis could have been conducted through the use of the BlueSky simulator with the created plugin. However, for ease of use and to save some development effort, a "UAV start log" was created alongside each scenario file. The "UAV start log", as presented in table 4.6, logged every instance of a UAV once access to the airspace was granted from the UTM system. The UAV start log consisted of information such as the timestamp of when the UAV was granted access to the

airspace, the pre-calculate route distance, and more. The instances were logged as Comma-Separated Values (CSV), and as a consequence the files were stored in ".csv" format. By storing the data in CSV format, the analysis of the data was made simpler as will be discussed in section 4.9.

As presented in the table 4.6, the creation time value was the second the UAV was provided access to the airspace from the UTM system. If a UAV was provided access 2 minutes after the simulation started, the value would have been 120 seconds. The UAV ID was the identifier of the UAV. In this thesis, the identifier was the word "UAV" with an incrementing number behind it, starting from 1, for example, "UAV1". The UAV type was the identifying name of the UAV's corresponding specification, which could be either of the four UAV types presented in section 4.4. The distance from the origin to the destination was the direct route distance from the origin- to destination coordinate. The route distance was the UTM system calculated route distance provided. Lastly, the max altitude, max horizontal speed, and max vertical speed were all planned maximum variables for the UAV thought its route, which the UTM calculated in the planning process for the UAV.

While the UAV start log was generated alongside the scenario files, the other logs were created through the custom logger plugin called "LOGGY", on the simulator side. The plugin had direct access to all of the BlueSky modules, quickly accessing necessary logging data, for the most part, the traffic module. For each instance of the plugin, the plugin created three separate log files, "Loss of Separation log", "Conflict log", and the "UAV end log". Similar to the "UAV start log", these logs were stored in CSV format. However, they were saved as ".log" files and later converted into ".csv" files. Moreover, the logging functions within the plugin were called in a time interval of one second to collect as accurate data as possible. While the logging interval could have been even shorter, large amounts of data would have been gathered with limited benefits.

Table 4.7: LoS log

| Data | Description |
|----------------------|---|
| Time [s] | The second the LoS is true between the two UAVs |
| UAV1 [string] | The first UAV in LoS occurrence |
| UAV2 [string] | The second UAV in LoS occurrence |
| Distance between [m] | The horizontal distance between the two UAVs |

The LoS log, as presented in table 4.7, logged every instance of a separation violation, with the two included UAVs, including the timestamp of the occurrence. In addition, the geographical distance between the two UAVs was also logged for each time step. Based on this data, we were able to calculate the number of unique LoS pairs, the average LoS duration, the average LoS distance, and the number of instances

where UAVs were within 10m of each other, as discussed in section 4.7.

Table 4.8: Conflict log

| Data | Description |
|---------------|---|
| Time [s] | The second the UAVs activated conflict resolution |
| UAV1 [string] | The first UAV in the conflict |
| UAV2 [string] | The second UAV in the conflict |

The conflict log, as presented in table 4.8, logged every instance where maneuvering were required in order to prevent a potential LoS. Consequently, for each time step, when UAVs needed to maneuver, the two included UAVs were logged, along with the timestamp. Based on this data, we were able to calculate the number of conflicts, as discussed in section 4.7.

Table 4.9: UAV end log

| Data | Description |
|-----------------------------------|--|
| Deletion time [s] | The second the UAV landed and was deleted from the simulation |
| UAV ID [string] | The identifier of the UAV |
| Distance flown [m] | The horizontal distance the UAV have flown |
| Distance away from coordinate [m] | The distance away from the planned destination the UAV managed to land |

The UAV end log, as presented in table 4.9, logged each of the instances of UAVs once they landed and had been removed from the simulation scene. The UAV end log collected information about the UAVs, such as the deletion time, the UAV identifier, the horizontal distance traveled, and the geographical distance from their deletion coordinate to the original destination coordinate. Based on this data, we were able to calculate the average travel time based on the start time from the start log and end time from the end log. Moreover, we were able to calculate the average route deviation based on the planned route distance compared to the distance traveled. We were able to calculate the average number of UAVs not utilizing the corridor based on the direct route compared to the planned route. Finally, we were able to calculate the direct deviation based on the planned route compared to the direct route.

4.9 Data Analysis

As discussed in section 4.8, each simulational scenario generated four separate log files. However, in their plain state, limited useful information could be drawn. As such, analysis of the data was necessary to calculate the KPIs and make sense of the results. Due to the structuring of the project and the utilization of python throughout, two different python script files were created for the data analysis portion of the thesis. The first python script file analyzed the generated log files. With this file, pandas were used to load the CSV files onto DataFrames, and based on a set of pre-defined calculational functions created based on the KPI values as discussed in section 4.7, the KPIs were calculated. Consequently, a result file would be outputted as a final result file. Moreover, the second script file was created to analyze the pooled results, in other words, calculating the mean and standard deviation, providing a final analyzed result file. In table 4.10, the structure of the final result file is presented.

Table 4.10: Data analysis output file with a description of the different stored values

| Data | Description |
|--|--|
| Average number of UAVs not utilizing the corridor [number] | The average number of UAVs that were not provided corridor access by the UTM |
| Average travel time [s] | The average travel duration for the UAVs to reach their destination |
| Average number of conflicts [number] | The average number of occurrences where UAVs needed to maneuver to avoid LoS |
| Average number of LoS [number] | The average number of unique occurrences where UAVs were not able to avoid LoS |
| Average LoS duration [s] | The average number of seconds two UAVs are violating the separation distance |
| Average LoS distance [m] | The average LoS distance between LoS pairs |
| Average route deviation [m] | The average deviation from the calculated- and provided route by the UTM |
| Average direct deviation [m] | The average direct deviation from the calculated- and provided route by the UTM |
| Average near mid-air collisions [m] | The average number of instances where two UAVs were closer than 10m from each other in a LoS |

4.10 Statistical Significance Testing

As the experimental results gathered throughout this thesis was based on random traffic simulations, in other words, random samples, to address the significance of the results, two-sample t-tests were con-

ducted. A sample, in this thesis, was defined as a set of experimental results gathered from experiments where parameters and rules were equal, with the only variance being the randomized traffic. In this thesis, the sample size was chosen to be five due to time constraints, computational power, and an initial sample comparison between sizes five and ten, where the differences did not vary to a great extent. However, ideally, even further simulations should have been conducted to achieve greater accuracy in the results.

Due to the small sample size used in this thesis, the t-test was the most viable option for significance testing. By conducting hypothesis testing between two values, we determined how certain we were that two samples were greater, lesser, or equal. Moreover, general details of how the t-tests were conducted are presented by example. For two samples, A and B, we start by calculating the mean value by using the formula presented below [84].

$$\bar{X} = \frac{\sum X}{N}$$

Here, \bar{X} is the mean value, X is the sample value, and N is the sample size. Furthermore, afterward, the standard deviation for each sample is calculated using the formula below [84].

$$\sigma = \sqrt{\frac{\sum (x_i - \bar{X})^2}{N}}$$

In the formula, σ is the standard deviation, x_i is the different sample values, \bar{X} is the sample mean, and N is the sample size. Now that we have both the mean and the standard deviation for samples A and B, we calculate the t-test statistic value, defined by t in the formula below [85].

$$t = \frac{\bar{X}_A - \bar{X}_B}{\sqrt{\frac{S_A^2}{N_A} + \frac{S_B^2}{N_B}}}$$

Now that we have the t-test statistic, we need to find the degrees of freedom. Since the standard deviations for the values in this thesis were usually different, we used the Welch's t-test formula for the degrees of freedom. The formula is as presented below [84].

$$df = \frac{\left[\frac{S_A^2}{N_A} + \frac{S_B^2}{N_B} \right]^2}{\left(\frac{S_A^2}{N_A} \right) \left(\frac{1}{N_A - 1} \right) + \left(\frac{S_B^2}{N_B} \right) \left(\frac{1}{N_B - 1} \right)}$$

Based on the currently accumulated data, we can use the t-test table [86] to conduct a hypothesis tests on the different samples. If we wish to determine if there was a significant difference or if one sample is lesser or greater than the other, we can use two-tailed or one-tailed values, respectively. Furthermore, an alpha level is chosen based on how high of confidence we wish to test the hypothesis. In this thesis, a p-value of <0.05 was chosen to determine whether something was statistically significant.

Chapter 5

Experiments

In this chapter, the experiments conducted to answer the thesis research questions as discussed in section 1.3, are presented. The experiments conducted is based on the methodological approach adopted as discussed in chapter 4. The corridor type comparison experiment is presented in section 5.1. Furthermore, for the related rules and parameter change experiments are presented in section 5.2. Finally, the corridor placements experiment is presented in section 5.3. Moreover, an additional unstructured free-flight experiment was conducted, which is presented in section 5.4.

5.1 Corridor Types

As explored in the literature, there are a variety of proposed, and some simulated, corridor types with different rules and parameters, ranging in complexity and airspace utilization. In this thesis, we have limited the scope of the corridor type research question, as presented in section 1.3, to focus on the structuring of the airspace within a corridor, essentially comparing different corridor types. As such, based on the literature discussed in chapter 3, three different corridor types were compared largely based on the proposed corridor types as presented in [8].

The first corridor type simulated in this thesis was the "bi-directional corridor". The bi-directional corridor allowed for travel in both directions of the corridor structure, with multiple concurrent Unmanned Aerial Vehicles (UAVs)s at any time. Consequently, the corridor structure consisted of two lanes, each with a width of 200m, ensuring enough room for route deviation, merging, operational error, and similar. To allow for the inclusion of various ranges of UAV specifications to access the corridor, the speed limit within the corridor was placed at 12.86 m/s. However, a consequence of the lower speed limit was that higher-end UAVs were not able to travel closer to their maximum altitude and speed limit. An illustrative figure of the bi-directional corridor is presented in figure 5.1.

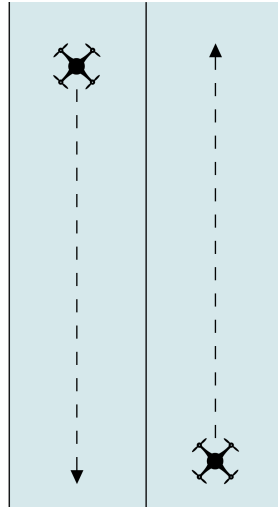


Figure 5.1: Bi-directional corridor

The second corridor simulated in this experiment was the "unstructured layered bi-directional corridor". Similarly to the bi-directional corridor, the unstructured layered bi-directional corridor allowed for multiple concurrent UAVs traveling in either direction. However, unlike the bi-directional corridor, the unstructured layered bi-directional corridor had a total of four different layers at different altitudes. By having additional altitude layers, the capacity of the corridor greatly increased, and it allowed for less complexity with growing traffic density. Similarly to the bi-directional corridor, to ensure the corridor was accessible to a range of different UAV specifications, the corridor speed limit was equal to the bi-directional corridor. As such, traffic was randomly distributed amongst the different corridor layers. An illustration of the unstructured layered bi-directional corridor is presented in figure 5.2, with the different layer altitudes presented in figure 5.3

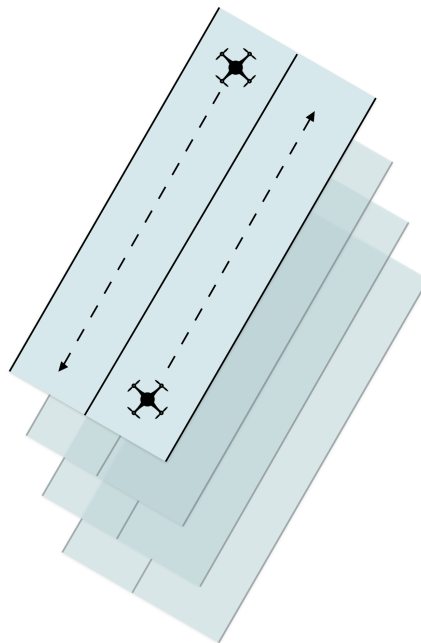


Figure 5.2: Layered bi-directional corridor

Finally, the last corridor type that was simulated in this thesis was the "structured layered bi-directional corridor". Similarly to the bi-directional- and unstructured layered bi-directional corridor, it allowed for travel in both directions with multiple concurrent UAVs. However, while the unstructured layered bi-directional corridor utilised the layers as a form of spread of the traffic, the structured layered bi-directional corridor separated the UAVs into the different layers depending on their UAV specifications. By separating the UAVs based on their specifications, all of the UAVs traveled closer to their optimal travel speed and altitude. Consequently, the lower layers of the corridors were assigned to the lower-end UAVs, while the upper layers were assigned to the higher-end UAVs. As such, the speed limits for each layer was as follows, in increasing altitude layer order, 12.86 m/s, 15.43 m/s, 18 m/s, and 20.57 m/s. However, a trade-off with this corridor, compared to the unstructured layered bi-directional corridor, was that each tier of UAV had less available airspace which they could be assigned. An illustration of the structured layered bi-directional corridor is presented in figure 5.2, while a figure of the layer segregation is presented in figure 5.4



Figure 5.3: Unstructured corridor layers

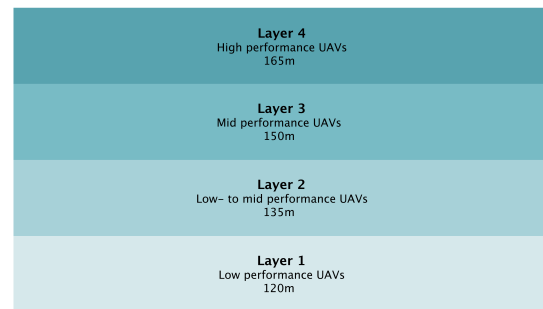


Figure 5.4: Structured corridor layers

A corridor grid placement was used for this experiment consisting of 16 junctions (4x4), with the structuring as presented in chapter 4. Moreover, in an effort to gain further insight into the different corridor types safety and efficiency impact on the traffic, three different traffic densities were simulated for each of the corridors. The first traffic density was a lower traffic density of 1,500, the second traffic density increased to 2,000, and the last traffic density increased the traffic density to 2,500 UAVs. In appendix A, and in the table A.1, the simulational specifications for the corridor types experiment are presented.

5.2 Rules and Parameters

In the previous experiment, as presented in section 5.1, we conducted a corridor type experiment to compare their effect on traffic efficiency and safety. However, this section presents the rules and parameters' experiments performed in this thesis, aimed at answering the rules and parameter research questions as presented in section 1.3. In the previous experiment, three corridor types were defined and compared, with significant differences in the utilization and structuring of the airspace between the bi-directional- and layered structured bi-directional corridor. Due to their significant differences, these two corridor types were used in the conduction of the experiments in this section, with the highest traffic density presented in the previous experiment of 2,500 UAVs. Furthermore, the same corridor placement adopted for the

corridor type experiment was utilized in the conduction of the experiments presented in this section.

Parameter changes refer to changes to the corridor or traffic that do not directly change the main rules of the corridor, rather the structural properties of the corridor, or parameters on the UAVs which does not directly effect the corridor rules. Examples of this are lane widths within the corridor, look-ahead times for the UAVs, or resolution zones. On the other hand, rule changes are how the UAVs collectively behave inside the corridor, their approach towards the corridor, or similar. For instance, some rules could be corridor speed limits, separation distances, a queue for the UAVs to access the corridor, exit altitude change when leaving the corridor, junction protocols, and similar. While there were a lot of different alternatives for rules and parameters to explore, in this thesis, we have explored three different rule and parameter changes, separation distances, speed limits, and look-ahead times as these are important elements for the efficiency and safety of the traffic.

5.2.1 Separation Distances

Separation distance is defined by the minimum distance away from each other the UAVs are allowed to operate, both inside and outside of the corridor structure. The separation distance in the previous experiment was 50m, based on observations by papers such as [6][65][87], and their experiences. However, as the corridor structure in this thesis have significant parameter and rule differences compared to the existing literature, the aim of the separation distance experiment was to explore and observe how different separation distances would effect the traffic efficiency and safety with the methodological approach taken in this thesis. In this case, with the use of the bi-directional- and layered bi-directional corridor. In table 5.1, a complete list of the different separation distances simulated are presented.

Table 5.1: A list of the different separation distances simulated for the bi-directional- and structured layered bi-directional corridor

| Separation distances [m] | 20 | 40 | 60 | 80 |
|--------------------------|----|----|----|----|
|--------------------------|----|----|----|----|

5.2.2 Speed Limits

Speed limits, similarly to ground traffic on structures such as highways, are defined by how fast the vehicles on the structure are allowed to travel. However, while a speed limit presents a rule of conduct does not mean that the vehicles will consistently follow the speed limit. A consequence of this, could be due to instances such as collision avoidance. In the previous experiment, as presented in section 5.1, consistent speed limits were simulated for the different corridor types. However, in this experiment, we explored how lower and higher speed limits might effect the efficiency and safety of the traffic for the bi-directional- and structured layered bi-directional corridor. In table 5.2, the different speed limits simulated in this experiment are presented. However, since the structured layered bi-directional corridor had different speed limits in each layer as a default, compared to the bi-directional corridor, the bottom layer was provided the presented speed limit in the table, with an increase of an additional 2.57 m/s for each layer. In other

words, if the speed limit for the base layer was 10.29 m/s, the upper layer speed limits was as follows 12.86 m/s, 15.43 m/s and 18.01 m/s.

Table 5.2: A list of the different speed limits simulated for the bi-directional- and structured layered bi-directional corridor

| Speed limits [m/s] | 10.29 | 12.86 | 15.43 | 18.00 |
|--------------------|-------|-------|-------|-------|
|--------------------|-------|-------|-------|-------|

5.2.3 Look-Ahead Times

Look-ahead times are apart of the state-based algorithm used in this thesis, as discussed in section 4.6, to find potential occurrences where UAVs would not uphold the provided separation distance. The state-based algorithm uses a look-ahead time in seconds, along with other parameters of the UAVs, as discussed in section 4.6, to look a distance into the future. However, due to the algorithmic construct of the state-based algorithm, a look-ahead time of 15s was adopted for the previous experiment, presented in section 5.1, to avoid occurrences where false conflicts would occur with on-going corridor traffic. However, in this experiment, we simulated different look-ahead times to explore their effect on the efficiency and safety on the traffic for the bi-directional- and structured layered bi-directional corridor. In table 5.3, the simulated look-ahead times are presented.

Table 5.3: A list of the different look-ahead times simulated for the bi-directional- and structured layered bi-directional corridor

| Look-ahead times [s] | 10 | 12 | 14 | 16 |
|----------------------|----|----|----|----|
|----------------------|----|----|----|----|

5.3 Corridor Placements

In order to answer corridor placement research question presented in section 1.3, a corridor placement experiment was conducted. In this experiment, we aimed to explore how different corridor placements might effect the traffics efficiency and safety. Based on this information, to gain some interesting results, six different corridor placements were explored, varying in complexity and number of junctions. The corridor placements explored were based on both the existing literature and personal adaptation. For instance, in the literature, a variety of different corridor grid networks have been simulated [6]. Furthermore, in the literature it has been suggested to place corridors above water or highways to mask the noise and visual pollution of the UAVs [55]. For this experiment, the structured layered bi-directional corridor was adopted, as presented in section 5.1, with the same three traffic densities simulated in the corridor types experiment, as presented in section 5.1.

In the experiments presented in section 5.1 and 5.2, a 4x4 grid network placement was adopted. Similarly, in this experiment, for the first corridor placement a 4x4 grid network was simulated consisting of 16 junctions covering larger portions of the simulated area. An illustration of the 4x4 corridor grid place-

ment is presented in figure 5.6. However, in addition to the 4x4 corridor grid placement, an additional 3x3 grid network was simulated for the second corridor placement. The corridor placement consists of 9 junctions, covering lesser areas, avoiding noise and visual pollution of high density traffic for larger areas. An illustration of the 3x3 grid network is presented in figure 5.5.

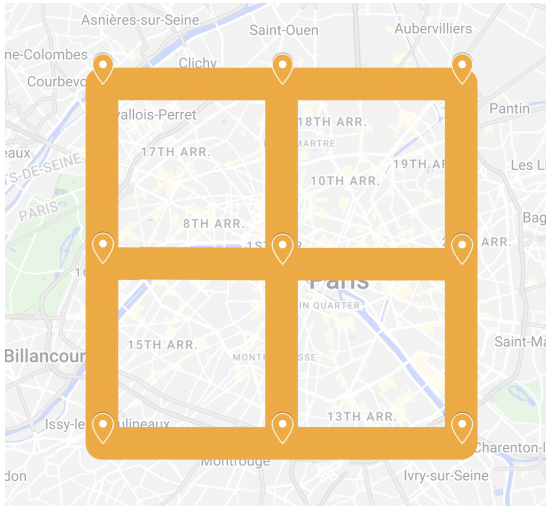


Figure 5.5: A 3x3 corridor grid network above the metropolitan area of Paris

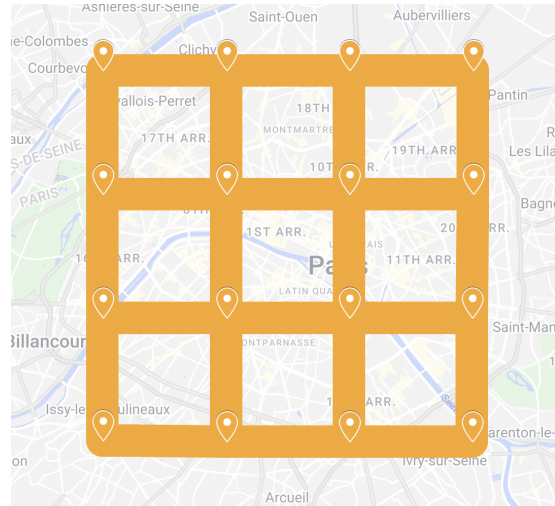


Figure 5.6: A 4x4 corridor grid network above the metropolitan area of Paris

For the third corridor placement, a corridor network was created based on smaller and larger parks in the metropolitan area of Paris. As such, a total of fourteen parks were used in the creation of the corridor network. An illustration of the park network is presented in figure 5.7. Moreover, for the fourth corridor placement, the inner ring-road of Paris was adopted, also called "Boulevard Périphérique". The "Boulevard Périphérique" is a two-way ring road around the metropolitan area of Paris and is the up-most inner ring-road. A corridor placement was constructed above the ring-road with a total of 20 junctions to best fit the ring-road. An illustration of the ring-road is presented in figure 5.8.



Figure 5.7: A corridor network based of the locations of smaller and larger parks in the metropolitan area of Paris

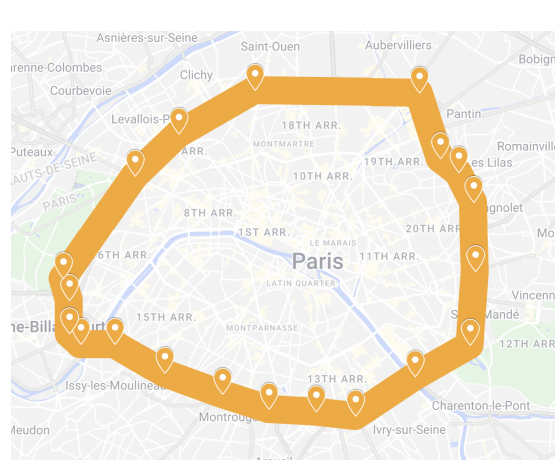


Figure 5.8: A corridor structure around the "Boulevard Périphérique" in the metropolitan area of Paris

For the fifth corridor placement, a corridor placement was adopted above the water running through the metropolitan area of Paris. The river is called the "Seine" river, and runs from the lower portion of the metropolitan area of Paris through the middle, and back to the lower area of the metropolitan area of Paris. A corridor placement consisting of 9 junction was created above the river to ensure the corridor followed the river. An illustration of the corridor river placement is presented in figure 5.9. Lastly, for the last corridor placement, the locations of larger roundabout, both with and without the right of way, was used in the creation of a roundabout network, consisting of 27 junctions. An illustration of the roundabout network is presented in figure 5.10

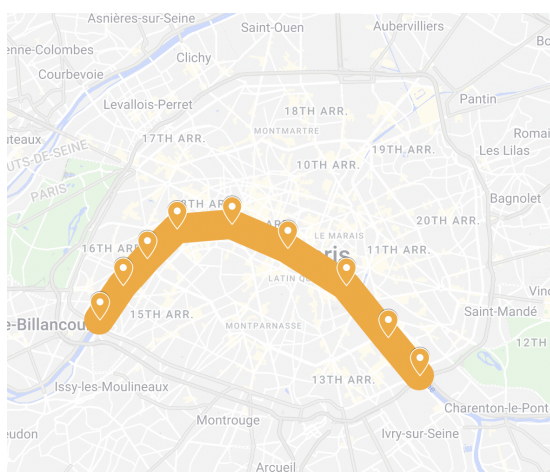


Figure 5.9: A corridor structure above the "Seine" river in the metropolitan area of Paris



Figure 5.10: A corridor structure above a roundabout network in the metropolitan area of Paris

The coordinates and interconnected junctions for the relevant corridor placements are presented in appendix B.

5.4 Unstructured Free-Flight

In addition to the main aim of the thesis, an unstructured free-flight experiment was conducted to compare the feasibility of unstructured free-flight compared to a corridor structure as part of a simple Unmanned Aircraft System Traffic Management (UTM) system. In this case, the structured layered bi-directional corridor as presented in section 5.1.

The unstructured free-flight experiment conducted in this thesis was a continuation of the work performed by the researchers in the paper [6]. From their experimental results, the researchers observed that unstructured free-flight is only feasible for up to 10,000 flights a day in an area the size of the San Francisco Bay Area, and anywhere above the given range will need a more complex and mature management system. Furthermore, the authors compared the unstructured free-flight results to a simple corridor structure in the same paper and observed benefits of structuring the airspace in such a manner. However, the comparison was limited as there was no data collected within the corridor structure, limiting the comparability of

the results. Consequently, this experiment aimed to address and fill the gap by comparing unstructured free-flight to the structured layered bi-directional corridor as presented in section 5.1.

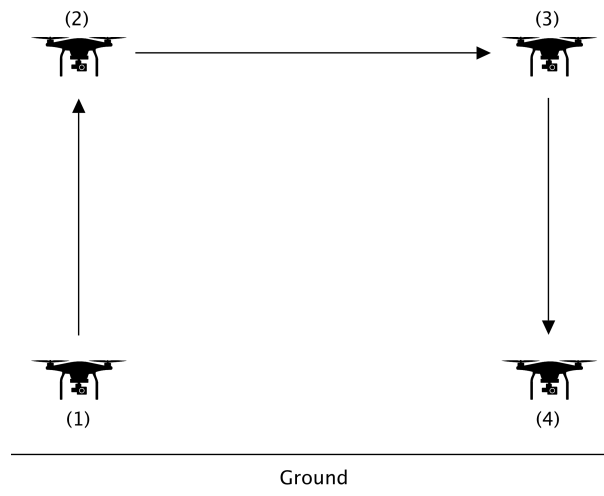


Figure 5.11: The UAV flight protocol for the unstructured free-flight simulations

In our experiment, a similar methodology was adopted as conducted by the researchers in [6]. Consequently, in this experiment, all UAVs had the same protocol, with a uniform speed and travel altitude of 120m and 15.4 m/s, respectively. In figure 5.11, the unstructured free-flight protocol is presented. In the first step, the UAV ascended to the travel altitude. In the second step, once the UAV reached the travel altitude, the UAV traveled directly to its destination. In the third step, once the UAV was close to its destination, it would decrease its speed, and once the destination was reached, it would stop and descend to the ground. Lastly, the UAV would be removed from the simulation once the ground was reached. Moreover, similar to the corridor type and placement experiments, the same three traffic densities were simulated. Lastly, more information on the traffic pattern for the corridor simulation as part of the simple UTM system is discussed in section 4.4.

Chapter 6

Results

In this chapter, the results collected from the experiments conducted, as discussed in chapter 5, are presented. The numerical results and standard deviations the statistical analysis and figures were based on are presented in appendix C. All of the figures used in the chapter use the standard deviation, represented as the vertical black line(s) on the figures. In the first section 6.1, the corridor type comparison results are shown. In subsections 6.2.1, 6.2.2, and 6.2.3, the separation distances, speed limits, and look-ahead times results for the bi-directional and structured layered bi-directional corridor are shown. In section 6.3, the results gathered from the corridor placements experiment is shown. Finally, in section 6.4 the results for the unstructured free-flight comparison to the corridor structure as part of a simple Unmanned Aircraft System Traffic Management (UTM) system is shown.

6.1 Corridor Types

In this section we discuss the results obtained from the experiment conducted on the impact of different corridor types on traffic safety and efficiency, as per the experiment presented in chapter 5, section 5.1.

The obtained results on the average number of conflicts for the different corridor types are shown in the figure 6.1. Based on the statistical analysis, it was observed a significant increase in the average number of conflicts for the bi-directional corridor compared to the unstructured- and structured layered bi-directional corridor for all traffic densities. However, no significant increasing or decreasing trends were observed between the unstructured- and structured layered bi-directional corridors. For the highest traffic density, an average of 444.6 conflicts was observed for the bi-directional corridor, compared to 256.0 and 249.8 for the unstructured- and structured layered bi-directional corridor.

From the experiment, the results obtained on the average number of Loss of Separation (LoS) occurrences for the different corridor types are presented in figure 6.2. From our statistical analysis, it was observed an increase in the average number of LoS occurrences for the bi-directional corridor compared to the unstructured layered bi-directional corridor. Furthermore, a significant increase in the average number of

LoS was observed for the bi-directional corridor compared to the structured bi-directional corridor for the two highest traffic densities. Moreover, no significant increase or decrease was observed between the unstructured- and structured bi-directional corridors for any of the traffic densities.

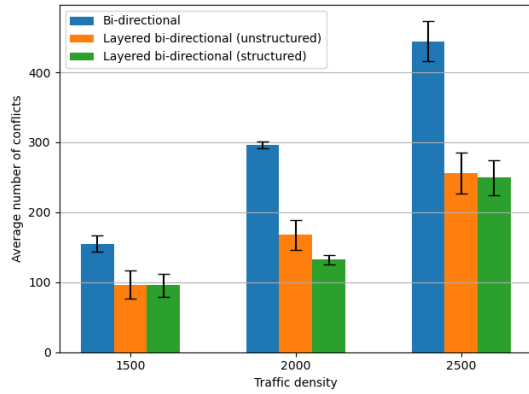


Figure 6.1: A figure of the average number of conflicts for the different corridor types

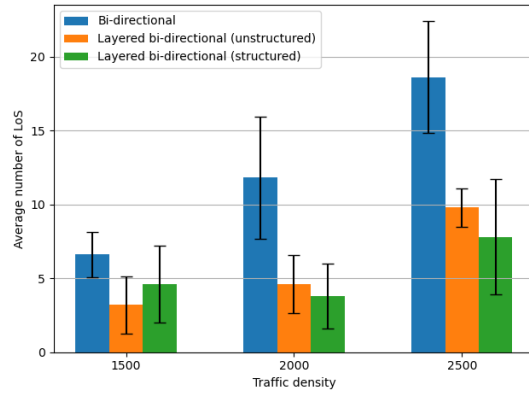


Figure 6.2: A figure of the average number of LoS for the different corridor types

The results obtained on the average LoS duration for the different corridor types and the average LoS distance for the different corridor types are shown in figures 6.3 and 6.4 respectively. From the figures, it can be observed that there is no significant trend between the different corridor types or the different traffic densities.

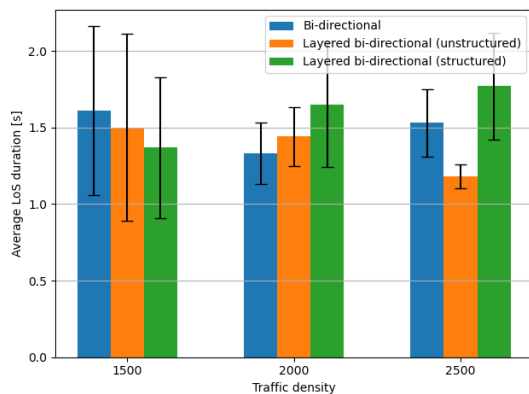


Figure 6.3: A figure of the average LoS duration for the different corridor types

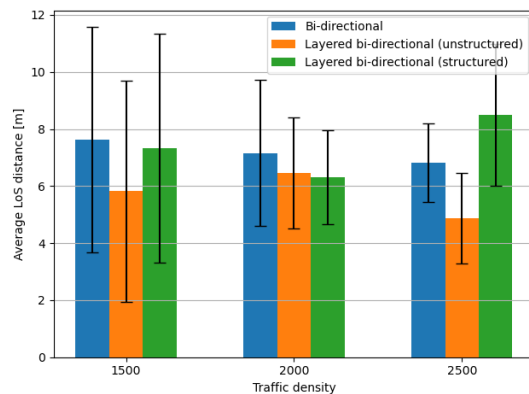


Figure 6.4: A figure of the average LoS distance for the different corridor types

The results attained on the average travel time for the different corridor types are presented in figure 6.5. The statistical analysis indicates a significant decrease in the average travel time for the structured layered bi-directional corridor compared to the other corridor types. However, no significant increase or decrease between the bi-directional and unstructured layered bi-directional corridor was observed. For the highest traffic density, it was observed an average travel time of 9.25 minutes for the structured layered bi-directional corridor and 10,62 minutes and 10,59 minutes for the bi-directional- and unstructured layered bi-directional corridor.

From the experiment, the results collected on the average route deviation for the different corridor types are shown in figure 6.6. A significant route deviation was found for the structured layered bi-directional corridor compared to the two other corridor types for all of traffic densities. However, no significant increase or decrease was found between the bi-directional- and the unstructured layered bi-directional corridor.

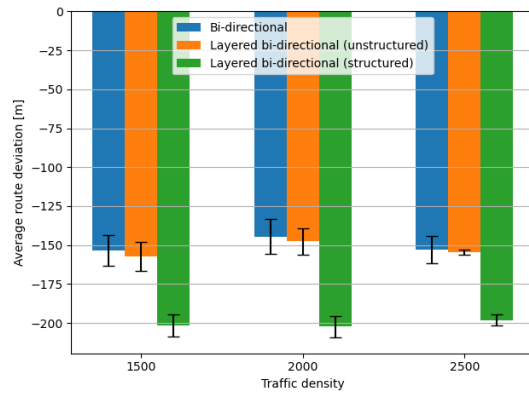
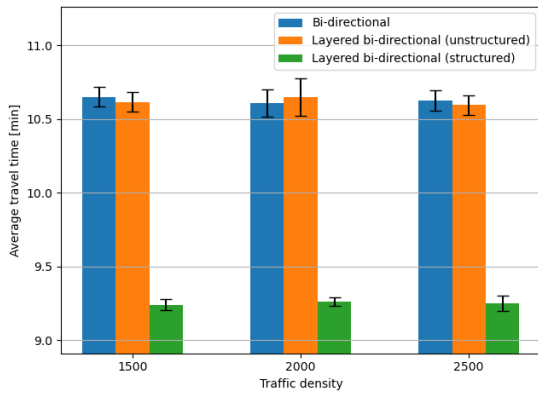


Figure 6.5: A figure of the average travel time for the different corridor types

Figure 6.6: A figure of the average route deviation for the different corridor types

The obtained results on the average number of near mid-air collisions for the different corridor types are presented in figure 6.7. Based on the simulational corridor type results, no trends or patterns were observed between any of the corridor types, or the different traffic densities.

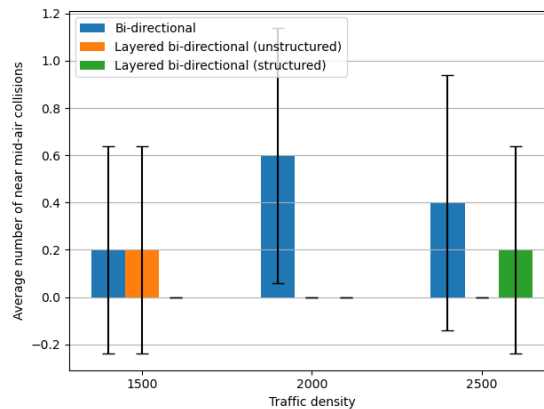


Figure 6.7: A figure of the average number of near mid-air collisions for the different corridor types

6.2 Rules and Parameters

In this sections the collected results for the rules and parameter experiments conducted, as discussed in chapter 5, section 5.2, are presented.

6.2.1 Separation Distances

In this subsection we discuss the results obtained from the separation distances experiment conducted, as per the experiment presented in chapter 5, subsection 5.2.1.

The results collected on the average number of conflicts for the bi-directional- and structured layered bi-directional corridor are presented in figure 6.8. The statistical analysis indicates a significant increasing conflict trend for both the bi-directional- and structured layered bi-directional corridors with the increase in separation distance. For the bi-directional corridor an increase from 147.8 conflicts to 856.8 conflicts was observed from the lowest separation distance to the highest. Similarly, for the structured layered bi-directional corridor it was observed an increase from 80.2 conflicts to 454.8 conflicts.

The average number of LoS occurrences for the bi-directional and structured layered bi-directional corridor are presented for the different separation distances in figure 6.9. Similarly to the average number of conflicts, as presented in the figure 6.8, an increasing trend of the average number of LoS was observed for both the bi-directional- and structured layered bi-directional corridor with the increase in separation distance. For the bi-directional corridor an increase from 6 to 38 LoS was observed with a separation distance of 20m to 80m. However, for the structured layered bi-directional corridor, an increase from 1.4 to 18.4 was observed.

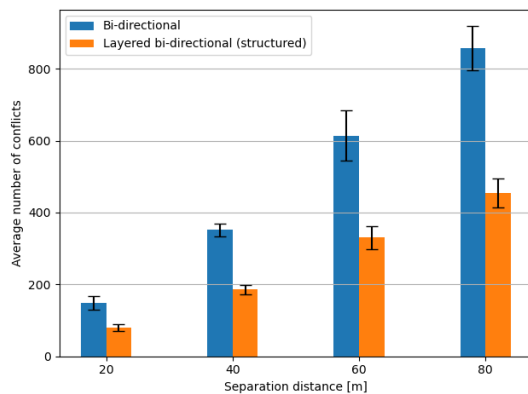


Figure 6.8: A figure of the average number of conflicts for the bi-directional- and layered bi-directional (structured) corridor for the different separation distances

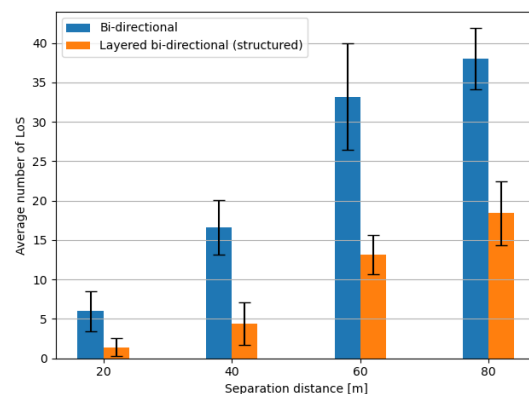


Figure 6.9: A figure of the average number of LoS for the bi-directional- and layered bi-directional (structured) corridor for the different separation distances

The attained results on the average LoS duration for the bi-directional and structured layered bi-directional corridor are presented for the different separation distances in figure 6.10. For the bi-directional corridor, it was observed a significant decrease in the average LoS duration for the lowest separation distance compared to the other separation distances. However, for the structured layered bi-directional corridor a significant decrease was observed for the lowest separation distance compared to the two highest separation distances.

The results collected on the average LoS distance for the bi-directional and structured layered bi-directional corridor for the different separation distances is shown in figure 6.11. Based on the results, the statistical analysis indicates that a significant decrease in the separation distance was observed for the lowest separation distance compared to the higher separation distances for both of the corridor types. However, no significant increase or decrease was observed between the other separation distances for either of the corridor types.

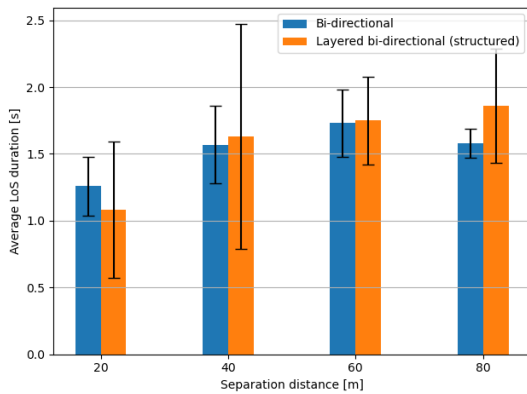


Figure 6.10: A figure of the average LoS duration for the bi-directional- and layered bi-directional (structured) corridor for the different separation distances

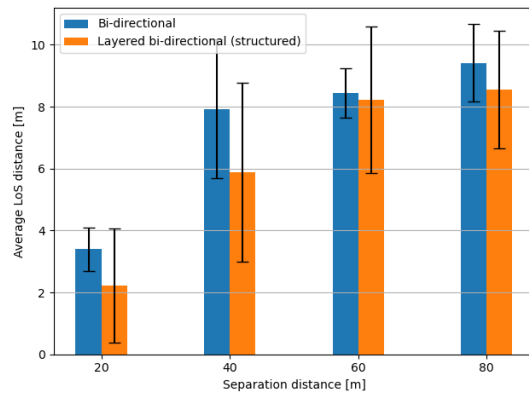


Figure 6.11: A figure of the average LoS distance for the bi-directional- and layered bi-directional (structured) corridor for the different separation distances

The attained results on the average travel time for the bi-directional- and structured layered bi-directional corridor are presented for the different separation distances in figure 6.12. Based on the statistical analysis of the results, no significant increase or decrease amongst the different separation distances for the corridor types was observed. Moreover, the results collected on the average route deviation for the different corridor types for the different separation distances is shown in figure 6.13. Based on the statistical analysis of the results, no significant increase or decrease was observed between the different separation distances for the bi-directional corridor. However, for the structured layered bi-directional corridor, a significant decrease in the average route deviation was observed with a separation distance of 60m. However, no other significant increases or decreases was observed.

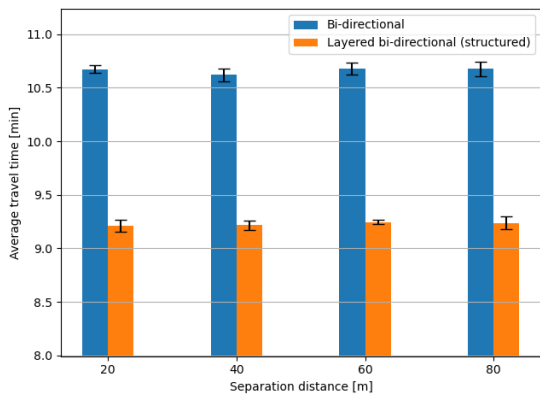


Figure 6.12: A figure of the average travel time for the bi-directional- and layered bi-directional (structured) corridor for the different separation distances

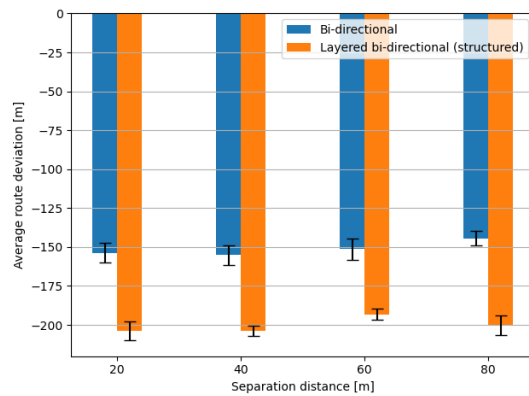


Figure 6.13: A figure of the average route deviation for the bi-directional- and layered bi-directional (structured) corridor for the different separation distances

The results collected on the average number of near mid-air collisions for the bi-directional- and structured layered bi-directional corridor is shown in figure 6.14. Based on statistical analysis of the results it was observed that for the bi-direction corridor, a significant decrease in the average number of near mid-air collisions for the highest separation distance of 80m compared to the lower separation distances. Furthermore, it was observed that a separation distance of 40m had a significant increase in the average number of near mid-air collisions compared to the other separation distances. However, for the structured layered bi-directional corridor, no significant increase or decrease was observed between any of the separation distances.

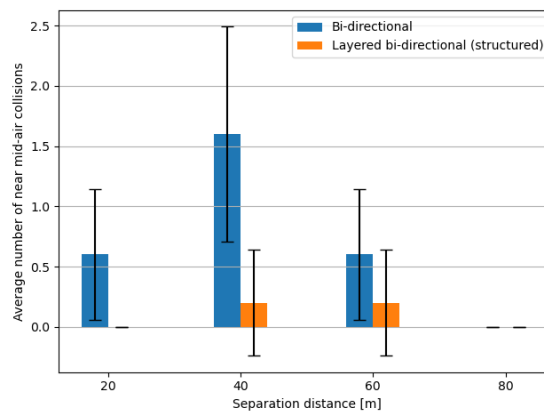


Figure 6.14: A figure of the average number of near mid-air collisions for the different separation distances

6.2.2 Speed Limits

In this subsection we discuss the results obtained from the speed limits experiment conducted, as per the experiment presented in chapter 5, section 5.2.2.

The results collected on the average number of conflicts for the bi-directional- and structured layered

bi-directional corridor for the different speed limits are presented in figure 6.15. The statistical analysis indicates a significant decrease in the average number of conflict between the lowest and highest speed limit for both corridor types. For the bi-directional corridor, a reduction of the average number of conflicts from 552.6 to 375 was observed from the lowest speed limit to the highest speed limit. For the structured layered bi-directional corridor a reduction from 252.8 to 224.25 was observed for the lowest speed limit to the highest speed limit.

The average number of LoS occurrences for the bi-directional- and structured layered bi-directional corridor for the different speed limits is shown in figure 6.16. For both the bi-directional and structured layered bi-directional corridor, the statistical analysis indicates there are no significant decrease or increase between the average number of LoS occurrences for any of the speed limits.

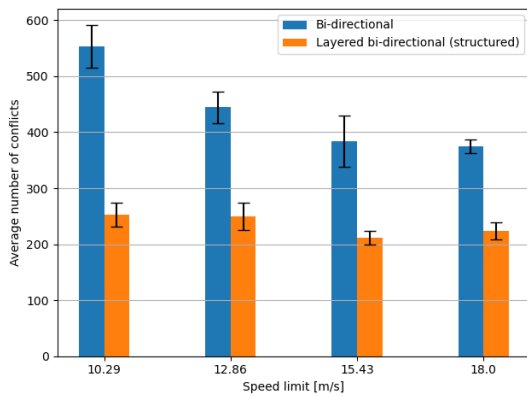


Figure 6.15: A figure of the average number of conflicts for the bi-directional- and layered bi-directional (structured) corridor for the different speed limits

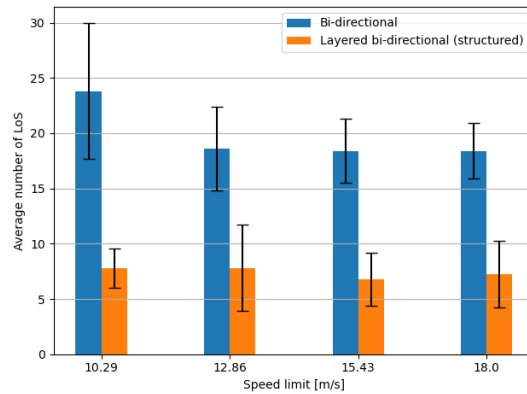


Figure 6.16: A figure of the average number of LoS for the bi-directional- and layered bi-directional (structured) corridor for the different speed limits

The average LoS duration for the bi-directional- and structured bi-directional corridor is presented in figure 6.17, while the average LoS distance is presented in figure 6.18. Based on the statistical analysis of the collected results, no significant increasing or decreasing trend was observed for either the LoS duration or the LoS distance for either of the different corridor types.

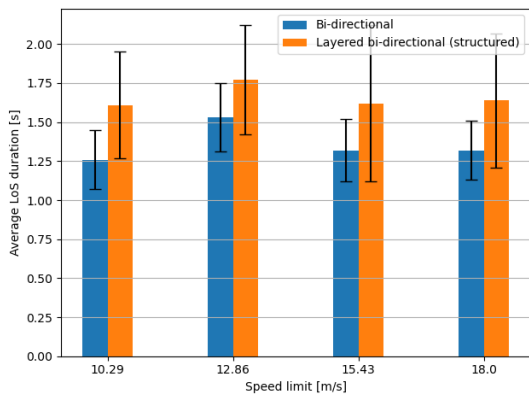


Figure 6.17: A figure of the average LoS duration for the bi-directional- and layered bi-directional (structured) corridor for the different speed limits

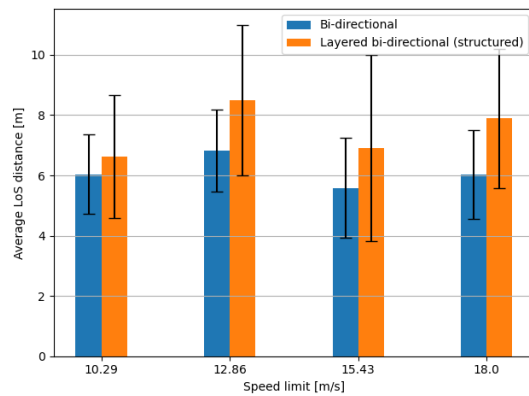


Figure 6.18: A figure of the average LoS distance for the bi-directional- and layered bi-directional (structured) corridor for the different speed limits

The average travel time is presented in figure 6.19 for the bi-directional and structured layered bi-directional corridor for the different speed limits. A significant decreasing trend in the travel time for both corridor types was observed, with a reduction from 12.34 minutes to 8.72 minutes for the bi-directional corridor from the lowest speed limit to the highest speed limit. On the other hand, a reduction from 10.27 minutes to 8 minutes was observed for the structured layered bi-directional corridor.

The results attained on the average route deviation for the bi-directional- and the structured layered bi-directional corridor on the different speed limits is presented in figure 6.20. A significant increase in route deviation was observed with an increase in the speed limit for both corridor types.

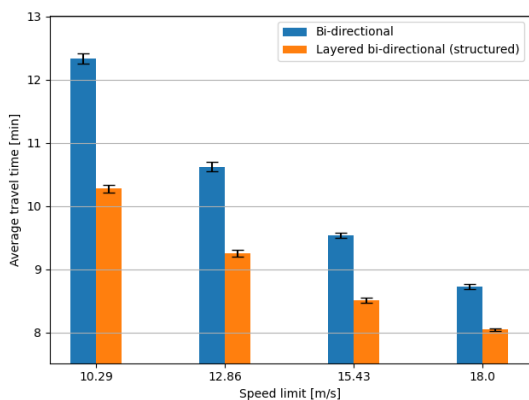


Figure 6.19: A figure of the average travel time for the bi-directional- and layered bi-directional (structured) corridor for the different speed limits

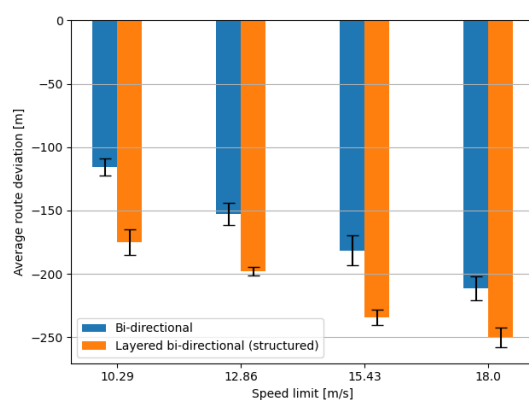


Figure 6.20: A figure of the average route deviation for the bi-directional- and layered bi-directional (structured) corridor for the different speed limits

The results attained on the average number of near mid-air collision are presented in figure 6.21. For both the bi-directional- and structure layered bi-directional corridor there was observed no significant increase or decrease between any of the speed limits for either of the corridor types.

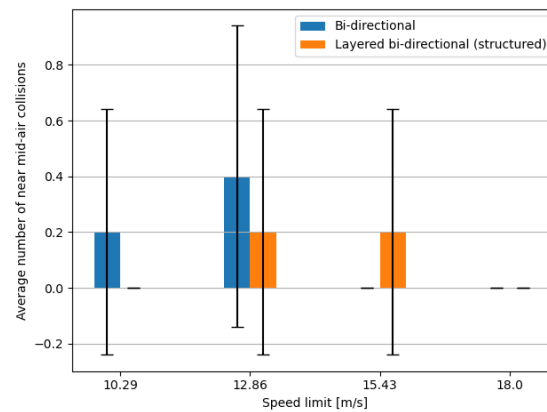


Figure 6.21: A figure of the average number of near mid-air collisions for the bi-directional- and layered bi-directional (structured) corridor for the different speed limits

6.2.3 Look-Ahead Times

In this subsection we discuss the results obtained from the look-ahead time experiment conducted, as per the experiment presented in chapter 5, section 5.2.3.

The results collected on the average number of conflicts for the bi-directional- and structured layered bi-directional corridor for the different look-ahead times are presented in figure 6.22. The statistical analysis indicates no significant increase or decrease in the number of conflicts for the bi-directional- or structured layered bi-directional corridor, despite an increase in look-ahead times.

The average number of LoS occurrences for the bi-directional- and structured layered bi-directional corridor for the different look-ahead times are shown in figure 6.23. For the bi-directional corridor no significant increase or decrease was observed between any of the look-ahead times. For the structured layered bi-directional corridor a significant decrease was observed between the lowest look-ahead time of 10s to 12s. However, no other significant increase or decrease amongst the values were observed for any of the corridor types.

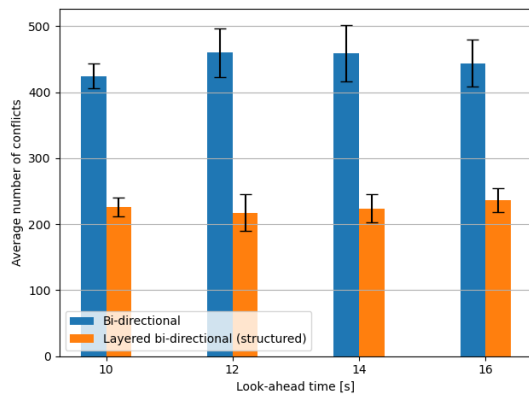


Figure 6.22: A figure of the average number of conflicts for the bi-directional- and layered bi-directional (structured) corridor for the different look-ahead times

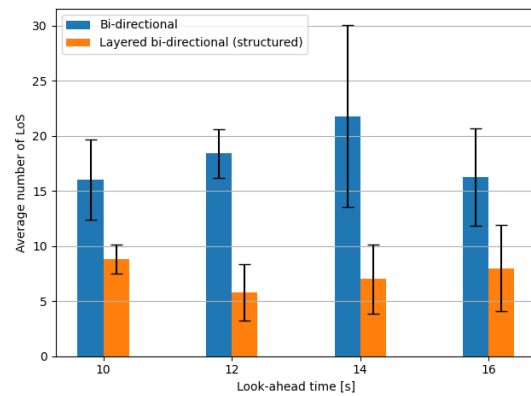


Figure 6.23: A figure of the average number of LoS for the bi-directional- and layered bi-directional (structured) corridor for the different look-ahead times

The results attained on the average LoS duration for the bi-directional- and structured layered bi-directional corridor for the different look-ahead times is shown in figure 6.24. Similarly, the collected results on the average LoS distances for the bi-directional- and structured layered bi-directional corridor for the different look-ahead times is shown in figure 6.25. A statistical analysis of the results showed that no significant increasing or decreasing trends for either of the corridor types were observed, despite different look-ahead times.

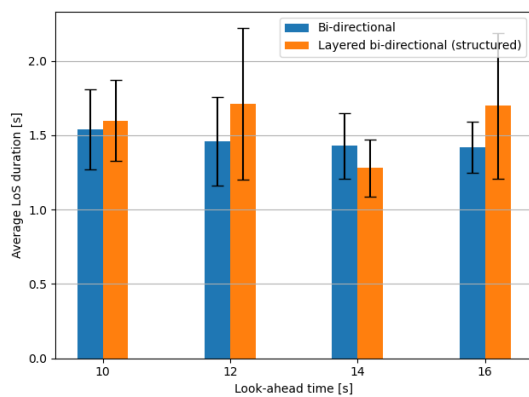


Figure 6.24: A figure of the average LoS duration for the bi-directional- and layered bi-directional (structured) corridor for the different look-ahead times

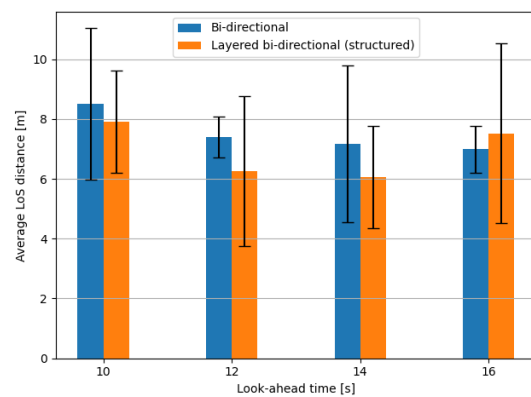


Figure 6.25: A figure of the average LoS distance for the bi-directional- and layered bi-directional (structured) corridor for the different look-ahead times

The average travel time for the bi-directional- and structured layered bi-directional corridor with the different look-ahead times is presented in figure 6.26. Moreover, in figure 6.27 the average route deviation for the bi-directional- and structured layered bi-directional corridor are presented for the different look-ahead times. The statistical analysis indicates there are no significant increases or decreases amongst the different look-ahead times and corridor types for the average travel time and the average route deviation.

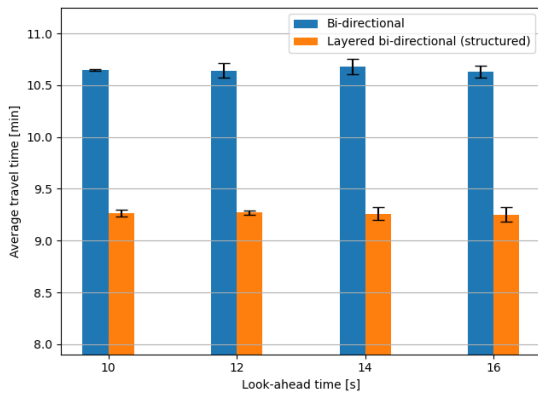


Figure 6.26: A figure of the average travel time for the bi-directional- and layered bi-directional (structured) corridor for the different look-ahead times

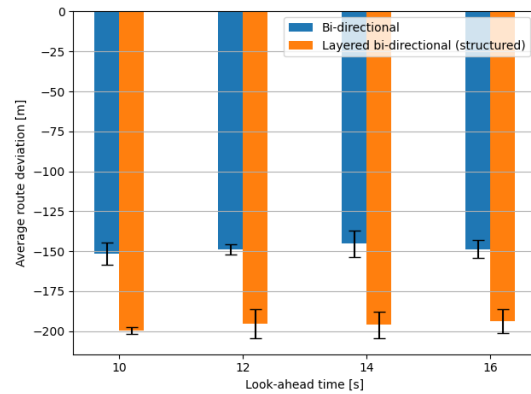


Figure 6.27: A figure of the average route deviation for the bi-directional- and layered bi-directional (structured) corridor for the different look-ahead times

The average number of near mid-air collisions for the bi-directional- and layered bi-directional corridor for the different look-ahead times are presented in figure 6.28. No significant increase or decrease was observed between any of the corridor types.

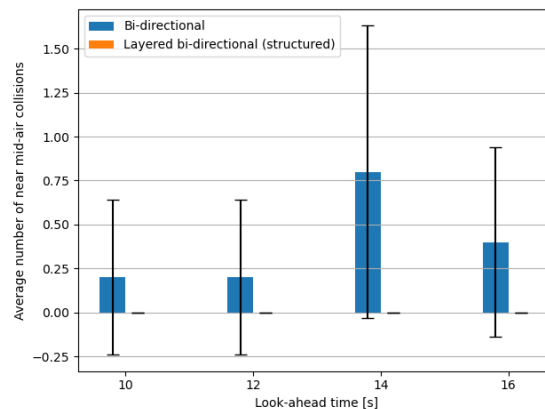


Figure 6.28: A figure of the average number of near mid-air collisions for the bi-directional- and layered bi-directional (structured) corridor for the different look-ahead times

6.3 Corridor Placements

In this section we discuss the results obtained from the experiment conducted on the impact of different corridor placements on traffic safety and efficiency, as per the experiment presented in chapter 5, section 5.3.

The data collected on the average number of Unmanned Aerial Vehicles (UAVs) not utilizing the corridor, due to viability, based on their placement, are presented in figure 6.29. From the statistical analysis, it was observed that the roundabout network had significantly less UAVs not using the corridor compared to the other corridor placements, with an average of 59 UAVs not using the corridor in the highest traffic density.

Further, it was observed that the 4x4 grid network placement was the second most accessible corridor placement, with a total of 129 UAVs not utilizing the corridor in the highest traffic density. Furthermore, the third most accessible corridor was observed to be the park network. Moreover, according to the statistical analysis it was observed that the corridor which was the least accessible was the river placement, with an average of 700 UAVs not utilizing the corridor. Lastly, no significant increase or decrease was observed between the 3x3 grid network and the ring road corridor placement.

The average UAV travel distance compared to the direct origin to destination route are presented for the different corridor placements in figure 6.30. For instance, if on average UAVs in one corridor placement travel 20% longer than their direct route, it would be represented as 1.2 in figure 6.30. From the statistical analysis, it was observed a significant increase in the direct route deviation for the two corridor grid network placements compared to the corridor placements. Furthermore, a significant increase in the direct route deviation for the 3x3 grid network was observed in comparison to the 4x4 grid network. Moreover, it was observed that the third and fourth corridor placements which deviated the UAVs the most from their direct routes were the park- and roundabout network. Lastly, it was observed that the two corridor placements with the least direct route deviation were the ring-road and river corridor placement. However, no consistent increase or decrease was observed between the two corridor placements.

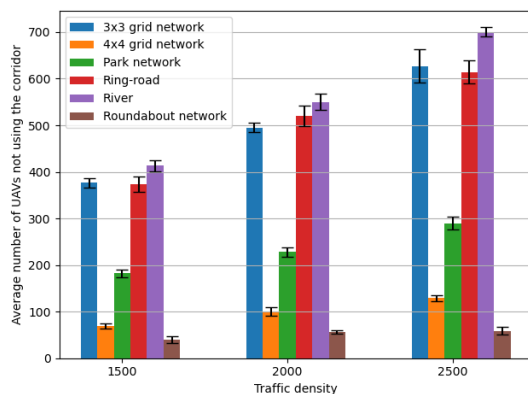


Figure 6.29: A figure of the average number of UAVs not utilizing the corridor depending on the corridor placement

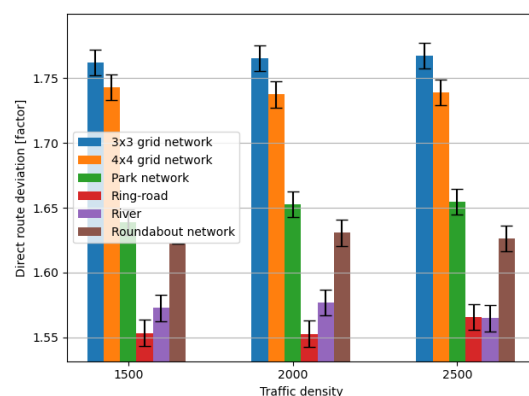


Figure 6.30: A figure of the average direct route deviation for the different corridor placements

The attained results on the average number of conflicts for the different corridor placements are presented in figure 6.31. Based on the statistical analysis conducted of the results, it was observed that the river corridor placement had a significant increase in the average number of conflicts compared to the other corridor placements, with an average of 565.2 conflicts for the highest traffic density. Amongst the other corridor placements the only significant decrease in the average number of conflicts which were observed was for the roundabout network compared to the parks- and river corridor placement. However, as the traffic density increased to 2,500, some clear differences emerged. In the highest traffic density, a significant decrease in the number of conflicts was observed for the roundabout network compared to all of the other corridor placements, with an average of 216.8 conflicts.

The average number of LoS occurrences for the different corridor placements are shown in figure 6.32. Based on the statistical analysis, no clear trend could be recognized between the different corridor placements. However, significant differences was observed throughout the different traffic densities. For the lowest traffic density, a significant increase in the LoS occurrences was observed between the 4x4 grid network and the ring-road placement. For the middle traffic density, a significant decrease in the number of LoS occurrences was observed for the ring-road and roundabout network, compared to the park network and river placement. Moreover, for the highest traffic density, the statistical analysis indicates there is a significant increase in the average number of LoS occurrences for the river corridor placement compared to the park network. Furthermore, a significant decrease in the number of LoS for the ring-road corridor placement, compared to the 3x3 grid network placement was observed.

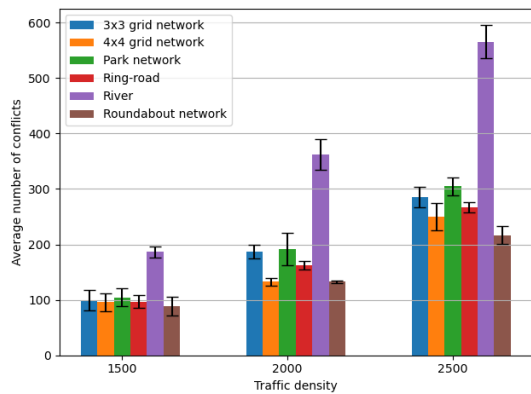


Figure 6.31: A figure of the average number of conflicts for the different corridor placements

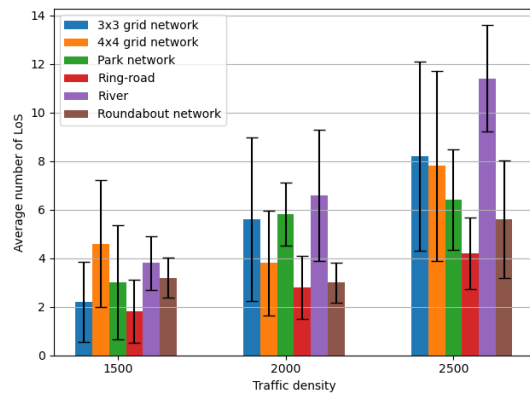


Figure 6.32: A figure of the average number of LoS for the different corridor placements

The collected results on the average the average LoS duration for the different corridor placements are presented in figure 6.33. Moreover, the attained results on the average LoS distance for the different corridor placements are presented in figure 6.34. Based on the statistical analysis no patterns or trends was observed for either of the corridor placements or the different traffic densities.

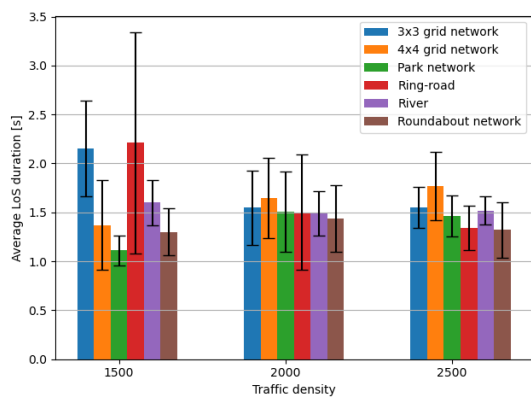


Figure 6.33: A figure of the average LoS duration for the different corridor placements

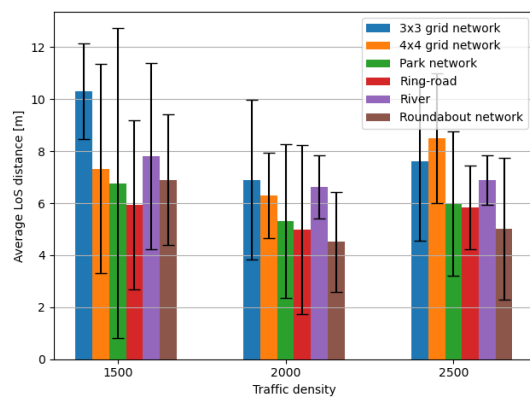


Figure 6.34: A figure of the average LoS distance for the different corridor placements

From the collected results, the average travel time for the corridor placement experiment are presented in figure 6.35. Based on the results, it was observed that the roundabout network yielded significant quicker travel times compared to the other corridor placements. Furthermore, it was observed that the 3x3 grid network and the river corridor placements significantly increased the average travel time compared to the other corridor placements. However, for the other corridor placements, no clear increasing or decreasing trend could be recognized.

The data collected on the average route deviation for the different corridor placements are presented in figure 6.36. The statistical analyses indicates a significant decrease in route deviation for the river corridor placement compared to the other placements. On the other end, the 3x3- and 4x4 grid network placement yielded the greatest route deviation for the lowest traffic density. However, no consistent significant increases or decreases were observed between them. Lastly, for the other traffic densities, the 3x3 grid network placement showed a significant increase in route deviation compared to the 4x4 grid network.

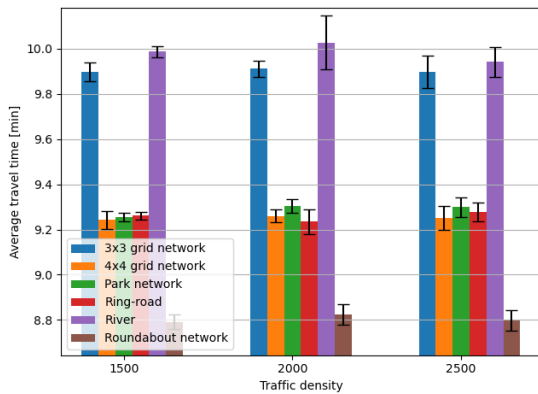


Figure 6.35: A figure of the average travel time for the different corridor placements

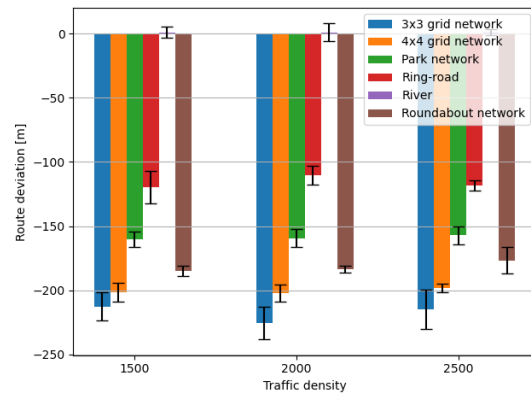


Figure 6.36: A figure of the average route deviation for the different corridor placements

From the collected results, the average number of near mid-air collisions for the different corridor placements are presented in figure 6.37. As can be seen in the figure, the only corridor placement where a near mid-air collision occurred was in the 4x4 grid network. However, no significant increase or decrease was observed amongst the different corridor placements.

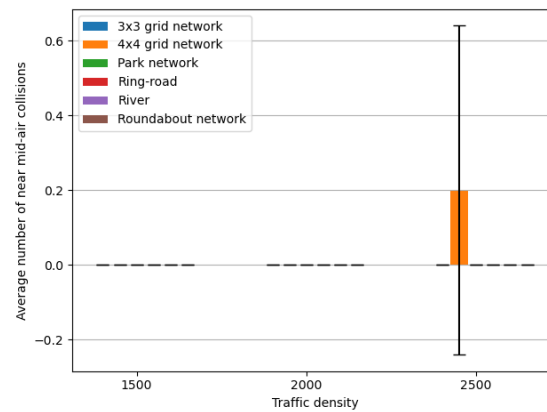


Figure 6.37: A figure of the average number of near mid-air collisions for the different corridor placements

6.4 Unstructured Free-Flight

In this section we discuss the results obtained from the experiment conducted on the comparison of unstructured free-flight compared to a corridor structure as part of a simple UTM system, as per the experiment presented in chapter 5, section 5.4.

The data attained on the average near mid-air collisions for unstructured free-flight and the structured layered bi-directional corridor are presented in figure 6.38. From the statistical analysis it was observed that the unstructured free-flight yielded a significant increase in the average number of near mid-air collisions compare to the structured layered bi-directional corridor for all traffic densities. Furthermore, it was observed a significant increase in the average number of near mid-air collisions for the unstructured free-flight. However, no significant increase or decrease was observed for the structured layered bi-directional corridor.

The average number of LoS occurrences for the unstructured free-flight and the structured layered bi-directional corridor are shown in figure 6.39. Similarly to the average number of near mid-air collisions (figure 6.38), from the statistical analysis it was observed that the unstructured free-flight showed a significant increase in the number of LoS occurrences for all of the different traffic densities, with a significant increase in the average number of LoS. On the other hand, no significant increasing or decreasing trend was observed for the structured layered bi-directional corridor. For the highest traffic density, the unstructured free-flight had an average of 88.4 LoS occurrences, compared to 7.8 LoS for the structured layered bi-directional corridor.

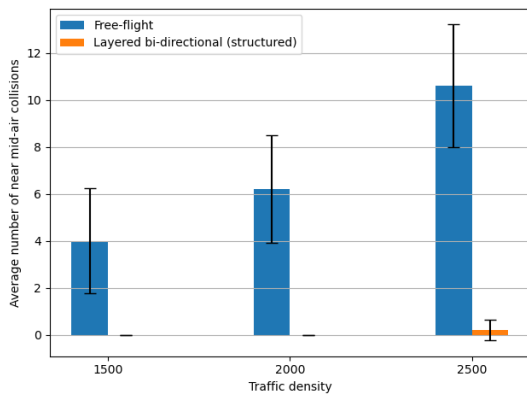


Figure 6.38: A figure of the average number of near mid-air collisions for the unstructured free-flight and layered bi-directional corridor (structured)

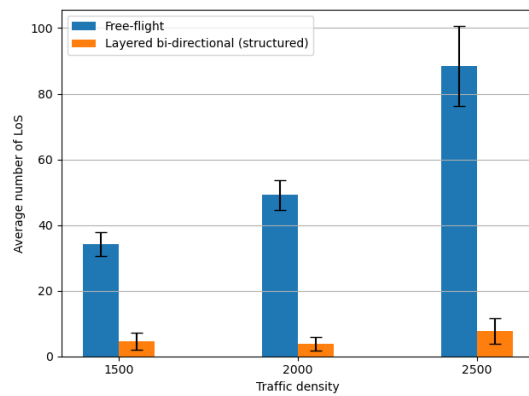


Figure 6.39: A figure of the average number of LoS for the unstructured free-flight and layered bi-directional corridor (structured)

The average LoS duration for the unstructured free-flight and structured layered bi-directional corridor are presented in the figure 6.40. The statistical analysis indicates a significant increase in the LoS duration for the unstructured free-flight compared to the structured layered bi-directional corridor. However, no significant increase in the LoS duration was observed with the increase in traffic density for either the unstructured free-flight nor the structured layered bi-directional corridor. For the highest traffic density, an average LoS duration of 4.08s and 1.77s was found for the unstructured free-flight and the structured layered bi-directional corridor respectively.

The data collected on the average LoS distance for the unstructured free-flight and the structured layered bi-directional corridor are presented in figure 6.41. Similar to the average LoS duration, as seen in figure 6.40, a significant increase in the LoS distance was observed for the unstructured free-flight compared to the structured layered bi-directional corridor. Furthermore, no significant increasing trend was observed with the increase in traffic density for either the unstructured free-flight or the structured layered bi-directional corridor.

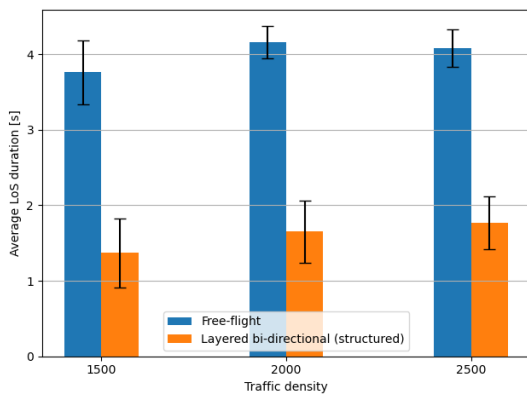


Figure 6.40: A figure of the average LoS duration for the unstructured free-flight and layered bi-directional corridor (structured)

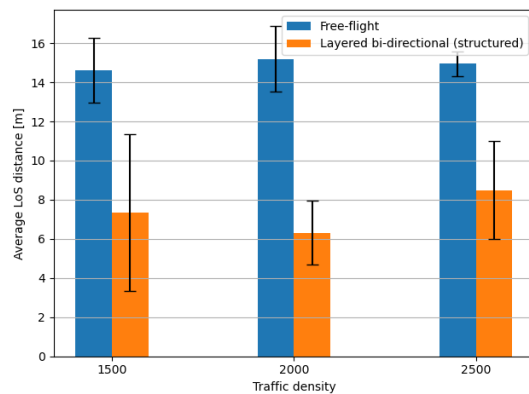


Figure 6.41: A figure of the average LoS distance for the unstructured free-flight and layered bi-directional corridor (structured)

The collected data on the average travel time for the unstructured free-flight and the structured layered bi-directional corridor are presented in figure 6.42. The statistical analysis indicates the corridor structure has a significant increase in the average travel time compared to the unstructured free-flight. For the highest traffic density, the unstructured free-flight had an average travel time of 5.32m, compared to 9.25m for the corridor structure. Moreover, no significant increasing or decreasing trend was observed for the increase in traffic density.

The average route deviation are presented for the unstructured free-flight and the structured layered bi-directional corridor in figure 6.43. The statistical analysis indicates a significant increase in the route deviation for the structured layered bi-directional corridor compared to the unstructured free-flight for all traffic densities. Moreover, no significant increasing or decreasing trends were observed with the increase in traffic density for either the unstructured free-flight or the structured layered bi-directional corridor.

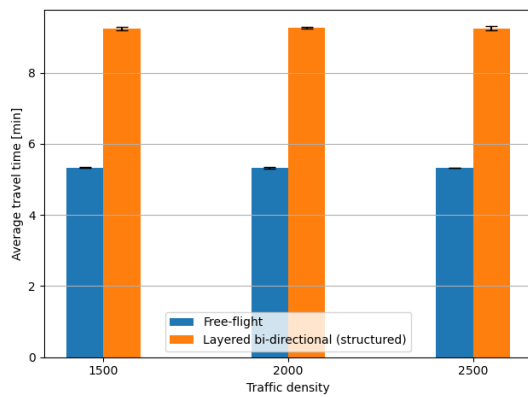


Figure 6.42: A figure of the average travel time for the unstructured free-flight and layered bi-directional corridor (structured)

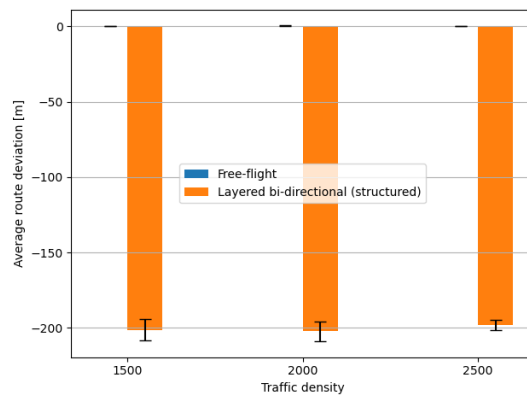


Figure 6.43: A figure of the average route deviation for the unstructured free-flight and layered bi-directional corridor (structured)

Chapter 7

Discussion

In this chapter, a discussion of the results presented in chapter 6 will be provided, discussing interpretations and conclusions from the results and positioning the results into the existing literature. Moreover, to simplify the readability of the discussion chapter, it has been divided into three sections. In the first section 7.1, we will present the work performed in this thesis. In the second section 7.2, we will interpret the results, conclude the observations, and position it into the literature. Lastly, in section 7.3, we will summarise the discussion chapter and discuss how this thesis has contributed to the existing literature.

7.1 Introduction

In this thesis, we compared three different corridor types, looking into their efficiency and safety effect on the traffic. The first corridor type compared in this thesis was the bi-directional corridor. The bi-directional corridor allowed for flights in either direction while keeping a low uniform corridor speed limit, allowing all types of Unmanned Aerial Vehicles (UAVs) to utilize it. The second corridor was the unstructured layered bi-directional corridor. Like the bi-directional corridor, it allowed for multiple concurrent UAVs traveling in either direction with a low uniform speed limit. However, unlike the bi-directional corridor, which only had a single layer, the unstructured layered bi-directional corridor had four different layers. By utilizing additional altitude layers, the corridor's capacity was more significant, spreading out the traffic. The last corridor type compared in this thesis was the structured layered bi-directional corridor. Like the unstructured layered bi-directional corridor, it allowed for travel in both directions while also utilizing four layers. However, while the unstructured layered bi-directional corridor utilized the layers to spread out the traffic, the structured layered bi-directional corridor separated the UAVs into different layers depending on the UAV specification. Consequently, higher-end UAVs could travel closer to their optimal altitude and speed without being slowed down by lower-end UAVs.

Secondly, we experimented with different rules- and parameter changes to determine how they effect the traffic in the bi-directional and structured layered bi-directional corridor. In the first experiment, we explored how different separation distances would effect the different corridors, looking into four different

separation distances, 20m, 40m, 60m, and 80m. In the second experiment, we looked into how different speed limits might effect the corridors, experimenting with four different based speed limits, 10.29 m/s, 12.86 m/s, 15.43 m/s, and 18 m/s. However, for the structured layered bi-directional corridor, the speed limits presented were for the bottom layer, meaning additional increases were applied for each additional layer. Lastly, we explored how look-ahead times would effect traffic efficiency and safety, looking into four different look-ahead times, 10s, 12s, 14s, and 16s.

Thirdly, in this thesis, we experimented with how different corridor placements might effect the efficiency and safety of the traffic. Consequently, six different corridor placements were explored, all ranging in complexity. The first corridor placement was a 3x3 grid network above Paris, created from the origin coordinate of the simulated area. The second corridor placement extended the first corridor placement, appending extra nodes on the x- and y-axis, creating a 4x4 grid network. The third corridor placement was created based on different parks in the metropolitan area of Paris, creating an overall park network. The fourth corridor placement was above the inner ring road of the metropolitan area of Paris, called "Boulevard Périphérique". The fifth corridor placement was above the "Seine" river, running through the metropolitan area of Paris. Lastly, the sixth corridor placement was above smaller and larger roundabouts.

In addition to the main aim of this thesis, we also experimented with unstructured free-flight. In this experiment, the UAVs traveled directly from their origin to their destination at a global speed limit. The experiment simulated the current large-scale Beyond Visual Line of Sight (BVLOS) operation, comparing it to a simple Unmanned Aircraft System Traffic Management (UTM) system utilizing the structured layered bi-directional corridor.

7.2 Discussion of Results

In this section we will interpret the results, conclude our findings, and position it into the literature. In subsection 7.2.1 the corridor types results are discussed. In subsection 7.2.2 the different rules- and parameter experiments are discussed. In subsection 7.2.3 the corridor placements results are discussed. Lastly, in subsection 7.2.4 the unstructured free-flight results are discussed.

7.2.1 Corridor Types

Significant differences between the corridor types were observed in the corridor type comparison experiment. The results suggest that the bi-directional corridor, on average, has more conflicts compared to the other two corridor types (figure 6.1). Likely, this is caused by the fact that the bi-directional corridor has less available airspace than the two other corridors, causing additional maneuvering to avoid Loss of Separation (LoS). However, similar conflicts were observed for both the unstructured- and structured layered bi-directional corridor despite the higher speed limits in the different layers for the structured layered bi-directional corridor. Furthermore, a similar trend was observed for the average number of LoS for the different corridor types (figure 6.2). It was observed that with the increase in traffic density, a significant

decrease in the average number of LoS could be observed for the unstructured- and structured layered bi-directional corridor compared to the bi-directional corridor. Similar to the conflicts, this was likely caused by the bi-directional corridor having less available airspace, causing more UAVs to occupy a smaller portion of the airspace, resulting in increased traffic complexity, causing difficulties in avoiding LoS. While some near mid-air collisions were observed for all of the different corridor types throughout the different simulations and traffic densities (figure 6.7), no clear pattern was observed, and the instances seem coincidental. The instances could result from complex junction traffic, where two UAVs did not have sufficient available airspace to perform an avoidance maneuver.

Interestingly, the results indicates there is no correlation between the corridor types and the average LoS duration and distance, despite the increase in traffic density (figure 6.3 and 6.4). As the structured layered bi-directional corridor had higher speed limits in the upper layers, it was believed that the LoS violations would be more severe. However, this is not the case based on the results. Moreover, as expected, since the structured layered bi-directional corridor separates the UAVs based on their specifications, the average travel time for the structured layered bi-directional corridor was significantly shorter compared to the bi-directional- and unstructured layered bi-directional corridor (figure 6.5). Lastly, a significant route deviation was observed for all corridor types, with the structured layered bi-directional corridor showing a significantly greater route deviation compared to the two other corridor types (figure 6.6). Since UAVs follow route waypoints to stay within the corridor, in sharp turns, UAVs will turn before traveling above the route waypoint to ensure the route is followed. Consequently, the faster the speed of the UAVs, the earlier the UAV will need to turn to stay on course, which explains why the structured layered bi-directional corridor has significantly greater route deviations than the other corridor types.

Based on the observations in the corridor types experiment, we have found that layering the airspace in the corridors is beneficial for the safety and efficiency of the traffic. Furthermore, we observed that structuring the layers based on different UAV specifications increased the efficiency of the traffic, allowing UAVs to travel closer to their optimal altitude and speed. Currently, the exploration and comparison of different corridor types are limited. The existing corridor literature often largely varies in the traffic and corridor concept approaches, making it difficult to compare the numerical results to existing literature. However, based on the collected results, we have observed that further efficiency and safety benefits can be yielded by segregating the corridor airspace into different layers. Consequently, corridor concepts such as [9], which have been proposed to have a single directional layer, could yield additional safety and efficiency benefits by further layering directional traffic, increasing capacity, and reducing traffic complexity. Moreover, our results support the corridor approaches proposed by the researchers in [13], of allowing UAVs to travel in different layers in the corridor structures. However, our results found it additionally beneficial to segregate traffic in different layers based on the specifications of the UAVs, allowing a vast range of different UAV types to access the corridor without slowing down faster UAVs, increasing efficiency.

7.2.2 Rules and Parameters

In this subsection a discussion of the collected and analyzed rules- and parameter results will be conducted. In the first part [7.2.2.1](#) we will discuss the separation distances results. In the second part [7.2.2.2](#) we will discuss the speed limits results. In the last part [7.2.2.3](#) we will discuss the look-ahead times results.

7.2.2.1 Separation Distances

In the separation distances experiment, as would be expected, an increase in the separation distance resulted in an increasing conflict trend for both of the corridor types (figure [6.8](#)). Since the increase of separation distance increases the area around the UAVs, which are prohibited for other UAVs to operate within, conflicts will more commonly occur due to the less accessible airspace. Consequently, an increasing trend was expected. Furthermore, a similar trend was observed for the average number of LoS occurrences for both of the corridor types (figure [6.9](#)). Similarly to the average number of conflicts (figure [6.8](#)), the same trend was expected. Due to the decrease in available airspace, the traffic becomes more complex, and there is less available airspace to both operate and maneuver, causing an increase in LoS. For the average number of near mid-air collisions (figure [6.14](#)), while there was one occurrence in both the 40m and 60m separation distance for the structured layered bi-directional corridor, no significant increase or decrease was observed. However, a significant increase was observed for the 40m separation distance compared to the other separation distances for the bi-directional corridor. However, further experiments will need to be conducted to verify that a separation of 40m is less safe than a lower or higher separation distance. The instance could also have been coincidental, which is why additional simulations should have been conducted for each scenario, in order to get more accurate results. Moreover, it was observed that the shortest separation distance of 20m caused a lower LoS duration and distance compared to the higher separation distances for both corridor types (figure [6.11](#)). Similar to both the average number of conflicts and the average number of LoS, this is likely due to the additionally available airspace and the lesser area to violate, causing the LoS duration and distance to be less. Interestingly, a trend could not be observed. However, this could be caused by a low traffic density or even the effectiveness of the Conflict Resolution (CR) algorithm.

Overall, the results indicate that a separation distance of 20m is beneficial for both corridor types in terms of efficiency and safety. The observations made in this thesis support the findings by Busulu et al. in the papers [[6](#)][[71](#)]. The authors observed that a lower separation distance decreased the observed clusters. Similarly, in this thesis, we observed that a decrease in separation distance decreased the number of conflicts and the general complexity of the airspace and operations within the corridor. Moreover, this thesis further supports the findings by Aarts et al. in the paper [[69](#)]. The authors found that larger separation distances reduced the capacity of the corridor grid network. Similarly, in this thesis, it was observed that an increase in separation distance increased the complexity of the corridor airspace and consequently limited its capacity. However, in the paper [[68](#)], written by Ho et al., the authors observed that an increase in separation distance increased the route deviation. In this thesis, no evidence suggests any significant

increase in route deviation with the increase of separation distance, despite an increase in conflicts. However, this could be caused by the complex environment and routes utilized in this thesis compared to the direct routes simulated by the authors. On the other hand, the authors further observed that an increase in separation distance increased the number of LoS, which was also observed in this thesis. However, while a low separation distance of 20m in this thesis caused the least number of conflicts and LoS, the separation between UAVs during LoS is significantly less than the higher separation distance, not leaving significant room for error. Furthermore, the results are based on perfect global knowledge and perfect weather conditions, which are not guaranteed in the real world, and, depending on the speed of the UAVs, different separation distances might be beneficial. For instance, two UAVs traveling at 20 m/s, with a separation distance of 20m, could be problematic if rapid speed reductions are performed. However, if two UAVs are traveling at a speed of 10 m/s with a separation distance of 20m, some room for error is present. Consequently, even higher traffic densities and greater sample sizes should be performed to explore the viability of such a small separation distances.

7.2.2.2 Speed Limits

In the speed limits experiment, it was observed a reduction in the average number of conflicts for the higher speed limits compared to the lower speed limits (figure 6.15). This was unexpected due to an increase in speed limit increases the look-ahead distance of the UAVs, which increases the possibility of conflicts being raised. However, a plausible explanation for the result is that a higher speed limit results in fewer concurrent UAVs utilizing the corridor simultaneously, consequently causing fewer conflicts. However, while a reduction in the number of conflicts was observed for the higher speed limits, no significant decrease was observed for the LoS occurrences (6.16)). With a decrease in the average number of conflicts, we would expect the average number of LoS to go down due to fewer potential LoS scenarios. However, with an increase in the speed limit, we would also expect it to be more challenging to avoid sudden potential LoS scenarios. Consequently, a trade-off is potentially occurring. Another possible explanation is that the traffic density was too low to observe any significant differences, or the sample size was too low to find a significant difference. Moreover, as expected, the average travel time significantly decreased for each increase in speed limits for both corridor types 6.19. Lastly, the results also indicate a significant increase in the route deviation with the increase in the speed limit (figure 6.20). This is due to the UAVs maneuvering earlier from the corridor waypoints to stay on route, and such turns are more rapidly performed with the increase in speed limit.

Overall, the results indicate that the different corridor types benefit from having a higher speed limit in terms of efficiency and safety. The observations in this thesis support the findings by Aarts et al. in the paper [69], where the authors found that by increasing the corridor speed limit the maximum density was not effected, while the network flow rate increased, overall improving the efficiency of their traffic. In this thesis, similar observations were made. However, unlike the authors, in this thesis, we also observed safety benefits to the traffic with an increase in speed, causing fewer conflicts and ultimately less complex corridor traffic. Similar observations were made by Sacharny et al. in the paper [66], supporting the indication

of both safety and efficiency improvements with an increase in speed limit.

7.2.2.3 Look-Ahead Times

In the look-ahead time experiment, no significant trends could be drawn from the results. Initially, it was expected that an increase in the look-ahead time would cause more conflicts due to the increased look-ahead distance while also causing fewer LoS due to earlier maneuvering. However, the results indicate no significant trends for either the average number of conflicts or the average number of LoS (figure 6.22 and 6.23). The lack of significant results could be a consequence of a conservative look-ahead range, too low traffic density, or even a too small sample size. However, as a state-based Conflict Detection (CD) algorithm is used to detect conflicts, a relatively low look-ahead time was used to avoid false conflicts with the ongoing traffic in the corridor. Consequently, it would have been interesting to simulate even higher traffic densities or adapt the state-based CD algorithm to dynamically discover potential conflicts based on its future behavior, simulating with even greater look-ahead times. Another approach could have also been to divide the ongoing traffic into additionally different layers, as proposed in the paper [9], to then simulate with even higher look-ahead times.

Overall, no significant increases or decreases were observed for the different look-ahead times for either of the corridor types. The observations made in this thesis does not corresponding to the observations made by Ho et al. in the paper [68]. The authors found that a greater look-ahead time increased the route deviation. However, in this thesis, no significant increase or decrease in the route deviation was observed for the different corridor types. However, this is likely caused by the more complex environment and the fact that the UAVs rarely fly in a direct route like the UAVs in the paper written by the authors, causing the average route deviations to be more difficult to distinguish, in addition to what has already been mentioned.

7.2.3 Corridor Placements

In the corridor placement experiment, significant differences were observed in the level of accessibility depending on the placement of the corridor (figure 6.29). As expected, the results indicate that the corridor placements with more significant numbers of junctions, extending over larger central areas of the metropolitan area of Paris, are the most accessible corridors. Consequently, corridor placements such as the 4x4 grid network, park network, and the roundabout network, were the most accessible corridor placements. On the other hand, placements with fewer junctions, such as the 3x3 grid network, ring-road, and river placement, were significantly less accessible. Moreover, the results indicate that the corridor placement significantly effects the distances the UAVs need to travel to reach their destination. On average, it was observed that the grid networks required the UAVs to travel longer than the other corridor placements. On the other hand, the river and ring-road placement required the UAVs to travel the shortest distances (figure 6.30). However, the river and ring-road placement were also the two placements that were the least accessible, meaning the average direct route deviation will be effected by the number of UAVs not using the corridor and flying directly to their destination. Moreover, significant differences in the average number

of conflicts were observed (figure 6.31). Significant increases in the average number of conflicts compared to the other placements were observed for the river placement. On the other hand, the roundabout network had the least number of conflicts. Due to the shortness and compactness of the river placement, UAVs are more likely to accumulate in the junctions, ultimately causing additional conflicts. However, as the roundabout network expands over greater areas, the traffic is more spread, ultimately causing fewer conflicts. For the average LoS, no clear trends or patterns were observed (figure 6.32). However, as the traffic density increased to 2,500, a significant increase in the number of LoS occurrences was observed for the river placement, which is likely due to the lack of available airspace due to the number of UAVs utilizing the corridor. For the average travel time, it was observed that the roundabout network yielded the shortest travel time, while the 3x3 grid network and the river placement yielded the longest (figure 6.35). Due to the spread and number of junction points for the roundabout network, UAVs have more accessible and efficient routes to their destination, causing a shorter travel time. However, the 3x3 grid network and the river placement have less spread and fewer junction points, causing UAVs to be assigned less efficient routes.

Overall, the results indicate that the corridor placement has a significant impact on the efficiency and safety of the traffic. The results indicate that a more spread-out corridor placement with a high number of junctions is beneficial for both efficiency and safety, in this case, the roundabout network. Moreover, it was observed that the number of conflicts and LoS occurrences was prevalent for corridor placements with fewer junction points, causing congestion and complex traffic patterns, reducing both traffic safety and efficiency. However, the traffic complexity was observed to be reduced by spreading out the traffic. The results observed in this thesis support the findings by Sacharny et al. that different corridor placements affect the safety of the traffic [66]. The authors found that the number of conflicts differed depending on three different corridor placements, with the grid structure being the less safe placement. Interestingly, a similar observation was made in this thesis. We observed that the 3x3- and 4x4 grid networks yielded significant conflicts compared to the more expanded and complex corridor placement for higher traffic densities. Moreover, this thesis supports the findings of Oosedo et al., who observed that coverage and efficiency are improved by having a more spread-out corridor network [65]. However, while the observations in this thesis are comparable to the two papers, different approaches and aims can be recognized. In the paper [66], the authors created a corridor network based on vertiports, where UAVs traveled to and from different vertiports, simulating a package delivery system. On the other hand, in the paper [65], the authors created on-demand corridors based on static vertiports, where only one UAV utilized the corridor at a single time delivering packages within a radius. In this thesis, we simulated random traffic in the metropolitan area of Paris, where the UAVs utilized a static corridor with different placements, observing the traffic safety and efficiency impact in terms of accessibility, conflicts, LoS, travel time, route deviation, and more.

7.2.4 Unstructured Free-Flight

In the unstructured free-flight experiment, as expected, a significant increase in the number of near mid-air collisions was observed for the unstructured free-flight compared to the structured layered bi-directional corridor (figure 6.38). Since the structured layered bi-directional corridor relies on a great level of information sharing amongst the UAVs and structuring of the airspace, they can keep a safe distance from one another. However, as the unstructured free-flight relies on simple onboard instruments, a significant decrease in safety can be recognized. Furthermore, a similar pattern was observed for the average number of LoS occurrences (figure 6.39). An immense LoS complexity growth was observed for the unstructured free-flight compared to the structured layered bi-directional corridor. Additionally, a significant increase in both the LoS duration and distance was observed for the unstructured free-flight, with more than double the LoS duration for the unstructured free-flight and slightly below double the average LoS distance (figure 6.40 and 6.41). However, as the unstructured free-flight allows for UAVs to travel the shortest route to their destination, a significant decrease in the average travel time was observed for the unstructured free-flight compared to the structured layered bi-directional corridor (figure 6.42).

Overall, it was observed that the simple UTM system utilizing the structured bi-directional corridor yielded significant safety improvements compared to the unstructured free-flight. However, the increased safety of the structured layered bi-directional corridor came at the expense of efficiency, as the UAVs, on average, travel further to reach their destination. Our observations support the findings and claims by Bulusu et al. that unstructured free-flight is only feasible up until a certain point and that a mature management system is required in order to sustain a level of safety [6]. Moreover, our observations further support the claim of another paper published by Bulusu et al. that cooperative conflict resolution increases the feasibility of high-density traffic [71].

7.3 Summary

In this thesis, an exploration of corridors as part of a simple UTM system has been explored, looking into different corridor types, rules, parameters, and placements, while also exploring unstructured free-flight. The literature on the topic of corridor exploration was found to be limiting, with varying degrees of realistic simulations and a range of different corridor concepts. Furthermore, most of the literature uses the concept of vertiports to simulate traffic or even generate traffic directly into the airspace. However, in reality, the traffic will likely be more dynamic, and UAVs will Vertical Take-Off and Landing (VTOL) in available airspace. In this thesis, we have contributed to the literature by exploring three different corridor types in a more realistic setting, observing characteristics of three different corridor types which might be beneficial in terms of efficiency and safety for the improvements and insight into future corridor development. Furthermore, in this thesis, we have contributed to the literature by exploring different rules and parameter changes to two different corridor types, exploring how they would effect the efficiency and safety of the traffic.

The literature on how different corridor placements might effect the efficiency and safety of traffic was also found to be limiting, with papers only addressing that various factors will limit the available airspace and that corridors will most likely be restricted to operate above highways, road networks, rivers, or similar. Furthermore, parts of the literature have observed that different vertiport placements and interconnecting networks effect efficiency and safety of the traffic. However, these papers have not addressed more realistic traffic and placements and have collected limited data. Consequently, in this thesis, we have contributed to the literature by simulating and comparing different corridor placements, looking into their effect on the safety and efficiency of the traffic, with more realistic traffic patterns as part of a simple UTM system, simulating suggested placements such as above rivers and ring roads, as well as placements simulated in the literature, such as different grid networks.

Lastly, the thesis has contributed to the literature by simulating and comparing unstructured free-flight with a corridor structure as part of a simple UTM system, comparing their efficiency and safety impact on the traffic. While a similar experiment has previously been conducted in the literature [6], the corridor structure compared was oversimplified by not logging data within the corridor, limiting its comparability. Therefore, in this thesis, we have contributed to the literature and covered the gap by simulating a more realistic corridor structure and comparing it to unstructured free-flight with even further data.

Chapter 8

Conclusions and Future Work

This chapter concludes the thesis by providing a brief summary and presenting the key findings. Furthermore, a list of possible future directions for the work conducted in this thesis will be presented.

8.1 Conclusion

With the increasing interest and utilization of Unmanned Aerial Vehicles (UAVs) current predictions and simulations of the future airspace have found that the existing approach toward UAV operation is not sufficient to ensure traffic safety. To cope with the future demand, structuring the airspace has been found beneficial and necessary. As such, various Unmanned Aircraft System Traffic Management (UTM) concepts have been proposed on how to manage the future airspace, with various concepts suggesting the adaptation of UAV corridors. UAV corridors are similar to roads and highways and provide rules of engagement to navigate and improve traffic safety. Due to the complexity of the urban and rural environments, the operational safety, social acceptance, integration into the existing Air Traffic Management (ATM), technological capabilities, and more will likely restrict the allowed operational airspace. As such, future corridor placements and UAV operation will need to confine to future rules and regulations.

Currently, the exploration and comparison of different corridor types, rules, parameters, and placements are limited. Their exploration is essential in determining beneficial characteristics for traffic efficiency and safety. Therefore, in this thesis, we aimed to explore different corridor types, comparing their efficiency and safety impact on the traffic while also exploring how different rules and parameters might effect traffic efficiency and safety for two of the corridor types simulated in this thesis. Additionally, we aimed to explore how different corridor placements might effect the efficiency and safety of the traffic.

In order to answer the research questions in this thesis, we created a simulational environment in the BlueSky simulator. We adopted the metropolitan area of Paris as our simulational area and created randomized UAV traffic across a twelve-hour period to simulate future traffic demand. Furthermore, four different UAV specifications were used to represent four different tiers of UAVs. Corridor structures were

created based on geographical coordinates and were adapted to the experiments conducted. To manage the airspace, a simple UTM system was created, permitting UAVs access to the airspace and corridor routes to reach their destination, if viable.

In our first experiment, we compared three different corridor types with different airspace structuring, comparing their efficiency and safety impact on the traffic. In our second, third, and fourth experiment, we conducted rules- and parameter change simulations on two of the corridor types compared in this thesis, explicitly exploring separation distances, speed limits, and look-ahead times. For our fifth experiment, we compared six different corridor placements on their efficiency and safety impact on the traffic. Lastly, in addition to the main aim of this thesis, we conducted an unstructured free-flight experiment, comparing the unstructured free-flight to a simple UTM system utilizing a corridor structure in terms of efficiency and safety.

For our corridor type experiment, we observed that different corridor types do have an effect on the efficiency and safety of the traffic. We found that layering the corridor airspace into different layers is beneficial for safety and efficiency of the traffic. Furthermore, we found that structuring the corridor airspace into different layers depending on the specifications of the UAVs increases the efficiency of the traffic without decreasing the safety. For the parameter and rule change experiment, it was observed that a lower separation distance of 20m increases both the safety and efficiency of both the corridor types simulated. Secondly, it was observed that increasing the speed limit within both of the corridor types increased both efficiency and safety of the traffic. Lastly, it was observed that there was no change in the safety and efficiency by changing the look-ahead time. For the corridor placement experiment, we observed that different corridor placements do have an effect on the efficiency and safety of the traffic. We observed that a corridor placement expanding from the center of the simulated area with a higher number of junctions increased the safety and efficiency of the traffic. In addition to the main aim of the thesis, we also observed that a simple UTM system utilizing a corridor structure significantly improved the safety of the traffic compared to unstructured free-flight.

8.2 Future Work

Various interesting future work topics have been recognized through the exploration and experimentation with different corridor types, rules, parameters, corridor placements, and unstructured free-flight.

- A state-based algorithm was used for all experiments in this thesis. However, its algorithmic structure limited possible look-ahead times, speed limits, and separation distances which could be adopted in a corridor structure with ongoing traffic. Consequently, as an extension of this work, future work should focus on how to make the algorithm dynamically recognize the future behavior of the UAVs, eliminating false conflicts.
- This thesis explored three different corridor types. However, the literature on the simulational com-

parison of different corridor types is still limited, and further research should be conducted to observe other beneficial corridor characteristics. For instance, future work could focus on segregating ongoing traffic in additional layers, and comparing it to the results collected in this thesis.

- Access protocols were neglected for the corridors in this thesis. Therefore, it would be interesting to experiment with different access protocols, looking into methods of queuing and merging traffic, comparing their efficiency and safety impact on the traffic compared to the more dynamic self-managed approach adopted in this thesis.
- The same entrance and exit protocol were used in this thesis for all experiments. However, different protocols could be compared, exploring their impact on the safety and efficiency of the traffic.
- For Conflict Resolution (CR), both heading and speed changes were allowed in this thesis. However, future work could explore different CR methods impact on the efficiency and safety of the traffic.
- For the corridor placements experiment conducted in this thesis, the junctions of the geographical based corridor placements were randomly selection. However, future research could explore if consistent entrance and exit junctions would effect the results. For instance, exit and entrance junctions every 400m on the corridor structure.

References

- [1] Amazon, *Amazon: Prime air*, (Last accessed: 23.05.2022). [Online]. Available: <https://www.amazon.com/Amazon-Prime-Air/b?ie=UTF8&node=8037720011>.
- [2] Military Advantage, *Military drones*, (Last accessed: 23.05.2022). [Online]. Available: <https://www.military.com/equipment/drones>.
- [3] Santosh Devasia and Alexander Lee, "Scalable low-cost unmanned-aerial-vehicle traffic network", *Journal of Air Transportation*, vol. 24, no. 3, pp. 74–83, 2016.
- [4] Therese Jones, "International commercial drone regulation and drone delivery services", RAND Santa Monica, CA, USA, Tech. Rep., 2017.
- [5] SESAR Joint Undertaking, *Europe needs to prepare for drone market boom, says new study*, (Last accessed: 23.05.2022), 2016. [Online]. Available: <https://www.sesarju.eu/newsroom/all-news/europe-needs-prepare-drone-market-boom-says-new-study>.
- [6] Vishwanath Bulusu, Raja Sengupta, and Zhilong Liu, "Unmanned aviation: To be free or not to be free?", in *7th International Conference on Research in Air Transportation*, 2016.
- [7] Nichakorn Pongsakornsathien, Suraj Bijjahalli, Alessandro Gardi, Angus Symons, Yuting Xi, Roberto Sabatini, and Trevor Kistan, "A performance-based airspace model for unmanned aircraft systems traffic management", *Aerospace*, vol. 7, no. 11, p. 154, 2020.
- [8] An Binh Nguyen, "Analysis of corridor type routing in unmanned air traffic management (utm)", M.S. thesis, University of South-Eastern Norway, 2020.
- [9] SESAR Joint Undertaking, "Catalogue of generic conops", 2020.
- [10] Karthik Balakrishnan, Joe Polastre, Jessie Mooberry, Richard Golding, and Peter Sachs, "Blueprint for the sky: The roadmap for the safe integration of autonomous aircraft", *Airbus UTM*, San Francisco, CA, 2018.
- [11] Quan Quan, Mengxin Li, and Rao Fu, "Sky highway design for dense traffic", *IFAC-PapersOnLine*, vol. 54, no. 2, pp. 140–145, 2021.
- [12] Lima Agnel Tony, Ashwini Ratnoo, and Debasish Ghose, "Corridrone: Corridors for drones, an adaptive on-demand multi-lane design and testbed", *arXiv preprint arXiv:2012.01019*, 2020.

- [13] Dae-Sung Jang, Corey A Ippolito, Shankar Sankararaman, and Vahram Stepanyan, "Concepts of airspace structures and system analysis for uas traffic flows for urban areas", in *AIAA Information Systems- AIAA Infotech@ Aerospace*, 2017, p. 0449.
- [14] Jacco M Hoekstra and Joost Ellerbroek, "Bluesky atc simulator project: An open data and open source approach", in *Proceedings of the 7th international conference on research in air transportation*, FAA/Eurocontrol USA/Europe, vol. 131, 2016, p. 132.
- [15] Sezer ÇOBAN and Tuğrul OKTAY, "Unmanned aerial vehicles (uavs) according to engine type", *Journal of Aviation*, vol. 2, no. 2, pp. 177-184, 2018.
- [16] Pilot Institute, *What's the difference between drones, uav, and uas? definitions and terms*, (Last accessed: 23.05.2022), 2020. [Online]. Available: <https://pilotinstitute.com/drones-vs-uav-vs-uas/>.
- [17] Mario Poljak, *What are the disadvantages of drones?*, (Last accessed: 23.05.2022). [Online]. Available: <https://dronetechplanet.com/what-are-the-disadvantages-of-drones/>.
- [18] Circuits Today, *Types of drones - explore the different types of uav's*, (Last accessed: 23.05.2022), 2017. [Online]. Available: <http://www.circuitstoday.com/types-of-drones>.
- [19] James Rennie, *Drone types: Multi-rotor vs fixed-wing vs single rotor vs hybrid vtol*, (Last accessed: 23.05.2022), 2016. [Online]. Available: <https://www.auav.com.au/articles/drone-types/>.
- [20] Lauren Rawlins, *Uncrewed aerial vehicles (uavs)*, (Last accessed: 23.05.2022). [Online]. Available: <http://www.antarcticglaciers.org/glacial-geology/uncrewed-aerial-vehicles-uavs/>.
- [21] ForestTech, *Types of drones (uavs)*, (Last accessed: 23.05.2022), 2017. [Online]. Available: <https://foresttech.events/types-of-drones-multi-rotor-vs-fixed-wing-vs-single-rotor-vs-hybrid-vtol/>.
- [22] Anunay Gupta, Tanzina Afrin, Evan Scully, and Nita Yodo, "Advances of uavs toward future transportation: The state-of-the-art, challenges, and opportunities", *Future Transportation*, vol. 1, no. 2, pp. 326-350, 2021.
- [23] Mike Ball, *Hybrid gas-electric multirotor drone breaks endurance record*, (Last accessed: 23.05.2022), 2021. [Online]. Available: <https://www.unmannedsystemstechnology.com/2021/03/hybrid-gas-electric-multirotor-drone-breaks-endurance-record/>.
- [24] heliguy, *Dji matrice 100 test flights*, (Last accessed: 23.05.2022), 2020. [Online]. Available: <https://www.heliguy.com/blogs/posts/dji-matrice-100-test-flights>.
- [25] Delair, *Fixed-wing uav: Delair introduces most advanced lidar surveying uav*, (Last accessed: 23.05.2022), 2018. [Online]. Available: <https://delair.aero/press/delair-introduces-industrys-advanced-fixed-wing-uav-lidar-based-aerial-surveying-3d-mapping/>.

- [26] PRODRONE, *The nation's first long-distance delivery experiment by single helicopter drone will start. the agreement has been signed among the cities of shima, gamagori and omaezaki, kddi and pro-drone*, (Last accessed: 23.05.2022), 2019. [Online]. Available: <https://www.prodrone.com/release-en/6096/>.
- [27] Wing, *Wing*, (Last accessed: 23.05.2022). [Online]. Available: <https://wing.com/>.
- [28] Alan Levin, *Alphabet jumps into drone air-traffic control with flight app*, (Last accessed: 23.05.2022), 2021. [Online]. Available: <https://www.bloomberg.com/news/articles/2021-06-29/alphabet-jumps-into-drone-air-traffic-control-with-flight-app>.
- [29] The SOARIZON Team, *What are vlos, evlos and bvlos? why do they affect drone operations?*, (Last accessed: 23.05.2022), 2020. [Online]. Available: <https://www.soarizon.io/news/what-are-vlos-evlos-and-bvlos-why-do-they-affect-drone-operations>.
- [30] Mahashreveta Choudhary, *What is bvlos and why is it important for drone industry?*, (Last accessed: 23.05.2022), 2019. [Online]. Available: <https://www.geospatialworld.net/blogs/what-is-bvlos-and-why-is-it-important-for-drone-industry/>.
- [31] The SOARIZON Team, *What are vlos, evlos and bvlos? why do they affect drone operations?*, (Last accessed: 23.05.2022), 2020. [Online]. Available: <https://www.scaleflyt.com/news/what-are-vlos-evlos-and-bvlos-why-do-they-affect-drone-operations>.
- [32] Karim Tolba, *Uae bans all drones and light sports aircraft with immediate effect*, (Last accessed: 23.05.2022), 2022. [Online]. Available: <https://www.commercialdroneprofessional.com/uae-bans-drones-and-light-aircraft-with-immediate-effect/>.
- [33] CCA Norway, *Terms used in unmanned air traffic*, (Last accessed: 23.05.2022). [Online]. Available: <https://luftfartstilsynet.no/en/drones/commercial-use-of-drones/about-dronesrpa/terms-used-in-unmanned-air-traffic/>.
- [34] JU SESAR, "European drones outlook study unlocking the value for europe", *Siebert, JU, Nov*, 2016.
- [35] FlyNex Team, *Utm and atm - this is the difference*, (Last accessed: 23.05.2022), 2020. [Online]. Available: <https://www.flynex.io/software-en/utm-and-atm-this-is-the-difference/>.
- [36] William Harris and Craig Freudenrich, *How airports work*, (Last accessed: 23.05.2022). [Online]. Available: <https://science.howstuffworks.com/transport/flight/modern/airport.htm>.
- [37] Lillian Gipson, *Utm 101*, (Last accessed: 23.05.2022). [Online]. Available: <https://www.nasa.gov/aeroresearch/utm-101/>.
- [38] Parimal H Kopardekar, "Unmanned aerial system (uas) traffic management (utm): Enabling low-altitude airspace and uas operations", *Tech. Rep.*, 2014.
- [39] Federal Aviation Administration, *Unmanned aircraft system traffic management (utm)*, (Last accessed: 23.05.2022). [Online]. Available: https://www.faa.gov/uas/research_development/traffic_management/.

- [40] Thomas Prevot, Joseph Rios, Parimal Kopardekar, John E Robinson III, Marcus Johnson, and Jaewoo Jung, "Uas traffic management (utm) concept of operations to safely enable low altitude flight operations", in *16th AIAA Aviation Technology, Integration, and Operations Conference*, 2016, p. 3292.
- [41] SESAR Joint Undertaking, *Sesar joint undertaking | history*, (Last accessed: 23.05.2022). [Online]. Available: <https://www.sesarju.eu/discover-sesar/history>.
- [42] SESAR JU, *Sesar joint undertaking | u-space*, (Last accessed: 23.05.2022). [Online]. Available: <https://www.sesarju.eu/U-space>.
- [43] NextGen, "Unmanned aircraft system (uas) traffic management (utm) conops v1", 2018.
- [44] FAA NextGen, "Unmanned aircraft system (uas) traffic management (utm) conops v2", 2020.
- [45] Marcus Johnson, Jaewoo Jung, Joseph Rios, Joey Mercer, Jeffrey Homola, Thomas Prevot, Daniel Mulfinger, and Parimal Kopardekar, "Flight test evaluation of an unmanned aircraft system traffic management (utm) concept for multiple beyond-visual-line-of-sight operations", in *USA/Europe Air Traffic Management Research and Development Seminar (ATM2017)*, 2017.
- [46] CORUS, "U-space concept of operations", vol. 2, 2019.
- [47] EUROCONTROL, *Concept of operations for european utm systems (corus) | eurocontrol*, (Last accessed: 23.05.2022). [Online]. Available: <https://www.eurocontrol.int/project/concept-operations-european-utm-systems>.
- [48] SESAR Joint Undertaking *et al.*, "U-space: Blueprint.", 2017.
- [49] GUTMA, "Designing utm for global success v3", 2020.
- [50] SESAR Joint Undertaking *et al.*, "Supporting safe and secure drone operations in europe: A preliminary summary of sesar u-space research and innovation results (2017-2019).", 2020.
- [51] Sabrina Islam Muna, Srijita Mukherjee, Kamesh Namuduri, Marc Compere, Mustafa Ilhan Akbas, Péter Molnár, and Ravichandran Subramanian, "Air corridors: Concept, design, simulation, and rules of engagement", *Sensors*, vol. 21, no. 22, p. 7536, 2021.
- [52] EmbraerX, Atech, and Harris-Corporation, "Flight plan 2030: An air traffic management concept for urban air mobility", 2019.
- [53] Governor Kathy Hochul, *Governor hochul announces new york's 50-mile drone corridor to host first-in-the-nation 5g test network for unmanned aircraft*, (Last accessed: 23.05.2022), 2021. [Online]. Available: <https://www.governor.ny.gov/news/governor-hochul-announces-new-yorks-50-mile-drone-corridor-host-first-nation-5g-test-network>.
- [54] UNICEF Malawi, *Humanitarian drone corridor launched in malawi: How drones are helping the poorest, hardest-to-reach communities access aid and information*, (Last accessed: 23.05.2022), 2017. [Online]. Available: <https://www.unicef.org/stories/humanitarian-drone-corridor-launched-malawi>.
- [55] Aleksandar Bauranov and Jasenka Rakas, "Designing airspace for urban air mobility: A review of concepts and approaches", *Progress in Aerospace Sciences*, vol. 125, p. 100 726, 2021.

- [56] Jacco M Hoekstra, Joost Ellerbroek, Emmanuel Sunil, and Jerom Maas, "Geovectoring: Reducing traffic complexity to increase the capacity of uav airspace", in *International conference for research in air transportation, Barcelona, Spain*, 2018.
- [57] Malik Doole, Joost Ellerbroek, Jacco Hoekstra, Alberto Mennella, and Manuel Onate, "Drone information service requirements for u-space", *SESAR Innovation Days; SESAR Joint Undertaking: Brussels, Belgium*, 2018.
- [58] Jungwoo Cho and Yoonjin Yoon, "Extraction and interpretation of geometrical and topological properties of urban airspace for uas operations", in *13th USA/EUROPE Air Traffic Management R&D Seminar*, 2019.
- [59] Antonio J Torija, Zhengguang Li, and Rod H Self, "Effects of a hovering unmanned aerial vehicle on urban soundscapes perception", *Transportation Research Part D: Transport and Environment*, vol. 78, p. 102-195, 2020.
- [60] Parker D Vascik, Jungwoo Cho, Vishwanath Bulusu, and Valentin Polishchuk, "Geometric approach towards airspace assessment for emerging operations", *Journal of Air Transportation*, vol. 28, no. 3, pp. 124-133, 2020.
- [61] D Geister and B Korn, "Concept for urban airspace integration dlr u-space blueprint", *German Aerospace Center-Institut of Flight Guidance*, 2017.
- [62] Emmanuel Sunil, JM Hoekstra, Joost Ellerbroek, Frank Bussink, Dennis Nieuwenhuisen, Andrija Vidosavljevic, and Stefan Kern, "Metropolis: Relating airspace structure and capacity for extreme traffic densities", in *Proceedings of the 11th USA/Europe Air Traffic Management Research and Development Seminar (ATM2015), Lisbon (Portugal), 23-26 June, 2015*, FAA/Eurocontrol, 2015.
- [63] Emmanuel Sunil, Joost Ellerbroek, Jacco Hoekstra, Andrija Vidosavljevic, Michael Arntzen, Frank Bussink, and Dennis Nieuwenhuisen, "Analysis of airspace structure and capacity for decentralized separation using fast-time simulations", *Journal of Guidance, Control, and Dynamics*, vol. 40, no. 1, pp. 38-51, 2017.
- [64] Malik Doole, Joost Ellerbroek, Victor L Knoop, and Jacco M Hoekstra, "Constrained urban airspace design for large-scale drone-based delivery traffic", *Aerospace*, vol. 8, no. 2, p. 38, 2021.
- [65] Atsushi Oosedo, Hiroaki Hattori, Ippei Yasui, and Kenya Harada, "Unmanned aircraft system traffic management (utm) simulation of drone delivery models in 2030 japan", *Journal of Robotics and Mechatronics*, vol. 33, no. 2, pp. 348-362, 2021.
- [66] David Sacharny, Thomas C Henderson, and Vista Marston, "On-demand virtual highways for dense uas operations", in *2021 IEEE International Conference on Multisensor Fusion and Integration for Intelligent Systems (MFI)*, IEEE, 2021, pp. 1-6.
- [67] Bizhao Pang, Wei Dai, Thu Ra, and Kin Huat Low, "A concept of airspace configuration and operational rules for uas in current airspace", in *2020 AIAA/IEEE 39th Digital Avionics Systems Conference (DASC)*, IEEE, 2020, pp. 1-9.

- [68] Florence Ho, Ruben Gerales, Artur Goncalves, Marc Cavazza, and Helmut Prendinger, "Improved conflict detection and resolution for service uavs in shared airspace", *IEEE Transactions on Vehicular Technology*, vol. 68, no. 2, pp. 1231–1242, 2018.
- [69] Michiel Johannes Maarten Aarts, Joost Ellerbroek, and Victor Knoop, "Capacity of a constrained urban airspace: Influencing factors, analytical modelling and simulations", *Analytical Modelling and Simulations*,
- [70] Marta Ribeiro, Joost Ellerbroek, and Jacco Hoekstra, "Analysis of conflict resolution methods for manned and unmanned aviation using fast-time simulations", *9th SESAR Innovation Days*, 2019.
- [71] Vishwanath Bulusu, Raja Sengupta, Valentin Polishchuk, and Leonid Sedov, "Cooperative and non-cooperative uas traffic volumes", in *2017 International Conference on Unmanned Aircraft Systems (ICUAS)*, IEEE, 2017, pp. 1673–1681.
- [72] Wanchao CHI Da Yang TANA, Mohamed Faisal Bin Mohamed SALLEH, and KH LOWb, "Study on impact of separation distance to traffic management for small uas operations in urban environment", in *Transdisciplinary Engineering: A Paradigm Shift: Proceedings of the 24th ISPE Inc. International Conference on Transdisciplinary Engineering, July 10-14, 2017*, IOS Press, vol. 5, 2017, p. 39.
- [73] Nader Samir Labib, Grégoire Danoy, Jędrzej Musiał, Matthias R Brust, and Pascal Bouvry, "Internet of unmanned aerial vehicles—a multilayer low-altitude airspace model for distributed uav traffic management", *Sensors*, vol. 19, no. 21, p. 4779, 2019.
- [74] Sugjoon Yoon, Dongcho Shin, Younghoon Choi, and Kyungtae Park, "Development of a flexible and expandable utm simulator based on open sources and platforms", *Aerospace*, vol. 8, no. 5, p. 133, 2021.
- [75] Jose A Millan-Romera, José Joaquín Acevedo, Ángel R Castaño, Hector Perez-Leon, Carlos Capitán, and Añbal Ollero, "A utm simulator based on ros and gazebo", in *2019 Workshop on Research, Education and Development of Unmanned Aerial Systems (RED UAS)*, IEEE, 2019, pp. 132–141.
- [76] Amjed Al-Mousa, Belal H Sababha, Nailah Al-Madi, Amro Barghouthi, and Remah Younis, "Utsim: A framework and simulator for uav air traffic integration, control, and communication", *International Journal of Advanced Robotic Systems*, vol. 16, no. 5, p. 1729 881 419 870 937, 2019.
- [77] Chiao Hsieh, Hussein Sibai, Hebron Taylor, Yifeng Ni, and Sayan Mitra, "Skytrakx: A toolkit for simulation and verification of unmanned air-traffic management systems", in *2021 IEEE International Intelligent Transportation Systems Conference (ITSC)*, IEEE, 2021, pp. 372–379.
- [78] Mike Tigas, Kostya Esmukov, and ijl, *Geopy - pypi*, (Last accessed: 23.05.2022). [Online]. Available: <https://pypi.org/project/geopy/>.
- [79] Kenneth Gade, Kristian Svartveit, Brita Hafskjold Gade, and Per A. Brodtkorb, *Nvector - pypi*, (Last accessed: 23.05.2022). [Online]. Available: <https://pypi.org/project/nvector/>.
- [80] GeeksForGeeks, *Dijkstra's shortest path algorithm | greedy algo-7*, (Last accessed: 23.05.2022), 2022. [Online]. Available: <https://www.geeksforgeeks.org/dijkstras-shortest-path-algorithm-greedy-algo-7/>.

- [81] Ilker Bekmezci, Ozgur Koray Sahingoz, and Şamil Temel, "Flying ad-hoc networks (fanets): A survey", *Ad Hoc Networks*, vol. 11, no. 3, pp. 1254–1270, 2013.
- [82] Jacco M Hoekstra and Joost Ellerbroek, "Aerial robotics: State-based conflict detection and resolution (detect and avoid) in high traffic densities and complexities", *Current Robotics Reports*, vol. 2, no. 3, pp. 297–307, 2021.
- [83] Marta Ribeiro, Joost Ellerbroek, and Jacco Hoekstra, "Review of conflict resolution methods for manned and unmanned aviation", *Aerospace*, vol. 7, no. 6, p. 79, 2020.
- [84] thebmj, *Mean and standard deviation*, (Last accessed: 23.05.2022). [Online]. Available: <https://www.bmj.com/about-bmj/resources-readers/publications/statistics-square-one/2-mean-and-standard-deviation>.
- [85] Zach, *Welch's t-test: When to use it + examples*, (Last accessed: 23.05.2022), 2019. [Online]. Available: <https://www.statology.org/welchs-t-test/>.
- [86] San Jose State University, *T-table*, (Last accessed: 23.05.2022). [Online]. Available: <https://www.sjsu.edu/faculty/gerstman/StatPrimer/t-table.pdf>.
- [87] E Sunil, J Ellerbroek, and J Hoekstra, "Metropolis–urban airspace design-scenario definition report (d 1.2)", *TU Delft*, 2014.

Appendix A

Simulational Parameters

A.1 Corridor types simulation(s) specifications

Table A.1: The simulation rules and parameters for the corridor type comparison experiment

| Parameter | Bi-directional | Layered bi-directional (unstructured) | Layered bi-directional (structured) |
|---------------------------------------|----------------|---|---|
| Corridor speed limit(s) [m/s] | 12.86 | 12.86 | 12.86, 15.43, 18, 20.57 |
| Corridor layer altitude(s) [m] | 120 | 120, 135, 150, 165 | 120, 135, 150, 165 |
| Look ahead time [s] | 15 | 15 | 15 |
| Horizontal separation distance [m] | 50 | 50 | 50 |
| Vertical separation distance [m] | 6 | 6 | 6 |

Appendix B

Corridor Coordinates

B.1 Park coordinates

| Node | Connected node(s) | Coordinate |
|------|-------------------|---------------------|
| N1 | N4, N2 | (48.89128, 2.31413) |
| N2 | N1, N9, N3 | (48.8852, 2.34327) |
| N3 | N2, N5 | (48.89527, 2.3897) |
| N4 | N7, N8, N1 | (48.87926, 2.3088) |
| N5 | N9, N6, N3 | (48.88039, 2.38223) |
| N6 | N5, N13 | (48.88179, 2.3988) |
| N7 | N4, N10 | (48.86159, 2.28897) |
| N8 | N10, N11, N9, N4 | (48.86345, 2.32673) |
| N9 | N8, N12, N5, N2 | (48.86004, 2.35867) |
| N10 | N7, N14, N8 | (48.84098, 2.27555) |
| N11 | N8, N14, N12 | (48.84661, 2.33583) |
| N12 | N11, N13, N9 | (48.84436, 2.35988) |
| N13 | N12, N14, N6 | (48.83606, 2.38123) |
| N14 | N10, N13, N11 | (48.82211, 2.33767) |

Table B.1: Park coordinates

B.2 Roundabout coordinates

| Node | Coordinate | |
|------|--------------------|---------------------|
| N1 | N5, N2 | (48.90319, 2.31291) |
| N2 | N1, N7, N3 | (48.89578, 2.34615) |
| N3 | N2, N4 | (48.8932, 2.3635) |
| N4 | N3, N8, N9 | (48.89589, 2.37928) |
| N5 | N1, N10, N6 | (48.88502, 2.29727) |
| N6 | N5, N12, N7 | (48.88353, 2.3274) |
| N7 | N2, N6, N8 | (48.88054, 2.35236) |
| N8 | N7, N13, N14, N4 | (48.87808, 2.37028) |
| N9 | N4, N15 | (48.87713, 2.40673) |
| N10 | N5, N16, N11 | (48.87383, 2.29497) |
| N11 | N10, N12 | (48.86899, 2.31014) |
| N12 | N6, N11, N18, N13 | (48.86575, 2.34118) |
| N13 | N12, N17, N8 | (48.86471, 2.36462) |
| N14 | N8, N15 | (48.86493, 2.39846) |
| N15 | N9, N14, N20 | (48.86451, 2.40875) |
| N16 | N10, N21, N18 | (48.86307, 2.28712) |
| N17 | N13, N19, N20 | (48.8578, 2.38028) |
| N18 | N16, N22, N12 | (48.84792, 2.30161) |
| N19 | N25, N17 | (48.84738, 2.34063) |
| N20 | N17, N23, N15 | (48.84843, 2.39583) |
| N21 | N16, N24 | (48.83793, 2.257) |
| N22 | N18, N25 | (48.8372, 2.31831) |
| N23 | N27, N20 | (48.83961, 2.39581) |
| N24 | N21, N25 | (48.8275, 2.29246) |
| N25 | N22, N24, N26, N19 | (48.82791, 2.3268) |
| N26 | N25, N27 | (48.82238, 2.34672) |
| N27 | N26, N23 | (48.83155, 2.35558) |

Table B.2: Roundabout coordinates

B.3 Ring road coordinates

| Node | Coordinate |
|------|---------------------|
| N1 | (48.82758, 2.29207) |
| N2 | (48.83505, 2.27259) |
| N3 | (48.83513, 2.25893) |
| N4 | (48.83788, 2.25444) |
| N5 | (48.84643, 2.25456) |
| N6 | (48.85214, 2.2522) |
| N7 | (48.87857, 2.28041) |
| N8 | (48.88941, 2.29741) |
| N9 | (48.90068, 2.32733) |
| N10 | (48.89992, 2.39191) |
| N11 | (48.88308, 2.40028) |
| N12 | (48.87941, 2.40751) |
| N13 | (48.87169, 2.41311) |
| N14 | (48.85386, 2.41398) |
| N15 | (48.83497, 2.41182) |
| N16 | (48.82669, 2.39036) |
| N17 | (48.81651, 2.36676) |
| N18 | (48.81776, 2.35142) |
| N19 | (48.81844, 2.33288) |
| N20 | (48.82226, 2.31465) |

Table B.3: Ring road coordinates

B.4 River coordinates

| Node | Coordinate |
|------|---------------------|
| N1 | (48.84078, 2.26978) |
| N2 | (48.84914, 2.27845) |
| N3 | (48.85569, 2.28729) |
| N4 | (48.86297, 2.29836) |
| N5 | (48.86399, 2.31853) |
| N6 | (48.85806, 2.33922) |
| N7 | (48.84902, 2.36059) |
| N8 | (48.83648, 2.37605) |
| N9 | (48.82726, 2.38793) |

Table B.4: River coordinates

Appendix C

Numerical Results

C.1 Numeric corridor types results

Table C.1: Numerical results for the bi-directional corridor

| KPIs | 1,500 | 2,000 | 2,500 |
|--|--------------------------|-------------------------|-------------------------|
| Average travel time [s] | 639.06 (σ 3.99) | 636.56 (σ 5.7) | 637.58 (σ 4.26) |
| Average number of conflicts [number] | 155.0 (σ 11.73) | 295.8 (σ 4.87) | 444.6 (σ 28.31) |
| Average number of LoS [number] | 6.6 (σ 1.52) | 11.8 (σ 4.15) | 18.6 (σ 3.78) |
| Average number of near mid-air collisions [number] | 0.2 (σ 0.44) | 0.6 (σ 0.54) | 0.4 (σ 0.54) |
| Average LoS duration [s] | 1.61 (σ 0.55) | 1.33 (σ 0.2) | 1.53 (σ 0.22) |
| Average LoS distance [m] | 7.63 (σ 3.95) | 7.16 (σ 2.57) | 6.82 (σ 1.37) |
| Average route deviation [m] | -153.29 (σ 9.78) | -144.5 (σ 11.4) | -152.8 (σ 8.86) |

Table C.2: Numerical results for the unstructured layered bi-directional corridor

| KPIs | 1,500 | 2,000 | 2,500 |
|--|--------------------------|--------------------------|--------------------------|
| Average travel time [s] | 637.05 (σ 3.93) | 639.01 (σ 7.75) | 635.72 (σ 4.1) |
| Average number of conflicts [number] | 96.6 (σ 20.62) | 167.6 (σ 21.42) | 256.0 (σ 28.82) |
| Average number of LoS [number] | 3.2 (σ 1.92) | 4.6 (σ 1.95) | 9.8 (σ 1.3) |
| Average number of near mid-air collisions [number] | 0.2 (σ 0.44) | 0.0 (σ 0.0) | 0.0 (σ 0.0) |
| Average LoS duration [s] | 1.5 (σ 0.61) | 1.44 (σ 0.19) | 1.18 (σ 0.08) |
| Average LoS distance [m] | 5.82 (σ 3.87) | 6.46 (σ 1.96) | 4.88 (σ 1.59) |
| Average route deviation [m] | -157.05 (σ 9.28) | -147.64 (σ 8.43) | -154.55 (σ 1.89) |

Table C.3: Numerical results for the structured layered bi-directional corridor

| KPIs | 1,500 | 2,000 | 2,500 |
|--|--------------------------|--------------------------|--------------------------|
| Average travel time [s] | 554.52 (σ 2.3) | 555.63 (σ 1.69) | 555.02 (σ 3.17) |
| Average number of conflicts [number] | 95.6 (σ 16.41) | 132.6 (σ 6.73) | 249.8 (σ 25.07) |
| Average number of LoS [number] | 4.6 (σ 2.61) | 3.8 (σ 2.17) | 7.8 (σ 3.9) |
| Average number of near mid-air collisions [number] | 0.0 (σ 0.0) | 0.0 (σ 0.0) | 0.2 (σ 0.44) |
| Average LoS duration [s] | 1.37 (σ 0.46) | 1.65 (σ 0.41) | 1.77 (σ 0.35) |
| Average LoS distance [m] | 7.33 (σ 4.01) | 6.31 (σ 1.64) | 8.49 (σ 2.49) |
| Average route deviation [m] | -201.49 (σ 7.08) | -202.38 (σ 6.67) | -198.06 (σ 3.53) |

C.2 Numeric separation distances results

Table C.4: Numerical results for the different separation distance for the bi-directional corridor

| KPIs | 20m | 40m | 60m | 80m |
|--|--------------------------|--------------------------|-------------------------|--------------------------|
| Average travel time [s] | 640.38 (σ 2.1) | 637.1 (σ 3.51) | 640.52 (σ 3.35) | 640.5 (σ 3.96) |
| Average number of conflicts [number] | 147.8 (σ 18.85) | 351.8 (σ 17.18) | 614.2 (σ 69.06) | 856.8 (σ 61.32) |
| Average number of LoS [number] | 6.0 (σ 2.55) | 16.6 (σ 3.44) | 33.2 (σ 6.72) | 38.0 (σ 3.87) |
| Average number of near mid-air collisions [number] | 0.6 (σ 0.54) | 1.6 (σ 0.89) | 0.6 (σ 0.54) | 0.0 (σ 0.0) |
| Average LoS duration [s] | 1.26 (σ 0.22) | 1.57 (σ 0.29) | 1.73 (σ 0.25) | 1.58 (σ 0.11) |
| Average LoS distance [m] | 3.4 (σ 0.7) | 7.93 (σ 2.24) | 8.43 (σ 0.8) | 9.41 (σ 1.25) |
| Average route deviation [m] | -153.78 (σ 6.27) | -155.24 (σ 6.13) | -151.32 (σ 6.8) | -144.45 (σ 4.71) |

Table C.5: Numerical results for the different separation distances for the structured layered bi-directional corridor

| KPIs | 20m | 40m | 60m | 80m |
|--|--------------------------|--------------------------|--------------------------|--------------------------|
| Average travel time [s] | 552.61 (σ 3.38) | 552.99 (σ 2.59) | 554.57 (σ 1.21) | 554.25 (σ 3.58) |
| Average number of conflicts [number] | 80.2 (σ 8.87) | 185.8 (σ 12.87) | 330.4 (σ 32.28) | 454.8 (σ 39.9) |
| Average number of LoS [number] | 1.4 (σ 1.14) | 4.4 (σ 2.7) | 13.2 (σ 2.49) | 18.4 (σ 4.1) |
| Average number of near mid-air collisions [number] | 0.0 (σ 0.0) | 0.2 (σ 0.44) | 0.2 (σ 0.44) | 0.0 (σ 0.0) |
| Average LoS duration [s] | 1.08 (σ 0.51) | 1.63 (σ 0.84) | 1.75 (σ 0.33) | 1.86 (σ 0.43) |
| Average LoS distance [m] | 2.22 (σ 1.85) | 5.88 (σ 2.89) | 8.23 (σ 2.37) | 8.55 (σ 1.89) |
| Average route deviation [m] | -203.66 (σ 5.99) | -203.75 (σ 3.47) | -193.23 (σ 3.46) | -200.36 (σ 6.21) |

C.3 Numeric speed limits results

Table C.6: Numerical results for the different speed limits for the bi-directional corridor

| KPIs | 10.29 m/s | 12.86 m/s | 15.43 m/s | 18.00 m/s |
|--|-------------------------|-------------------------|---------------------------|--------------------------|
| Average travel time [s] | 740.61 (σ 4.85) | 637.58 (σ 4.26) | 572.13 (σ 2.56) | 523.48 (σ 2.37) |
| Average number of conflicts [number] | 552.6 (σ 38.23) | 444.6 (σ 28.31) | 383.6 (σ 45.41) | 375.0 (σ 12.39) |
| Average number of LoS [number] | 23.8 (σ 6.14) | 18.6 (σ 3.78) | 18.4 (σ 2.88) | 18.4 (σ 2.51) |
| Average number of near mid-air collisions [number] | 0.2 (σ 0.44) | 0.4 (σ 0.54) | 0.0 (σ 0.0) | 0.0 (σ 0.0) |
| Average LoS duration [s] | 1.26 (σ 0.19) | 1.53 (σ 0.22) | 1.32 (σ 0.2) | 1.32 (σ 0.19) |
| Average LoS distance [m] | 6.04 (σ 1.32) | 6.82 (σ 1.37) | 5.58 (σ 1.66) | 6.02 (σ 1.47) |
| Average route deviation [m] | -115.6 (σ 6.57) | -152.8 (σ 8.86) | -181.49 (σ 11.88) | -211.14 (σ 9.47) |

Table C.7: Numerical results for the different speed limits for the structured layered bi-directional corridor

| KPIs | 10.29 m/s | 12.86 m/s | 15.43 m/s | 18.00 m/s |
|--|-------------------------|--------------------------|--------------------------|--------------------------|
| Average travel time [s] | 616.78 (σ 3.69) | 555.02 (σ 3.17) | 510.49 (σ 2.14) | 482.9 (σ 1.26) |
| Average number of conflicts [number] | 252.8 (σ 20.69) | 249.8 (σ 25.07) | 211.4 (σ 11.78) | 224.25 (σ 15.24) |
| Average number of LoS [number] | 7.8 (σ 1.79) | 7.8 (σ 3.9) | 6.8 (σ 2.39) | 7.25 (σ 2.99) |
| Average number of near mid-air collisions [number] | 0.0 (σ 0.0) | 0.2 (σ 0.44) | 0.2 (σ 0.44) | 0.0 (σ 0.0) |
| Average LoS duration [s] | 1.61 (σ 0.34) | 1.77 (σ 0.35) | 1.62 (σ 0.5) | 1.64 (σ 0.43) |
| Average LoS distance [m] | 6.63 (σ 2.04) | 8.49 (σ 2.49) | 6.91 (σ 3.09) | 7.9 (σ 2.31) |
| Average route deviation [m] | -174.87 (σ 9.9) | -198.06 (σ 3.53) | -234.33 (σ 5.92) | -249.88 (σ 7.79) |

C.4 Numeric look-ahead times results

Table C.8: Numerical results for the different look-ahead times for the bi-directional corridor

| KPIs | 10s | 12s | 14s | 16s |
|--|--------------------------|--------------------------|--------------------------|-------------------------|
| Average travel time [s] | 638.68 (σ 0.59) | 638.55 (σ 4.27) | 640.73 (σ 4.34) | 637.78 (σ 3.63) |
| Average number of conflicts [number] | 424.75 (σ 18.34) | 459.8 (σ 36.36) | 458.6 (σ 42.79) | 444.0 (σ 35.29) |
| Average number of LoS [number] | 16.0 (σ 3.65) | 18.4 (σ 2.19) | 21.8 (σ 8.23) | 16.25 (σ 4.43) |
| Average number of near mid-air collisions [number] | 0.2 (σ 0.44) | 0.2 (σ 0.44) | 0.8 (σ 0.83) | 0.4 (σ 0.54) |
| Average LoS duration [s] | 1.54 (σ 0.27) | 1.46 (σ 0.3) | 1.43 (σ 0.22) | 1.42 (σ 0.17) |
| Average LoS distance [m] | 8.5 (σ 2.53) | 7.39 (σ 0.68) | 7.17 (σ 2.63) | 6.99 (σ 0.78) |
| Average route deviation [m] | -151.45 (σ 6.98) | -148.93 (σ 3.33) | -145.29 (σ 8.23) | -148.75 (σ 5.7) |

Table C.9: Numerical results for the different look-ahead times for the structured layered bi-directional corridor

| KPIs | 10s | 12s | 14s | 16s |
|--|--------------------------|-------------------------|--------------------------|--------------------------|
| Average travel time [s] | 555.95 (σ 2.13) | 556.34 (σ 1.19) | 555.58 (σ 3.61) | 554.99 (σ 4.19) |
| Average number of conflicts [number] | 226.2 (σ 14.17) | 217.4 (σ 28.13) | 223.8 (σ 21.56) | 236.4 (σ 17.84) |
| Average number of LoS [number] | 8.8 (σ 1.3) | 5.8 (σ 2.59) | 7.0 (σ 3.16) | 8.0 (σ 3.94) |
| Average number of near mid-air collisions [number] | 0.0 (σ 0.0) | 0.0 (σ 0.0) | 0.0 (σ 0.0) | 0.0 (σ 0.0) |
| Average LoS duration [s] | 1.6 (σ 0.27) | 1.71 (σ 0.51) | 1.28 (σ 0.19) | 1.7 (σ 0.49) |
| Average LoS distance [m] | 7.9 (σ 1.71) | 6.26 (σ 2.51) | 6.06 (σ 1.72) | 7.52 (σ 3.0) |
| Average route deviation [m] | -199.77 (σ 2.11) | -195.34 (σ 9.0) | -196.16 (σ 8.18) | -193.89 (σ 7.43) |

C.5 Numeric corridor placements results

Table C.10: Numerical results for the 3x3 grid network

| KPIs | 1,500 | 2,000 | 2,500 |
|--|---------------------------|---------------------------|---------------------------|
| Average travel time [s] | 593.79 (σ 2.52) | 594.67 (σ 2.16) | 593.87 (σ 4.39) |
| Average number of conflicts [number] | 99.4 (σ 18.88) | 187.2 (σ 12.58) | 285.2 (σ 18.75) |
| Average number of LoS [number] | 2.2 (σ 1.64) | 5.6 (σ 3.36) | 8.2 (σ 3.9) |
| Average number of near mid-air collisions [number] | 0 (σ 0.0) | 0 (σ 0.0) | 0 (σ 0.0) |
| Average LoS duration [s] | 2.15 (σ 0.49) | 1.55 (σ 0.38) | 1.55 (σ 0.21) |
| Average LoS distance [m] | 10.3 (σ 1.83) | 6.89 (σ 3.07) | 7.6 (σ 3.04) |
| Average route deviation [m] | -212.48 (σ 10.94) | -225.52 (σ 12.73) | -214.88 (σ 15.32) |
| Average direct deviation [m] | 1.76 (σ 0.01) | 1.77 (σ 0.01) | 1.77 (σ 0.01) |
| Average number of UAVs not using corridor [number] | 376.6 (σ 9.99) | 495 (σ 10.31) | 627.2 (σ 35.15) |

Table C.11: Numerical results for the 4x4 grid network

| KPIs | 1,500 | 2,000 | 2,500 |
|--|--------------------------|--------------------------|--------------------------|
| Average travel time [s] | 554.52 (σ 2.3) | 555.63 (σ 1.69) | 555.02 (σ 3.17) |
| Average number of conflicts [number] | 95.6 (σ 16.41) | 132.6 (σ 6.73) | 249.8 (σ 25.07) |
| Average number of LoS [number] | 4.6 (σ 2.61) | 3.8 (σ 2.17) | 7.8 (σ 3.9) |
| Average number of near mid-air collisions [number] | 0 (σ 0.0) | 0 (σ 0.0) | 0.2 (σ 0.44) |
| Average LoS duration [s] | 1.37 (σ 0.46) | 1.65 (σ 0.41) | 1.77 (σ 0.35) |
| Average LoS distance [m] | 7.33 (σ 4.01) | 6.31 (σ 1.64) | 8.49 (σ 2.49) |
| Average route deviation [m] | -201.49 (σ 7.08) | -202.38 (σ 6.67) | -198.06 (σ 3.53) |
| Average direct deviation [m] | 1.74 (σ 0.01) | 1.74 (σ 0.01) | 1.74 (σ 0.01) |
| Average number of UAVs not using corridor [number] | 69.2 (σ 5.38) | 101.2 (σ 9.17) | 129 (σ 6.72) |

Table C.12: Numerical results for the park network

| KPIs | 1,500 | 2,000 | 2,500 |
|--|--------------------------|-------------------------|-------------------------|
| Average travel time [s] | 555.35 (σ 1.12) | 558.28 (σ 1.78) | 557.91 (σ 2.65) |
| Average number of conflicts [number] | 104.6 (σ 15.63) | 192.0 (σ 29.33) | 304.6 (σ 16.74) |
| Average number of LoS [number] | 3.0 (σ 2.35) | 5.8 (σ 1.3) | 6.4 (σ 2.07) |
| Average number of near mid-air collisions [number] | 0 (σ 0.0) | 0 (σ 0.0) | 0 (σ 0.0) |
| Average LoS duration [s] | 1.11 (σ 0.15) | 1.51 (σ 0.41) | 1.46 (σ 0.21) |
| Average LoS distance [m] | 6.77 (σ 5.95) | 5.31 (σ 2.97) | 5.99 (σ 2.78) |
| Average route deviation [m] | -160.28 (σ 6.11) | -159.4 (σ 6.78) | -157.1 (σ 6.83) |
| Average direct deviation [m] | 1.64 (σ 0.01) | 1.65 (σ 0.01) | 1.65 (σ 0.01) |
| Average number of UAVs not using corridor [number] | 182.2(σ 7.85) | 228.4 (σ 10.20) | 290 (σ 14.05) |

Table C.13: Numerical results for the ring road

| KPIs | 1,500 | 2,000 | 2,500 |
|--|---------------------------|--------------------------|-------------------------|
| Average travel time [s] | 555.66 (σ 0.96) | 554.06 (σ 3.22) | 556.58 (σ 2.5) |
| Average number of conflicts [number] | 96.6 (σ 11.41) | 162.2 (σ 8.17) | 267.4 (σ 9.32) |
| Average number of LoS [number] | 1.8 (σ 1.3) | 2.8 (σ 1.3) | 4.2 (σ 1.48) |
| Average number of near mid-air collisions [number] | 0 (σ 0.0) | 0 (σ 0.0) | 0 (σ 0.0) |
| Average LoS duration [s] | 2.21 (σ 1.13) | 1.5 (σ 0.59) | 1.34 (σ 0.23) |
| Average LoS distance [m] | 5.94 (σ 3.25) | 4.98 (σ 3.25) | 5.84 (σ 1.61) |
| Average route deviation [m] | -119.83 (σ 12.57) | -110.47 (σ 7.34) | -118.3 (σ 3.83) |
| Average direct deviation [m] | 1.55 (σ 0.01) | 1.55 (σ 0.01) | 1.57 (σ 0.01) |
| Average number of UAVs not using corridor [number] | 373.6 (σ 15.96) | 520.4 (σ 21.58) | 614.2 (σ 24.83) |

Table C.14: Numerical results for the river

| KPIs | 1,500 | 2,000 | 2,500 |
|--|-------------------------|-------------------------|-------------------------|
| Average travel time [s] | 599.24 (σ 1.44) | 601.67 (σ 7.07) | 596.54 (σ 3.96) |
| Average number of conflicts [number] | 186.4 (σ 9.86) | 362.0 (σ 28.15) | 565.2 (σ 29.74) |
| Average number of LoS [number] | 3.8 (σ 1.1) | 6.6 (σ 2.7) | 11.4 (σ 2.19) |
| Average number of near mid-air collisions [number] | 0 (σ 0.0) | 0 (σ 0.0) | 0 (σ 0.0) |
| Average LoS duration [s] | 1.6 (σ 0.23) | 1.49 (σ 0.23) | 1.52 (σ 0.14) |
| Average LoS distance [m] | 7.82 (σ 3.58) | 6.62 (σ 1.22) | 6.89 (σ 0.95) |
| Average route deviation [m] | -46.08 (σ 4.26) | -50.47 (σ 6.68) | -45.18 (σ 2.44) |
| Average direct deviation [m] | 1.57 (σ 0.01) | 1.58 (σ 0.01) | 1.56 (σ 0.01) |
| Average number of UAVs not using corridor [number] | 413 (σ 12.55) | 550.4 (σ 18.20) | 700 (σ 10.19) |

Table C.15: Numerical results for the roundabout network

| KPIs | 1,500 | 2,000 | 2,500 |
|--|--------------------------|--------------------------|---------------------------|
| Average travel time [s] | 527.46 (σ 1.95) | 529.38 (σ 2.71) | 527.92 (σ 2.71) |
| Average number of conflicts [number] | 89.0 (σ 16.61) | 132.75 (σ 2.5) | 216.8 (σ 16.42) |
| Average number of LoS [number] | 3.2 (σ 0.84) | 3.0 (σ 0.82) | 5.6 (σ 2.41) |
| Average number of near mid-air collisions [number] | 0 (σ 0.0) | 0 (σ 0.0) | 0 (σ 0.0) |
| Average LoS duration [s] | 1.3 (σ 0.24) | 1.44 (σ 0.34) | 1.32 (σ 0.28) |
| Average LoS distance [m] | 6.89 (σ 2.51) | 4.51 (σ 1.91) | 5.02 (σ 2.72) |
| Average route deviation [m] | -184.91 (σ 3.99) | -183.56 (σ 2.84) | -176.78 (σ 10.39) |
| Average direct deviation [m] | 1.62 (σ 0.0) | 1.63 (σ 0.01) | 1.63 (σ 0.01) |
| Average number of UAVs not using corridor [number] | 40.2 (σ 6.91) | 56.25 (σ 3.03) | 59 (σ 8.87) |

C.6 Numeric unstructured free-flight results

Table C.16: Numerical results for the unstructured free-flight

| KPIs | 1,500 | 2,000 | 2,500 |
|--|-------------------------|-------------------------|-------------------------|
| Average travel time [s] | 319.86 (σ 0.64) | 319.57 (σ 0.92) | 319.51 (σ 0.45) |
| Average number of LoS [number] | 34.2 (σ 3.7) | 49.2 (σ 4.55) | 88.4 (σ 12.14) |
| Average number of near mid-air collisions [number] | 4 (σ 2.23) | 6.2 (σ 2.28) | 10.6 (σ 2.60) |
| Average LoS duration [s] | 3.76 (σ 0.42) | 4.16 (σ 0.21) | 4.08 (σ 0.25) |
| Average LoS distance [m] | 14.63 (σ 1.65) | 15.2 (σ 1.66) | 14.95 (σ 0.63) |
| Average route deviation [m] | 0.39 (σ 0.01) | 0.38 (σ 0.01) | 0.38 (σ 0.01) |